Performance Evaluation of Erosion and Sediment Control Practices

by

Jannell E. Clampitt

A thesis submitted to the Graduate Faculty of
Auburn University
in partial fulfillment of the
requirements for the Degree of
Master of Science

Auburn, Alabama
August 5, 2023

Keywords: construction stormwater, sediment control,
wattles, percent open area, flocculants, residual testing

Approved by

Michael A. Perez, P.E., Chair, Assistant Professor of Civil Engineering
Wesley N. Donald, Research Fellow IV, Civil Engineering
Xing Fang, P.E., Professor of Civil Engineering

ABSTRACT

Construction-generated stormwater runoff has the potential to negatively affect receiving water bodies downstream. Not only does eroded soil transport other pollutants, but sediment also remains suspended in water, where it can block sunlight and cause hypoxic conditions, resulting in a variety of other adverse environmental effects. Federal and state regulations stress the importance of erosion and sediment control on construction sites and mandate the implementation of effective stormwater pollution prevention plans. The regulations aim to prevent the impairment of receiving waterbodies by mandating the management of construction stormwater with appropriate design, implementation, and maintenance of erosion and sediment control practices.

This thesis explores practical methods to enhance wattle impoundment abilities and application of flocculants on construction sites. This research evaluates construction stormwater treatment through (1) modification of a wattle's encasement to improve impoundment abilities, (2) exploring possible flocculant detection methods for large-scale applications, and (3) conducting large-scale testing evaluations with flocculants to develop guidance on dosage and applications rates.

Temporary erosion and sediment control practices seek to minimize and reduce the effluent turbidity from a construction site by preventing sediment detachment and capturing suspended sediment particles, respectively. A common method to protect against erosive forces and allow sediment to settle out of suspension is to impound water. Wattle ditch checks are a common erosion and sediment control practice for slowing down water in channels to reduce those erosive forces. Wattle popularity is correlated to their price, weight, application versatility, range of fill materials, and installation process. According to previous research, the hydraulic performance of wattles is predominantly determined by the fill material. This study assessed the impact of

encasement material (e.g., netting, socking, etc.) on wattle hydraulic efficacy. In a two-phased process, two separate hydraulic flumes were used. Phase I evaluated configurations of wattle encasement fabric. In Phase II, select encasements were evaluated with 4.0 ft (1.2 m) long wattles with excelsior fill materials – heavy-duty synthetic plastic netting (control), polypropylene, polyester and polypropylene blend, and cotton woven encasements. The outcomes of each wattle test were normalized using ratios of impoundment length and depth. The results indicated that the percent open area (POA) had a direct relationship with the impoundment length and depth when the encasements were evaluated independently of the fill material; however, the encasement type had a greater effect on performance when the fill material was included. Using a cotton fabric increased the length and depth ratios of the impoundment by 30% and 24%, respectively, compared to a plastic netting encasement; these ratios increased to 52% and 44% when two additional cotton fabric layers surrounded the wattle.

Even though implementing erosion and sediment control practices can be highly effective at capturing sediment from stormwater, fine sediment and clay particles are difficult to capture as they can take days to settle out of suspension. Often times, practitioners do not have options to increase the detention time for impounded water for the time necessary to capture those fine particles before another storm event. Flocculants are a chemical additive that can be added to sediment-laden water to facilitate the efficient capture of fine sediment particles. Flocculants function by agglomerating fine sediment particles to produce flocs, which are larger colloids that facilitate settlement. Thus, greatly reducing detention time necessary for capturing fine particles. While effective, there are concerns that improper use of flocculants could create potential pollution to downstream waterways and harm aquatic life. The effectiveness of flocculants used in a variety of applications, including stormwater management, has been studied; however, there is a

knowledge gap regarding application techniques and dosage guidance for construction site applications.

When exploring flocculant detection methods for large-scale applications, methods that were simple and easy to perform without extensive lab training, cost-effective, capable of working with sediment-ladened samples, produced reliable results in a short time, and were capable of quantifying concentration ranges above and below manufacturer's recommended concentrations were periodized. A Cannon-Fenske Routine Viscometer and Brookfield Digital Viscometer were not sensitive enough to quantify the necessary concentration range needed, while a Laboratory Charge Analyzer could. Depending on the flocculant type and charge, the Laboratory Charge Analyzer could only accurately quantify low or high concentrations around the manufacturer's recommendations. Quantifying soil settling velocity remained to be the most consistent method that met all criteria for predicting residual flocculant concentrations. Research found that large-scale applications require sample temperature and pH to be accounted for in the settling velocity prediction equations to generate reliable results as the time of year and vegetation can influence the temperature and pH of stormwater, which, in addition to flocculant concentration, all significantly influence soil settling velocities.

Flocculant application placement and reapplication timing guidance on construction sites to achieve optimum dosing and mixing for granular and block form flocculants were determined by performing large-scale tests and using the soil settling velocity residual flocculant detection method that accounted for pH, temperature, and flocculant concentrations. Anionic granular polyacrylamide flocculant was spread across three wattles spaced over 43 ft (13 m) at a rate of 6.36 oz. (180 g) per wattle. Results found that during a 0.75 ft^3/s (0.07 m^3/s) flow event, the channel is initially dosed with 14 mg/L above the manufacturer's recommendations and

exponentially decreased over the first 25 minutes or 1,060 ft^3 (30 m^3) of flow to reach the recommended dosage of 5 mg/L. From this, it is recommended that reapplication of granular flocculant should be performed after 3600 ft^3 (101.9 m^3) of flow or 1.0 in. (2.54 cm) of runoff per acre (0.4 ha). Anionic block form polyacrylamide tests were conducted, and results indicated that six flocculant blocks provided optimum dosing for a flowrate of 1.80 ft^3/s (0.05 m^3/s) of channel flow in a 4 ft wide bottom channel; however, further analysis is necessary for accurate concentration predictions using block form flocculants. All flocculant applications evaluated indicated the need for at least one flocculant-free ditch check at the end of a channel to provide necessary mixing. Flocculants vary by manufacturer and are highly soil-dependent. Therefore results may vary based on the product manufacturer and soil type.

Effective application of flocculants on construction sites is possible with the correct dosage, dosage delivery mechanism, and application. This study provides practitioners with a framework for establishing flocculant implementation that effectively treats construction stormwater. The findings of this study enable advances in flocculant usage in construction stormwater treatment through new and revised guidelines, as well as an increased understanding of the use of flocculants in the erosion and sediment control business.

ACKNOWLEDGMENTS

Over the last two years of earning my master's degree, I have had the honor of working with a fantastic group of people. Dr. Michael A. Perez has been an incredible advisor who surpassed his mentorship and support throughout my master's journey and has given me the tools to be a successful researcher, presenter, networker, and planner, to name a few, through the countless opportunities he has given me to grow. He and his wife, Veronica Ramirez-Perez, have helped make Auburn my home away from home, and I could not be more thankful for their unconditional support and everything they have done for me. I am deeply grateful to Dr. Wesley N. Donald, Dr. Xing Fang, Dr. J. Blake Whitman, and Dr. Jeffery J. LaMondia for their mentorship, guidance, and time throughout these research efforts.

The flocculant research portion of this research could not have been possible without the support from the Alabama Department of Transportation, along with the Auburn University Department of Civil and Environmental Engineering and Samuel Ginn College of Engineering for both the wattle and flocculant portions of this research. I thank Mr. Kris Ansley for testing support and coordination at the Auburn University Stormwater Research Facility. I would also like to share my gratitude and make a special thank you to all my undergraduate research assistants Adam Craig, William Tyler Puckett, Matthew Ford, Logan Suddath, Patricia Barnes, Rustin Roberts, Joey Allison, Alma Lilly Smith, Joseph Faust, Amanda Pollard, Alex Clements, Zoey Thompson, and many more who have been the extra pairs of hands in the lab and at the facility to help me successfully execute labor and time intensive testing efforts in at all hours of the day.

I am most of all grateful to my immediate family for their unwavering love and support. This endeavor is a direct outcome of their encouragement and unconditional love. I want to express my endless gratitude and thank my mother, Jayne Clampitt, for encouraging me to follow

my dreams and giving me to tools to do so; my father, Greg Clampitt, for teaching me how to build and fix anything; my brother, Garrett Clampitt, for helping me when I needed it, and my sister, Jeannett Clampitt, for being by my side and my sounding board throughout the ups and downs. I would not have been here without my family, who has taught me the importance of education, hard work, and to never limit one's potential.

TABLE OF CONTENTS

LIST OF TABLES

LIST OF FIGURES

LIST OF ABBREVIATIONS

AM	Acrylamide
ADEM	Alabama Department of Environmental Management
ALDOT	Alabama Department of Transportation
B-PAM	Anionic Block H_{30} PAM Flocculant from Manufacturer A
G-PAM	Anionic Granular H_{30} PAM Flocculant from Manufacturer A
AOS	Apparent Opening Size
AU-SRF	Auburn University - Stormwater Research Facility
ANZECC	Australian and New Zealand Environment and Conservation Council
CGP	Construction General Permit
DOT	Department Of Transportation
E&SC	Erosion And Sediment Control
FDA	Food And Drug Administration
Fr	Froude Number
LCA	Laboratory Charge Analyzer
LC	Lethal Concentration
LD	Lethal Dose
MPC	Maximum Permissible Concentration
MLR	Multiple Linear Regression
NCAT	National Center For Asphalt Technology
NPDES	National Pollutant Discharge Elimination System
NRCS	National Resources Conservation Service
NPS	Nonpoint Source
NCDOT	North Carolina Department of Transportation
POA	Percent Open Area
PTW	Performance Target Window
PAM	Polyacrylamide
PAC	Polyaluminum Chloride
SDS	Safety Data Sheet
SWPPP	Stormwater Pollution Prevention Plan
SCD	Streaming Current Device
SCV	Streaming Current Value
US	United States
USEPA	United States Environmental Protection Agency

CHAPTER ONE: INTRODUCTION

1.1 BACKGROUND

A staggering 54% of the 3.5 million miles of rivers and streams in the United States (U.S.) are listed as impaired (ADEM 2020; NOAA 2022). A majority of these impairments are due to nonpoint source (NPS) pollution, which has continuously been a concern and challenge to monitor and regulate. Sediment discharge from construction sites is one major source of NPS pollution (USEPA 2022a). The Natural Resources Conservation Service estimated that an average of 20-200 tons/ac/yr (45-448 tonne/ha/yr) of sediment is lost at construction sites that use poor erosion and sediment control (E&SC) practices (USEPA 2007a). Erosion control is designed to protect against soil detachment through wind, water, or ice. Sediment control practices are designed to capture the detached sediment particles before they leave the site (USEPA 1992). Discharged sediment has the potential to bind to and carry excess nutrients and other chemicals, which can degrade water quality, increase turbidity, block necessary sunlight for aquatic plants, and cause eutrophication and hypoxia (Xepapadeas, 2011).

1.2 CONSTRUCTION EROSION AND SEDIMENT CONTROL

The U.S. Environmental Protection Agency (USEPA) created the National Pollutant Discharge Elimination System (NPDES) under the Clean Water Act to address point and NPS pollution (ADEM 2021). Under the Construction General Permit (CGP), construction sites that are greater than or equal to 1.0 ac (0.4 ha) of land disturbance threshold must have NPDES permit coverage that implements a Stormwater Pollution Prevention Plan (SWPPP) (ADEM 2021a; USEPA 2022b). A SWPPP outlines site-specific activities to implement and maintain effective E&SC and pollution prevention measures (USEPA 2007b). E&SC practices and products are continuously

evolving as the construction industry seeks efficient and cost-effective ways to meet environmental goals and commitments. Each state has its own installation standards and regulations to meet effluent requirements. There are a variety of products and practices that all strive to limit soil loss until permeant vegetation can be established. Such products and practices typically include various forms of straws or mulches to protect bare soil against splash erosion and aid in vegetation establishment; ditch check installations that work to intercept channelized flow and slow water down, reducing erosive forces; and sediment basins that collect the stormwater from the site, where any remaining sediment in the water can have one last opportunity be captured before the water is discharged off-site. However, research quantifying the performance of all E&SC products and practices is limited.

1.3 DEFINITION AND PURPOSE OF WATTLES

Wattles are one of the most widely used E&SC practices; they are tubular devices with a permeable encasement containing flexible media typically used for impounding or diverting runoff. They can be implemented as ditch checks, inlet protection, sediment barriers, and slope interrupters. Wattles are relatively low in cost, lightweight, easy to install, and available in various materials and dimensions (Donald et al., 2015). They are often filled with biodegradable materials, allowing them to decompose on-site after their useful life. While commonly specified on SWPPPs, there is currently a dearth of knowledge regarding the performance of various wattle materials. This research evaluates how encasement material and POA affect a wattle's hydraulic performance. Improving wattle's hydraulic performance can generate favorable conditions for E&SC measures and minimize material costs by decreasing the quantity of wattles required on site.

1.4 FLOCCULANT DEFINITION AND PURPOSE

Flocculants are a water-soluble chemical additive that bonds particles together through polarity differences, creating larger clumps - known as flocs - that settle out of suspension faster (Hancock, 2017; Kazaz et al., 2022; Pillai, 1997; Vajihinejad et al., 2019). They are used in a variety of water treatment practices as they are used to speed up the settling process of fine particles in water. Unlike coagulants which use a chemical process that neutralizes colloid charge that causes particles to repel each other, flocculants take coagulation a step further by using a physical process that adheres neutral particles together to form larger flocs that can settle out of suspension (Greenwood, 2022; SNF Floeger & de Milieux, 2003; Stechemesser & Dobiáš, 2005). The most popular polymer products among these flocculant types are synthetic flocculants (Dao et al., 2016), apart from the other three categories of inorganic, bio/natural, and stimuli-responsive flocculants (Vajihinejad et al., 2019). Synthetic flocculants are sought after for their water-soluble properties that come as polymeric flocculants that are categorized according to their net electrical charge: anionic, cationic, non-ionic, and amphoteric (Biesinger & Stokes, 1986; Dao et al., 2016; Xiong et al., 2018). Polyacrylamide (PAM) is a common form of commercial flocculant with the largest product volume as it's an extension of acrylamide (AM) which is a cost-effective product for being one of the most reactive monomers and high-water solubility (Dao et al., 2016). PAM is used in a variety of applications. Water and wastewater treatment commonly use PAM as a flocculating agent (Al Momani & Örmeci, 2014; Chang et al., 2008; Kurenkov et al., 2002; Long et al., 2020; Ma et al., 2019; Wong et al., 2006), agriculture soil conditioning and diapers use it for water absorption and retention (Druschel, 2014; Khoo et al., 2019; Xiong et al., 2018; Yu et al., 2021), cosmetics for a thickening agent (Anderson, 2005; Young et al., 2007), and petroleum corporations for enhanced oil recovery to name a few (Li et al., 2017; Maurya & Mandal, 2016; Zolfaghari et al., 2006). PAM flocculant is the most popular flocculant used in E&SC practices as it is highly

water-absorbent and, when it comes in contact with water, forms a soft gel which is used to help capture and remove suspended sediment particles (Rawat et al., 2012). Although flocculants have been found to be highly effective in assisting in removing fine particles suspended in water, their efficacy can be highly influenced by environmental conditions. Thus, even though there is a plethora of research on flocculants, there is still an abundance of questions that remain concerning BMPs on construction sites where environmental factors are difficult to control or predict.

1.5 RESEARCH OBJECTIVES

This research consists of three predominant components associated with the design, improvement, and application requirements of construction stormwater treatment, with specific emphasis on wattles and flocculants. The specific objectives of this research are as follows:

(1) Examine how various wattle encasement material types with low percent open areas or fill densities impact a wattle's impoundment abilities,
(2) Expand on large-scale applicable methods for residual flocculant concentration detection, and
(3) Provide flocculant application placement and reapplication guidance when used on construction sites to achieve optimum dosing and mixing for granular and block form flocculants.

To achieve these objectives, the following tasks were performed:

(1) Develop small-scale wattle prototype evaluation methods using a hydraulic flume for evaluating innovative product designs,
(2) Quantify various wattle encasement's percent open area and evaluate each encasement fabrics impoundment abilities, with and without wattle fill material,

(3) Assess increased fill densities with a large percent open area encasement to compare impoundment performance changes by encasement percent open area, fabric type, and increased fill density,

(4) Expand on existing flocculant detection methods for measuring residual concentration to assess their applicability to large-scale applications,

(5) Perform large-scale application testing using granular and block form flocculants for optimum dosage delivery and application evaluations, and

(6) Analyze collected data from flocculant detection methods and large-scale application testing to provide guidance for proper implementation.

1.6 EXPECTED OUTCOMES

The outcomes of this study will focus on how improving wattle's hydraulic performance can generate favorable conditions for E&SC measures and minimize material costs by decreasing the quantity of wattles required on site. Flocculant large-scale test evaluations provide insight on possible detection methods for quantifying flocculant concentrations in the field, the rate at which flocculant is being dosed in a channel during flow, when reapplication should be performed, guidance on the number of flocculant blocks that should be placed in a channel at a time, and placement of flocculant in a channel to achieve proper dosing and observed floc size during channel flow. The results from this study will provide designers and practitioners with the knowledge, resources, and educational outreach opportunities required to effectively select wattle materials to achieve maximum impoundment and effectively use flocculants without causing environmental harm. Future research should expand from this resreach to increase knowledge in construction erosion and sediment control practices using wattles and flocculants.

1.7 ORGANIZATION OF THESIS

This thesis is divided into four chapters outline different E&SC products outlined in the research objectives. Following this chapter, Chapter Two: *Wattles* provides an overview of current application and research performed on wattles. Subsequent sections withing this chapter outline the methodologies and results for *product evaluations*, *percent open area*, *encasement*, and *density* tests conducted on wattles. Chapter Three: *Flocculants* provides an overview of current uses of flocculants and implementation concerns on construction sites. Subsequent sections within this chapter outline the methodologies and results for *flocculant detection methods* and *large-scale application* testing. Chapter Four: *Conclusions* presents a summary of the accomplished research objectives while providing insight for future research directions to expand upon.

CHAPTER TWO: WATTLE PERFORMANCE EVALUATION

2.1 BACKGROUND

Kaufman (2000) and Chapman et al. (2014) first expressed the need for credible, scientific results for designing and implementing E&SC plans. Since then, recent research efforts for large-scale testing have focused on design enhancements, installation techniques, implementation strategies, and evaluation techniques.

In a controlled environment at the Auburn University - Stormwater Research Facility (AU-SRF), Donald et al. (2013) and Perez et al. (2015) evaluated wattle installation methods. They found that providing an underlay, along with teepee staking and sod staples, helped maintain contact between the wattle and channel bottom, improved the installation's structural integrity. Donald et al. (2013) reported a 95% difference in the length of subcritical flow impounded by the wattle when compared to an installation with teepee staking and without underlay or staples. Bhattarai et al. (2016) noticed similar undercutting and scour results when an underlay was not installed, and they also suggested installing an underlay. Schussler et al. (2021) implemented the findings of the AU-SRF studies at an active highway construction site in central Iowa. By changing the installation method from driving wooden stakes through the wattle center to a teepee staking pattern with sod staples and an erosion control blanket underlay, ditch check wattle installations increased sediment retention by 1,158% (Schussler et al., 2021).

Donald et al. (2015) examined the impact of wattle fill density, dimensions, and fill material on hydraulic performance. Flow rates of 0.570, 1.13, and 1.70 ft^3/s (0.0161, 0.0320, and 0.0481 m^3/s) were applied to Excelsior fiber, wheat straw, and synthetic fiber wattles with average densities of 2.25, 53.5, and 1.35 $lbs./ft^3$ (36.0, 53.5, and 21.6 kg/m^3), respectively. Despite being 147% less dense than the average wheat straw wattle density, synthetic fiber wattles produced

impoundments that were 23, 31, and 32% deeper than wheat straw wattles and 153, 112, and 87% greater than excelsior wattles at low, medium, and high flow rates, respectively.

Wattles operate by impounding water and reducing runoff velocity, thereby preventing erosion and promoting sedimentation (ASTM International D7208-14e1, 2018; Donald et al., 2013, 2016; Perez et al., 2015; Schussler et al., 2021; USEPA 2007a, USEPA 2007b; Whitman et al., 2021a; Xepapadeas, 2011). Donald et al. provided an example of a study that looked into the hydraulic performance of wattles as a performance indicator (Donald et al., 2013). In a following investigation, Donald et al. (2016) matched the dimensionless Froude number (Fr) to the ratio of depth to specific energy (y/E) to determine the ratio of potential to total energy in the runoff. When Fr is plotted against y/E, the connection provides manufacturers and practitioners with normalized minimum performance criteria (Donald et al., 2016). This connection produces an inflection point that reveals when flow parameters create favorable conditions for velocity reduction.

In the Larry Buss Hydrology Laboratory at Iowa State University, Whitman et al. (2021a) compared the hydraulic performance of different wattle fill materials using a 4.00 ft (1.22 m) wide flume. Experiments were carried out using wattles stuffed with excelsior wood fiber, wheat straw, coconut coir, synthetic fiber, wood chips, and miscanthus fiber. Wattles' impounding capacities were examined at flow rates of 0.25, 0.75, 1.25, and 2.00 ft^3/s (0.01, 0.02, 0.04, and 0.06 m^3/s) with longitudinal channel slopes of 3.50, 4.25, and 5.00%. To evaluate hydraulic efficiency, Whitman et al. (2021a) devised a method that uses the ratio of impoundment length to depth to determine subcritical flow conditions. Maximum impoundment depth (H_2) was measured, and the theoretical impoundment depth (H_1) was computed using the wattle installation height, as illustrated in Figure 2-1. Standing pool impoundment length (L_1) is estimated from the channel

slope and displayed in Figure 2-1; the impoundment length (L_2) is determined by comparing these two values. The distance from the channel bottom to the wattle crest (wattle installation height) is the theoretical impoundment depth (H_1), whereas the theoretical standing pool impoundment length (L_1) is the calculated subcritical pooled length from the wattle crest to the upstream channel bottom perpendicular to the wattle crest height. As illustrated in Figure 2-1, measured data for the water depth (H_2) from the channel base to the water surface and subcritical impoundment length (L_2) to the position of the hydraulic jump were acquired from the wattle face upstream of the wattle.

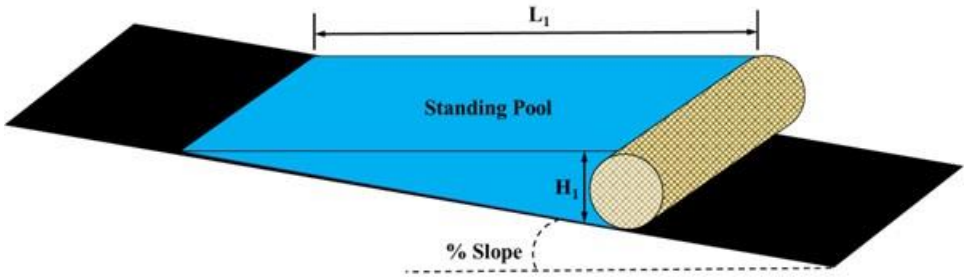

(a) theoretical impoundment depth and length

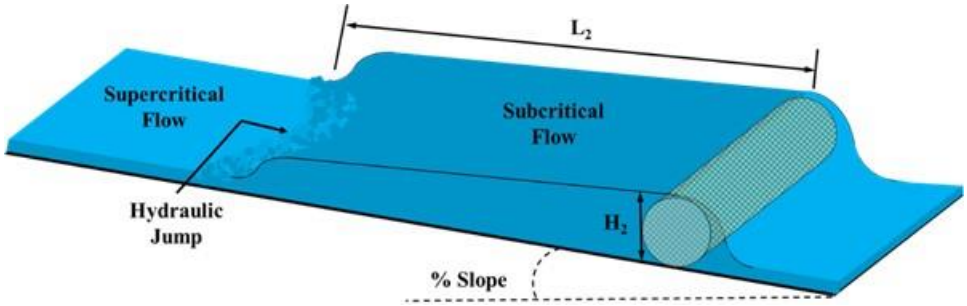

(b) measured impoundment depth and length

Figure 2-1. Wattle Flow Characteristics

Using depth and length ratios, the data were normalized and compared. Whitman et al. (2021a) explained that the ratio calculations expressed by Equations (2-1) and (2-2) represent the proportion of the theoretical design parameters obtained during testing.

$$Impoundment\ Depth\ Ratio = \frac{H_2}{H_1} \times 100\% \quad (2\text{-}1)$$

$$Impoundment\ Length\ Ratio = \frac{L_2}{L_1} \times 100\% \quad (2\text{-}2)$$

Where H_1 = theoretical impoundment depth (ft or m); H_2 = measured maximum impoundment depth (ft or m); L_1 = theoretical standing pool impoundment length (ft or m); and L_2 = measured subcritical flow length (ft or m). Whitman et al. (2021a) determined that synthetic fiber and miscanthus-filled wattles generate optimal hydraulic conditions throughout a broad range of flow rates and slopes. Whitman et al. (2021a) defined favorable conditions as obtaining an average impoundment length ratio greater than 80% and an impoundment depth ratio greater than 100%. Coconut coir and wood chips yielded favorable outcomes on average, although their performance varied across flow rates and slopes. Wattles filled with excelsior fibers and wheat straw were less consistent in their ability to provide suitable conditions over a range of slopes and flow rates, indicating that the wattle fill material should be considered when defining site-specific wattle impoundment objectives.

The most effective circumstances for a wattle are those that allow water to impound and overtop, rather than trying to filter sediment through the media, according to studies that analyzed fill material, density, installation, and performance evaluation methodology. This thesis details evaluation techniques used for innovative wattle designs, assessing the impacts of a fabric POA, and how various fabrics with ranging POAs can influence a wattle's impoundment abilities.

2.2 PRODUCT EVALUATIONS

With a constant drive to improve existing E&SC products, innovative encasement and fill materials arise and seek to be compared to existing products used in industry. This section focuses on the testing methodology used to evaluate wattle product prototypes that can help guide product designers make informed decisions on developing competitive products.

2.2.1 PRODUCT TESTING APPARATUS

The apparatus used in this testing was a 15.0 ft (4.57 m) long fiberglass hydraulic flume with a 1.00 ft (0.305 m) width and 1.50 ft (0.457 m) deep rectangular open channel (Figure 2-2) located in Auburn University's Harbert Engineering Center Hydrology Lab. Acrylic walls allow for profile measurements across the length of the flume. An actuated tilting mechanism can adjust the flume slope between -5% and 15%. An adjustable tailgate allows for variable flow depths to be achieved. Flow is introduced into the flume from an approximate 209.2-gal (792 L) supply sump located underneath the channel. Two Baldor industrial motor pumps with a 0.74 hp (0.56 kW) motor are capable of producing a peak flow capability of roughly 0.06 ft^3/s (0.002 m^3/s). Flow rates were measured using a piezometer for each pump that has an accuracy of ±0.5%.

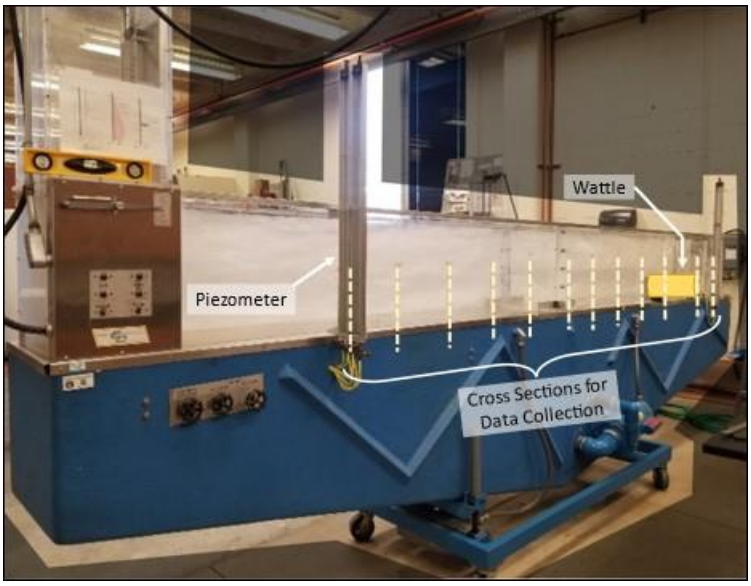

Figure 2-2. Testing apparatus: Auburn University Flume

Wattle samples were installed at the downstream end of the flume using eyehooks anchors and jute twine to simulate intimate contact with the channel surface (Figure 2-3). Three samples were tested for each of the evaluated wattles. One impervious barrier (control) constructed of plywood was used and tested two times to verify consistency in results. Each wattle was weighed and measured before installation to document product fill density.

Figure 2-3. Tie-down method used for all tests.

2.2.2 PRODUCT TESTING METHODOLOGY

The evaluation of wattles in this study involved two different slope conditions, 7% and 10%. A flow rate of 0.08 ft^3/s (0.002 m^3/s) was used for the 7% and 10% slopes, respectively. These slopes were selected due to the wattle installment heights and flume channel length. Any slope less than 7% would have resulted in the full impoundment length being lost if water overtopped the evaluated product. However, if a longer flume were used, the slope could be decreased to lower values if desired. The flow rates were determined using a piezometer that was built into the flume. To measure water depth, a total of 12 cross-sections were taken, spaced 1.00 ft (0.305 m) apart along the flume profile, as shown in Figure 2-2. The installed height was measured upon installation of the wattles, and impoundment depth was measured at the wattle face when steady-state flow conditions were achieved. These measurements were used to calculate the depth ratio of the product. Additionally, the impoundment length was measured from the centerline of the installed wattle to the location of the hydraulic jump within the flume. The ratio between the measured impoundment length and the theoretical impoundment length for a standing pool was computed to obtain the length ratio. These measurements mimicked the testing methodology used by Whitman et al. (2021a).

2.2.3 WATTLE PRODUCT COMPARISON AND PACKING

Depending on the diameter of the product prototype and discussions with the product designer, manufactured wattles with similar characteristics are recommended to be selected to compare results to inform the designer of how their product differs from what is already on the market. For this study, straw wattles were selected to compare the performance of the prototype. The straw wattles were sourced from two different manufacturers to account for variability between manufacturers. The two different straw wattles and wattle prototype were individually weighed

to determine their respective densities. Each straw wattle and prototype were then shortened to 1.00 ft (0.305 m) to fit in the hydraulic flume, while maintaining the original wattle density. Figure 2-4 shows the shortened wattle lengths of the various products evaluated.

(a) Straw 1 (b) Straw 2 (c) Product X

Figure 2-4. Wattle test samples

2.2.4 PRODUCT RESULTS AND DISCUSSION

Product X, Straw 1, and Straw 2 had a dry density of 4.36, 3.79, and 3.39 lb/ft^3 (69.9, 60.7, and 54.4 m^3/s), respectively. After testing, wattles were allowed to drain excess water prior to being weighed for saturated density. Product X, Straw 1, and Straw 2 wattles had a saturated density of 12.3, 12.3, and 9.52 lb/ft^3 (197, 197, and 152 kg/m^3), respectively. Absorption was calculated to be 283% for Product X, 325% for Straw 1, and 281% for Straw 2. Providing water absorption data to the product designer may be useful information to understand the various properties of the materials used in their prototype. Density and absorption data is summarized in Table 2-1.

Table 2-1: Averaged Density and Absorption Data

Wattle Evaluated	Measured diameter, ft (m)	Installed height, ft (m)	Weight, lbs/ft (kg/m)	Dry density, lbs/ft^3 (kg/m^3)	Saturated Weight, lb (kg)	Saturated Density, lb/ft^3 (kg/m^3)	Water Absorption, %
Product X	0.75 (0.23)	0.58 (0.18)	1.92 (2.86)	4.36 (69.86)	5.44 (2.47)	12.34 (197.59)	283%
Straw 1	0.77 (0.23)	0.62 (0.19)	1.76 (2.62)	3.79 (60.73)	5.72 (2.60)	12.31 (197.19)	325%
Straw 2	0.78 (0.24)	0.61 (0.19)	1.63 (2.43)	3.39 (54.38)	4.58 (2.08)	9.52 (152.56)	281%

Table 2-2 summarizes impoundment length and depth data collected during testing.

Table 2-2. Average Impoundment Length and Depth Results for each Product Evaluated

	7% Slope 0.08 ft^3/s (0.002 m^3/s)		10% Slope 0.08 ft^3/s (0.002 m^3/s)	
Wattle Evaluated	**Impoundment Length Ratio**	**Impoundment Depth Ratio**	**Impoundment Length Ratio**	**Impoundment Depth Ratio**
Control	116%	116%	95%	115%
Straw 1	105%	105%	79%	103%
Straw 2	103%	103%	78%	102%
Product X	111%	111%	83%	108%

Using the impoundment length and depth ratio plots developed by Whitman et al. (2021b)2021b), the performance target window (PTW) can be easily located in the upper right-hand corner of the plots listed in Figure 2-5. The PTW represents the ideal impoundment condition zone where water is overtopping the wattle with at least 80% of the theoretical standing pool impoundment length achieved. The impoundment length ratio minimum is set at 80% rather than 100% because the length is measured back to the center of the hydraulic jump, which inherently decreases the length measurement. Each data point in the plots in Figure 2-5 represents one wattle run at one flow rate and one slope.

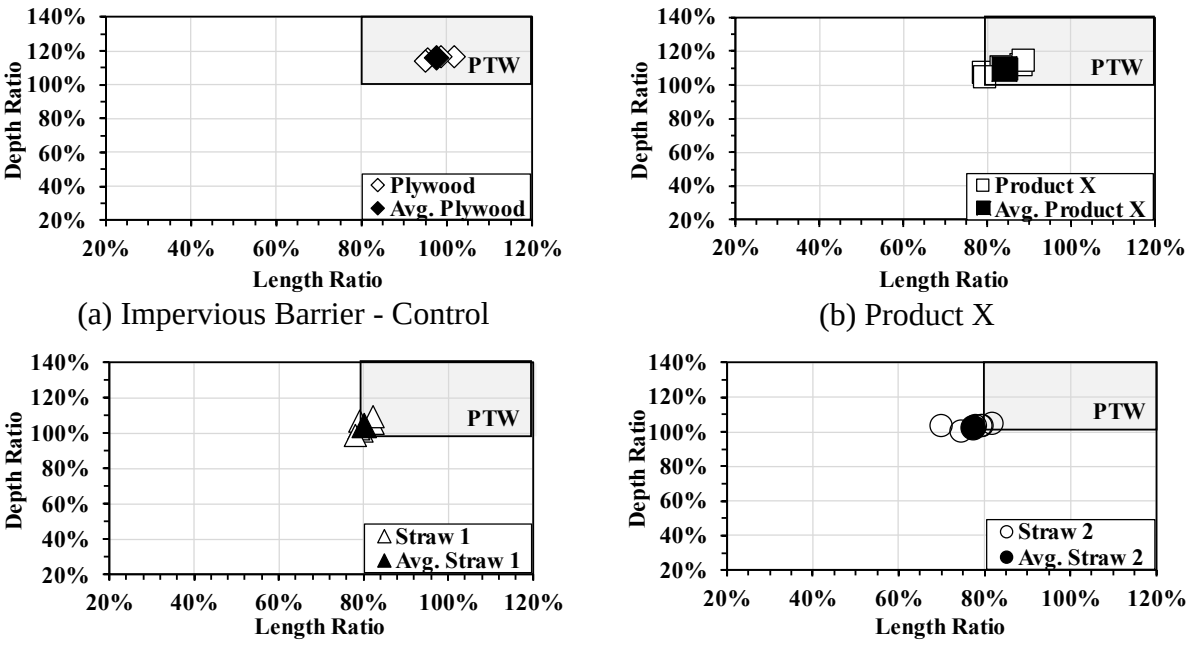

(a) Impervious Barrier - Control (b) Product X

(c) Straw 1 (d) Straw 2

Figure 2-5. Product Impoundment Depth and Length Ratio Plots

The products evaluated in this small-scale study performed exceptionally well across the board, seeing that the average all products evaluated were either within or along the border of the PTW. Figure 2-6 displays the visual differences in impoundment lengths and depths across each product evaluated for a 7% slope.

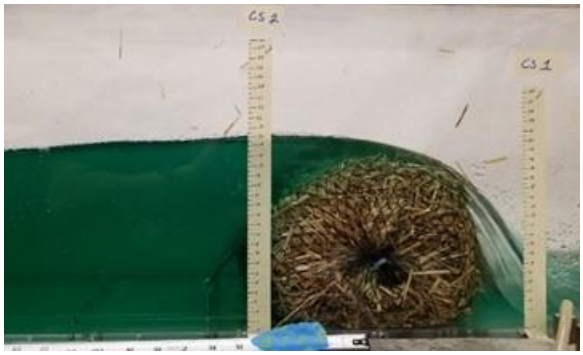

(a) Straw 1 impoundment depth

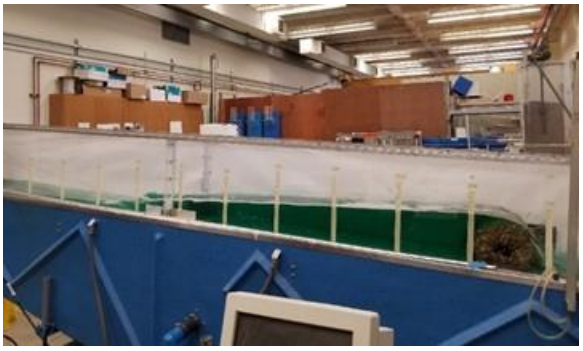

(b) Straw 1 impoundment length

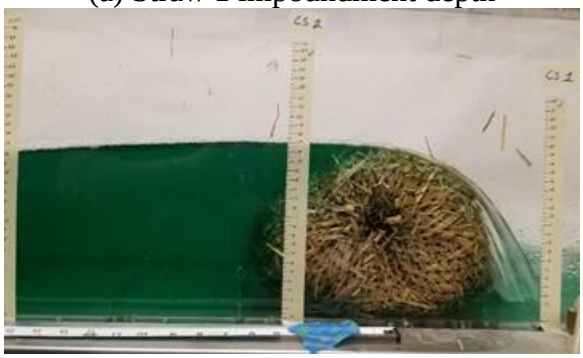

(c) Straw 2 impoundment depth

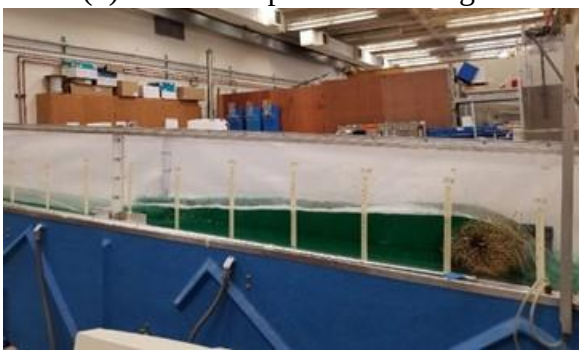

(d) Straw 2 impoundment length

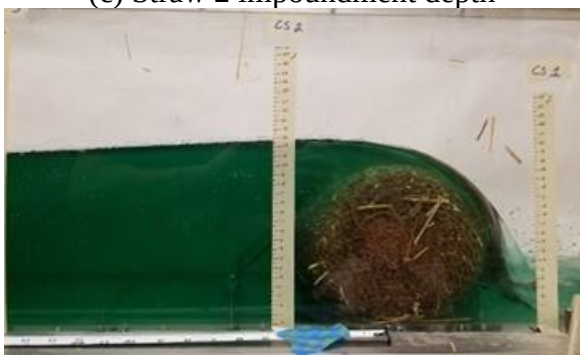

(e) Product X impoundment depth

(f) Product X impoundment length

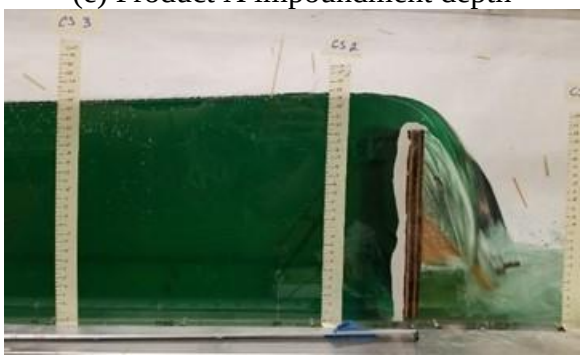

(g) Impervious Barrier impoundment depth

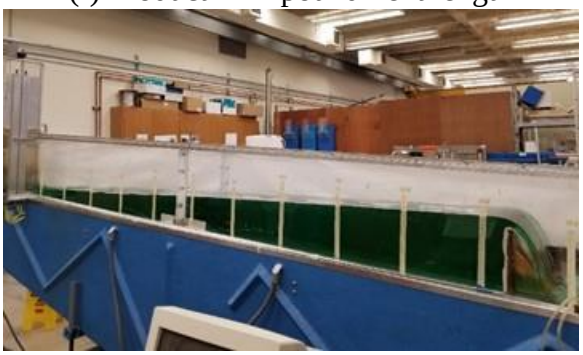

(h) Impervious Barrier impoundment length

Figure 2-6. 7% Slope and 0.08 ft^3/s (0.002 m^3/s) Flow Rate Impoundment Lengths and Depths for The Evaluated Products

Figure 2-7 displays the visual differences in impoundment lengths and depths across each product evaluated for a 10% slope.

(a) Straw 1 impoundment depth

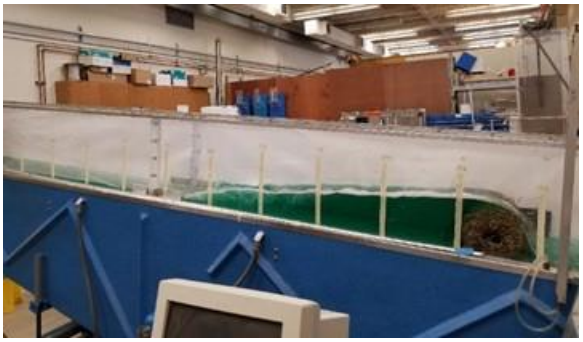

(b) Straw 1 impoundment length

(c) Straw 2 impoundment depth

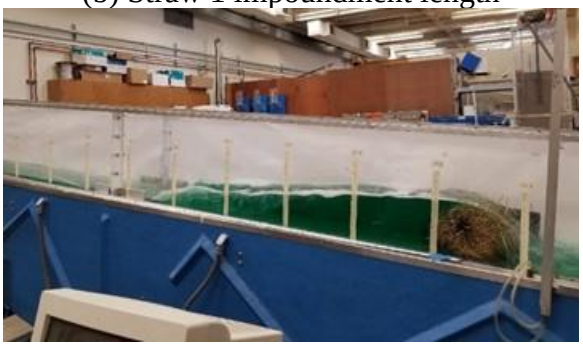

(d) Straw 2 impoundment length

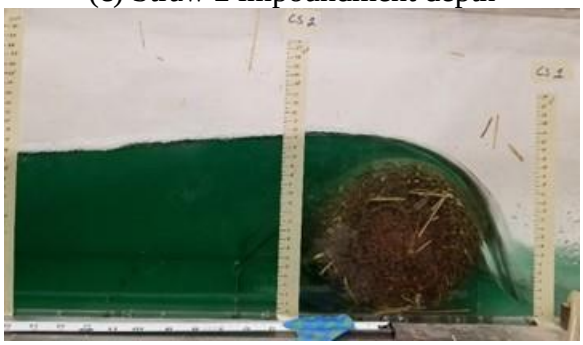

(e) Product X impoundment depth

(f) Product X impoundment length

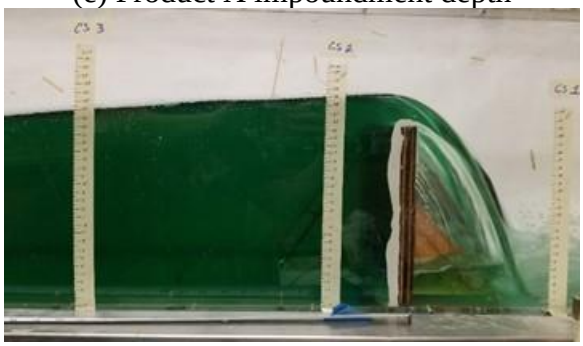

(g) Impervious Barrier impoundment depth

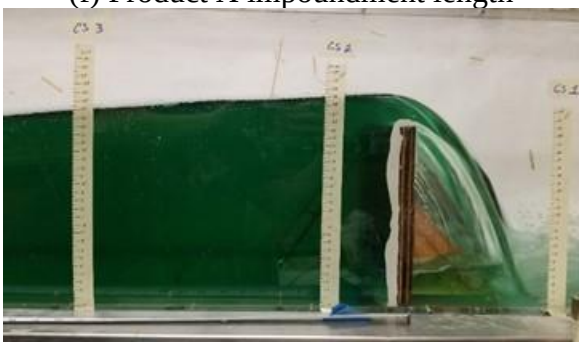

(h) Impervious Barrier impoundment length

Figure 2-7. 10% Slope and 1.07 ft^3/s (37.8 m^3/s) Flow Rate Impoundment Lengths and Depths for The Evaluated Products

2.3 PERCENT OPEN AREA

The POA and apparent opening size (AOS) of any E&SC application have received very little consideration as a potential factor influencing hydraulic performance. POA is the percentage of void space on the surface of a material (Christopher & Fischer, 1992). The AOS is the largest particle that can pass through a certain geotextile (ASTM International D4751-21a, 2021). Clogging is a common problem that arises when using geotextiles in E&SC applications. Calhoun (1972) established that geotextiles containing less than 4% POA are susceptible to clogging. Based on visual observations, Whitman et al. (2019) concluded that smaller AOS led to clogging, which decreased effluent flow-through rates and increased the hydrostatic strain exerted on E&SC products while evaluating manufactured sediment barriers for their durability and capability to retain sediment. Additional studies on AOS and POS as filters for geotextiles used in geotechnical and environmental engineering have been conducted (Liao & Bhatia, 2005; Narejo, 2003; Tolikonda & Quaranta, 2012), while others have evaluated software for precisely measuring (Aydilek & Edil, 2004) and predicting POA change when subjected to tensile strains (Tang et al., 2013).

Evaluating various fabric materials with various weaving patterns and POAs was done by subjecting each encasement through the same testing methodology used when evaluating a wattle. Evaluating each encasement by its impoundment abilities, independent of any fill material was conducted using a hydraulic flume. This section's results would guide ideal encasements to select for wattle testing applications.

Fabric samples were assessed in the flume, located in Auburn University's Harbert Engineering Center Hydrology Lab, with a constant flow and slope, and varied in weaving patterns, weaving tightness, and materials. The fabric with the greatest impoundment depth was evaluated with additional layers. Top-performing fabrics were modified and retested using the

same testing criteria. The highest-performing modified fabric was double- and triple-layered. Twenty fabric tests with three replicable test series were executed. Each series of tests were performed by maintaining a consistent flow rate across a fixed channel slope and inserting the fabric into a custom-made frame anchored inside the flume.

2.3.1 CHANNELIZED FLOW FABRIC TEST REGIME

Fabric evaluations were conducted by maintaining a constant flow of 0.04 ft^3/s (0.001 m^3/s) at a 5% slope. Measurements were taken five minutes after each fabric installation or until the flow reached equilibrium (i.e., sustained subcritical flow length measured from the fabric to the hydraulic jump) within the flume. This evaluation process involved measuring the upstream subcritical flow length and depth at the fabric face. Measurements were collected at twelve established cross-sectional locations that were spaced 1.00 ft (0.305 m) apart. Cross-sections were used to obtain water depth measurements from channel bottom to water surface elevation. Rulers were attached to the acrylic sidewalls at each cross-section location to visually obtain water depth readings throughout each experiment.

2.3.2 EVALUATED FABRICS

Fabrics were stapled to a 12.0 in. (30.5 cm) square wooden frame built from 0.50 in. (1.3 cm) square lumber. Fabric samples were installed at the downstream end of the flume using an aluminum frame cage, Figure 2-8(a), that was sealed in place with plumber's putty. A hardware cloth with 0.50 in. (1.3 cm) square openings was attached to the aluminum frame. The developed system prevented fabric samples from stretching due to the force of the flow simulating how the fabric would perform if filled with a media. Figure 2-8(b) shows the fabrics' appearance when installed in the flume.

(a) aluminum frame holding cage (b) holding cage with fabric installed

Figure 2-8. Fabric Installation Testing Method

Polypropylene, cotton, bamboo-cotton mix, and polyester-propylene mix encasements were investigated. Using ImageJ software (Rasband, n.d.), each fabric's POA was determined to range between 2.5% to 50.6%. Creating a scanned colorless image and changing the black and white color threshold revealed each fabric's POA. The software was used to compute POA by taking the area of each open space (black) and dividing it by the section's overall cross-sectional area. Samples portrayed in Figure 2-9 are representative of 0.787 $in.^2$ (2.00 cm^2) of each fabric.

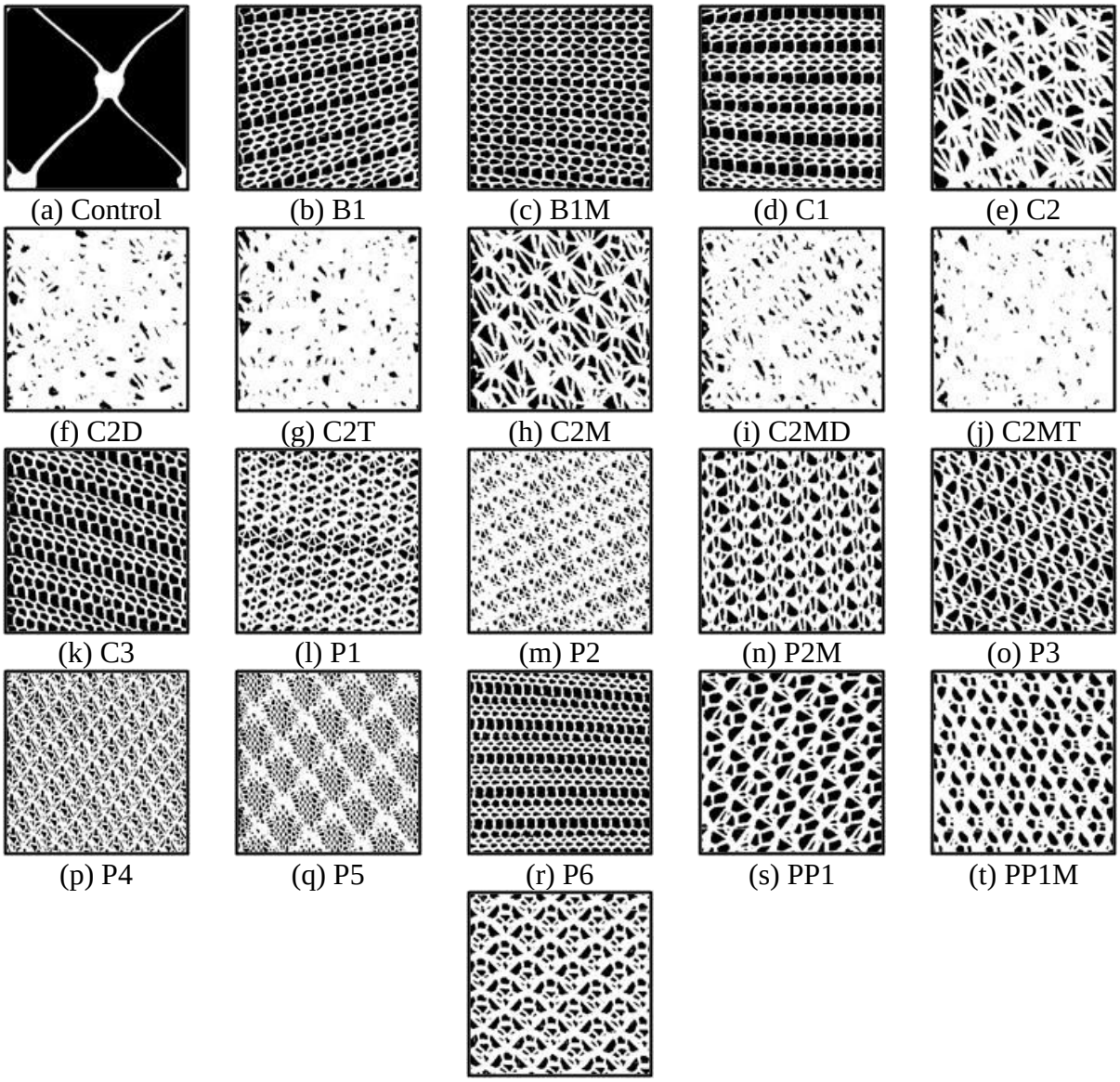

Figure 2-9. Fabric Netting Styles Outlined by the POA

Table 2-3 provides an overview of each fabric's identification code used throughout this study.

Table 2-3. Fabric Identification Codes

Encasement material	Layers	Identification
Bamboo Cotton Mix #1	Single	B1
Bamboo Cotton Mix #1 tighter weave	Single	B1M
Control – standard heavy-duty synthetic plastic net	Single	Control
Cotton #1	Single	C1
Cotton #2	Single	C2
Cotton #2	Double	C2D
Cotton #2	Triple	C2T
Cotton #2 tighter weave	Single	C2M
Cotton #2 tighter weave	Double	C2MD
Cotton #2 tighter weave	Triple	C2MT
Cotton #3	Single	C3
Polyester Polypropylene Mix #1	Single	P1
Polyester Polypropylene Mix #2	Single	P2
Polyester Polypropylene Mix #2 tighter weave	Single	P2M
Polyester Polypropylene Mix #3	Single	P3
Polyester Polypropylene Mix #4	Single	P4
Polyester Polypropylene Mix #5	Single	P5
Polyester Polypropylene Mix #6	Single	P6
Polypropylene #1	Single	PP1
Polypropylene #1 tighter weave	Single	PP1M
Polypropylene #2	Single	PP2

2.3.3 FABRIC EVALUATION CRITERIA

Each fabric was compared independently to assess impoundment depth and subcritical flow length. The impoundment depth was measured at the fabric's face. Measuring the distance from the fabric face to the hydraulic jump under stabilized flow conditions determined the subcritical length. High-performing fabrics maximized subcritical flow length.

A multiple linear regression (MLR) was used to analyze the impact of POA on impoundment depth and length for 20 textiles. A regression equation shows the extent the independent variable (i.e., POA) affects the dependent variables (i.e., impoundment depth and length) and the significance of that effect. Model findings show the link between POA and impoundment depth and length. The MLR regression model equation is shown in Equation (5)

$$f(x) = \beta_0 + \beta_1 x_1 + \beta_2 x_2 \quad (2\text{-}3)$$

where $f(x)$ = dependent variable (i.e., POA); β_0 = intercept coefficient; β_i = least squares coefficients; x_i = independent variable (i.e., impoundment length/depth).

2.3.4 FABRIC RESULTS AND DISCUSSION

Twenty fabrics were analyzed, where each installation was subjected to one flow and slope. Each installation was replicated three times. The fabric was removed between replications to allow supercritical flow to resume before the next installation. This phase of the study identified the fabric with the greatest impoundment capabilities, independent of fill. The study examined each fabric with the greatest impoundment ability as a wattle with excelsior fiber fill.

2.3.4.1 FABRIC ANALYSIS

Fabric length and depth impoundment values, in Table 2-4, were averaged so that one data point represents each fabric and plotted, Figure 2-10.

Table 2-4. Fabric Properties and Identification Code

Encasement material	Average Impoundment Length, in. (cm)	Average Impoundment Depth, in. (cm)	POA, %
Control	0.00 (0.00)	0.00 (0.00)	92.03%
B1	46.8 (119)	4.33 (11.0)	46.01%
B1M	27.7 (70.3)	3.67 (9.31)	50.64%
C1	44.3 (113)	4.17 (10.6)	43.08%
C2	56.7 (144)	4.75 (12.1)	28.08%
C2D	90.6 (230)	6.22 (15.79)	6.27%
C2T	118.3 (300)	7.33 (18.6)	6.32%
C2M	82.0 (208)	5.92 (15.0)	29.04%
C2MD	119.3 (303)	7.33 (18.6)	2.98%
C2MT	139.3 (353)	8.42 (21.4)	2.45%
C3	24.7 (62.7)	3.38 (8.59)	49.07%
P1	27.8 (70.7)	3.50 (8.89)	39.75%
P2	38.3 (97.2)	4.00 (10.2)	33.35%
P2M	30.5 (77.5)	4.00 (10.2)	37.24%
P3	24.8 (63.1)	3.42 (8.68)	38.56%
P4	27.2 (69.0)	3.45 (8.76)	29.14%
P5	30.1 (76.4)	3.67 (9.31)	29.48%
P6	15.0 (38.1)	2.97 (7.54)	47.30%
PP1	21.9 (55.7)	3.30 (8.38)	39.85%
PP1M	26.7 (67.7)	3.67 (9.31)	37.73%
PP2	25.9 (65.8)	3.33 (8.47)	29.05%

When compared to the control that had no impoundment length or depth, cotton fabrics (i.e., C2 and C2M) had the highest impoundments, starting with impoundment length and depth at 56.7 and 4.75 in. (144 and 12.2 cm), respectively, and were double- and triple-layered, which drastically increased their impoundment length and depth up to 139 and 8.42 in. (353 and 21.4 cm), respectively.

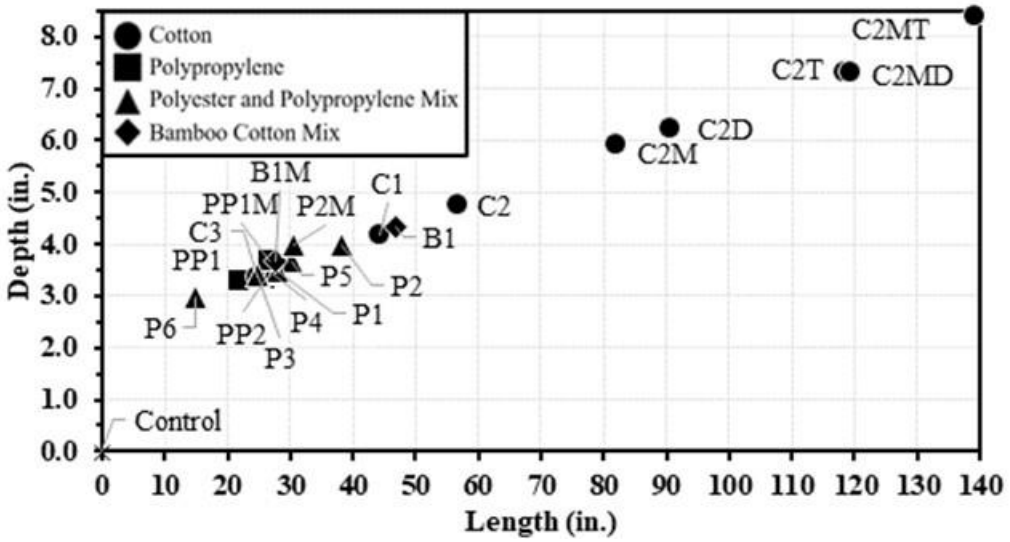

Figure 2-10. Fabric Impoundment Length and Depths (*Note: 1.00 in. = 2.54 cm*)

Figure 2-11 ranks the fabric's POA values in Table 2-4 from smallest to largest.

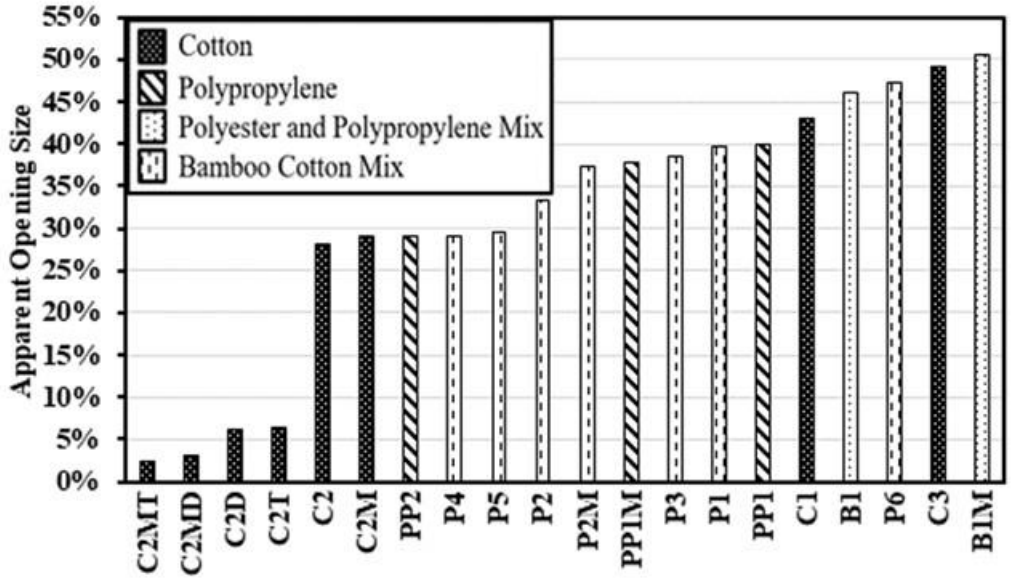

Figure 2-11. Fabric POA

Figure 2-12 displays a comparison of impoundment depths for each evaluated fabric subjected to a 0.04 ft^3/s (0.001 m^3/s) flow rate at a 5% longitudinal slope. POA was measured for each fabric and plotted to identify patterns in the fabric types.

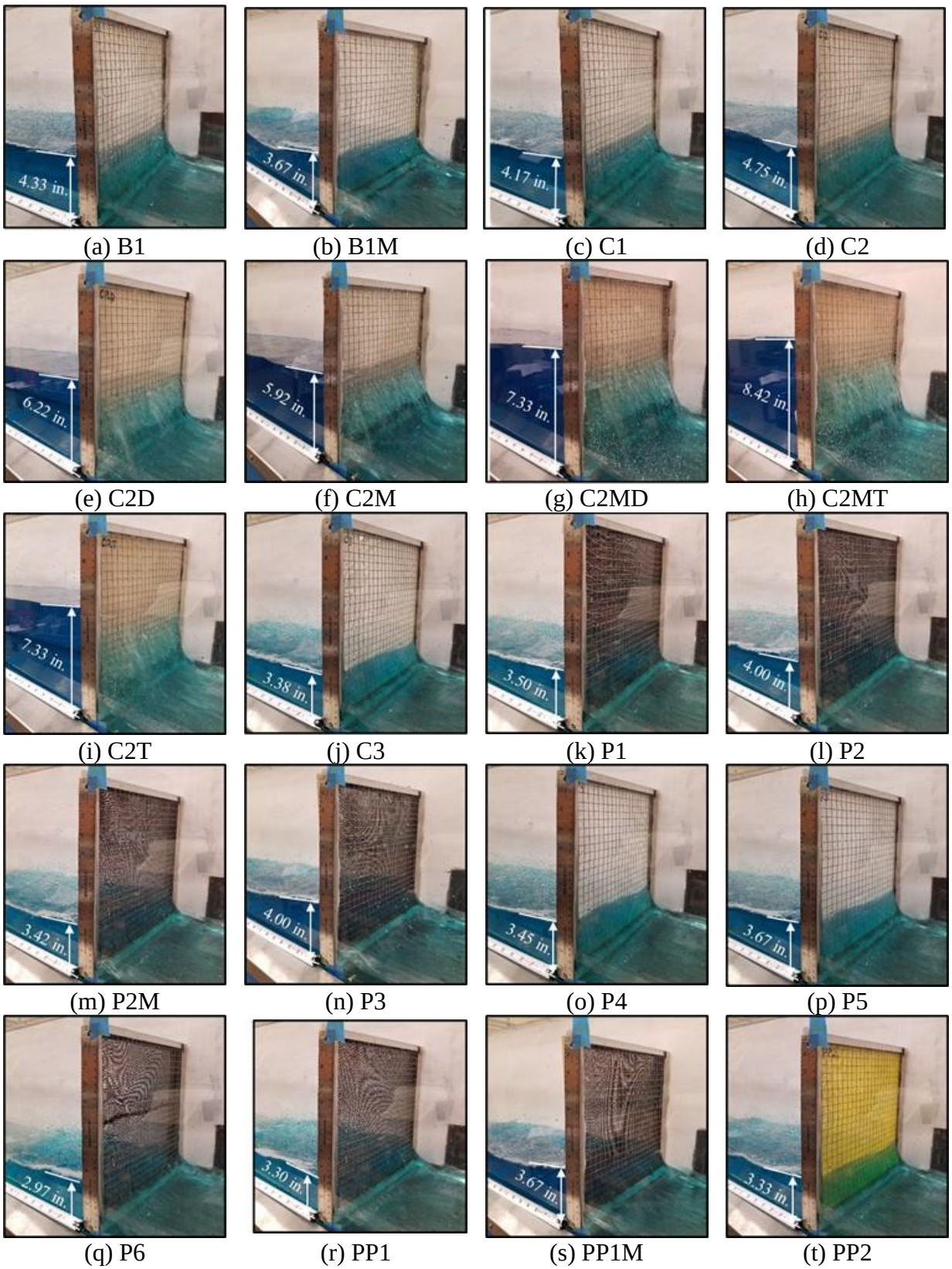

(a) B1 (b) B1M (c) C1 (d) C2

(e) C2D (f) C2M (g) C2MD (h) C2MT

(i) C2T (j) C3 (k) P1 (l) P2

(m) P2M (n) P3 (o) P4 (p) P5

(q) P6 (r) PP1 (s) PP1M (t) PP2

Figure 2-12. Fabric Impoundment Results, 0.04 ft^3/s (0.001 m^3/s), 5% Slope (*Note: 1.00 in. = 2.54 cm*)

Figure 2-13(a) and Figure 2-13(b) illustrate the POA and average impoundment length and depth, respectively. Two clusters of data points in both Figure 2-13(a) and Figure 2-13(b) group single- and multi-layered fabrics. These multi-layered fabrics enabled smaller POAs to be obtained as it was difficult to achieve tighter weaves Figure 2-13(a) and Figure 2-13(b) show that as POA increases the impoundment length and depth decrease.

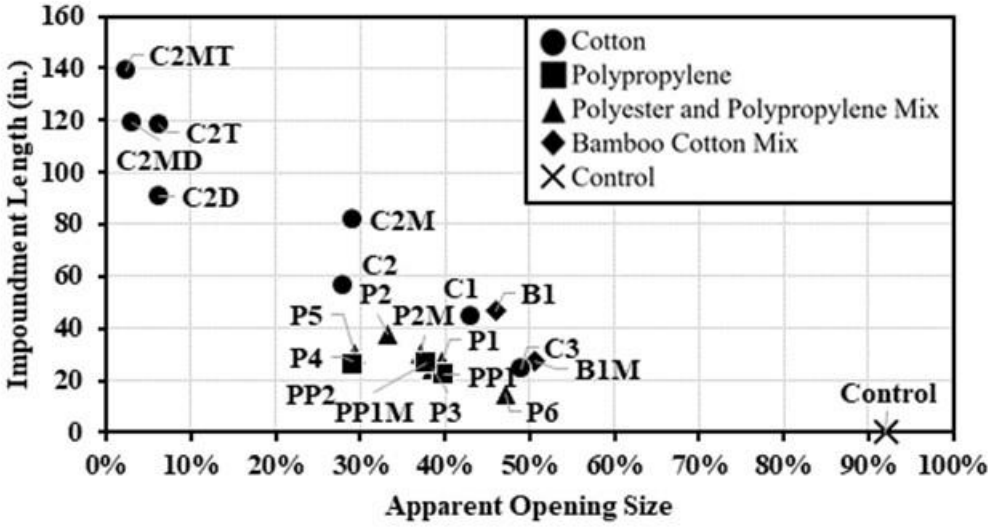

(a) impoundment length

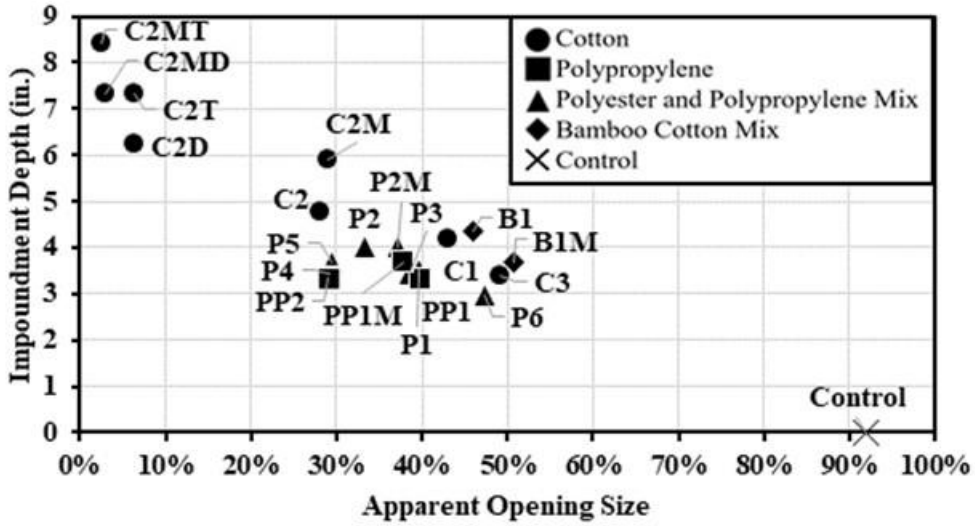

(b) impoundment depth

Figure 2-13. Fabric POA vs. Impoundment Performance (*Note: 1.00 in. = 2.54 cm*)

2.3.4.2 FABRIC STATISTICAL ANALYSIS

Relationships between fabric POA and impoundment length and depth were measured using a multiple linear regression (MLR). This regression estimated using results from 60 experiments (i.e., three iterations for each of the twenty fabrics). Fabrics were characterized by POA, and impoundment length and depth were measured for each experimental iteration. Results shown in Table 2-5 indicate that changing the POA had no significant effect on the impoundment length; however, as the POA increases, the impoundment depth significantly decreases. The dependent variables for this analysis were the impoundment length and impoundment depth, while the independent variable was the POA for each of the 21 evaluated fabrics.

Table 2-5. Fabric POA with Impoundment Length and Depth Linear Regression Analysis

Variables	Statistical Significance	
	Coefficients	*p*-value[s]
Intercept	0.894	<0.001
Impoundment Length	0.003	0.063
Impoundment Depth	-0.166	<0.001

Note: N/A = not applicable.
[a]Comparison to effects of base at 95% confidence interval and *p*-value <0.05.

Additionally, two series of unrelated means tests were conducted to determine if (a) the mean impoundment *length* was statistically different between every pair of fabrics and (b) the mean impoundment *depth* was statistically different between every pair of fabrics. The null hypothesis for each test was that fabric 1's impoundment length or depth would not be statistically different from fabric 2's impoundment length or depth. The alternative hypothesis for each test was that the impoundment length or depth between fabric 1 and fabric 2 statistically differed.

Figure 2-14(a) and Figure 2-14(b) display the *p*-values between each fabric comparison with respect to their impoundment length and depth means, respectively. The green cells identify pairs of fabrics with statistically different impoundment lengths or depths at a 95% confidence

level or greater. The red cells identify pairs of fabrics where the impoundment lengths or depths are not statistically different, at a 95% confidence level.

The results in Figure 2-14(a) and Figure 2-14(b) highlight that five pairs of fabrics with statistically different impoundment lengths, and 12 pairs of fabrics with statistically different impoundment depths, respectively. These results statistically show that cotton fabrics with larger POA performed equally regarding impoundment length and depth to synthetic materials (i.e., polypropylene and polyester-polypropylene mix).

	p-value[a]																		
Variable	B1	B1M	C1	C2	C2D	C2M	C2MD	C2MT	C2T	C3	P1	P2	P2M	P3	P4	P5	P6	PP1	PP1M	PP2
B1	-	<0.001	<0.001	<0.001	<0.001	<0.001	<0.001	<0.001	<0.001	<0.001	<0.001	<0.001	<0.001	<0.001	<0.001	<0.001	<0.001	<0.001	<0.001	<0.001
B1M		-	<0.001	<0.001	<0.001	<0.001	<0.001	<0.001	<0.001	<0.001	0.352	<0.001	<0.001	<0.001	<0.001	<0.001	<0.001	<0.001	<0.001	<0.001
C1			-	<0.001	<0.001	<0.001	<0.001	<0.001	<0.001	<0.001	<0.001	<0.001	<0.001	<0.001	<0.001	<0.001	<0.001	<0.001	<0.001	<0.001
C2				-	<0.001	<0.001	<0.001	<0.001	<0.001	<0.001	<0.001	<0.001	<0.001	<0.001	<0.001	<0.001	<0.001	<0.001	<0.001	<0.001
C2D					-	<0.001	<0.001	<0.001	<0.001	<0.001	<0.001	<0.001	<0.001	<0.001	<0.001	<0.001	<0.001	<0.001	<0.001	<0.001
C2M						-	<0.001	<0.001	<0.001	<0.001	<0.001	<0.001	<0.001	<0.001	<0.001	<0.001	<0.001	<0.001	<0.001	<0.001
C2MD							-	<0.001	0.071	<0.001	<0.001	<0.001	<0.001	<0.001	<0.001	<0.001	<0.001	<0.001	<0.001	<0.001
C2MT								-	<0.001	<0.001	<0.001	<0.001	<0.001	<0.001	<0.001	<0.001	<0.001	<0.001	<0.001	<0.001
C2T									-	<0.001	<0.001	<0.001	<0.001	<0.001	<0.001	<0.001	<0.001	<0.001	<0.001	<0.001
C3										-	<0.001	<0.001	<0.001	0.072	<0.001	<0.001	<0.001	<0.001	<0.001	<0.001
P1											-	<0.001	<0.001	<0.001	<0.001	<0.001	<0.001	<0.001	<0.001	<0.001
P2												-	<0.001	<0.001	<0.001	<0.001	<0.001	<0.001	<0.001	<0.001
P2M													-	<0.001	<0.001	<0.001	<0.001	<0.001	<0.001	<0.001
P3														-	<0.001	0.125	<0.001	<0.001	<0.001	<0.001
P4															-	<0.001	<0.001	<0.001	0.063	<0.001
P5																-	<0.001	<0.001	<0.001	<0.001
P6																	-	<0.001	<0.001	<0.001
PP1																		-	<0.001	<0.001
PP1M																			-	<0.001
PP2																				-

[a]Comparison to effects of base at 95% confidence interval and *p-value* <0.05.

(a) impoundment lengths

	p-value[a]																		
Variable	B1	B1M	C1	C2	C2D	C2M	C2MD	C2MT	C2T	C3	P1	P2	P2M	P3	P4	P5	P6	PP1	PP1M	PP2
B1	-	<0.001	<0.001	<0.001	<0.001	<0.001	<0.001	<0.001	<0.001	<0.001	<0.001	<0.001	<0.001	<0.001	<0.001	<0.001	<0.001	<0.001	<0.001	<0.001
B1M		-	<0.001	<0.001	<0.001	<0.001	<0.001	<0.001	<0.001	<0.001	<0.001	<0.001	<0.001	<0.001	<0.001	1.000	<0.001	<0.001	1.000	<0.001
C1			-	<0.001	<0.001	<0.001	<0.001	<0.001	<0.001	<0.001	<0.001	<0.001	<0.001	<0.001	<0.001	<0.001	<0.001	<0.001	<0.001	<0.001
C2				-	<0.001	<0.001	<0.001	<0.001	<0.001	<0.001	<0.001	<0.001	<0.001	<0.001	<0.001	<0.001	<0.001	<0.001	<0.001	<0.001
C2D					-	<0.001	<0.001	<0.001	<0.001	<0.001	<0.001	<0.001	<0.001	<0.001	<0.001	<0.001	<0.001	<0.001	<0.001	<0.001
C2M						-	<0.001	<0.001	<0.001	<0.001	<0.001	<0.001	<0.001	<0.001	<0.001	<0.001	<0.001	<0.001	<0.001	<0.001
C2MD							-	<0.001	1.000	<0.001	<0.001	<0.001	<0.001	<0.001	<0.001	<0.001	<0.001	<0.001	<0.001	<0.001
C2MT								-	<0.001	<0.001	<0.001	<0.001	<0.001	<0.001	<0.001	<0.001	<0.001	<0.001	<0.001	<0.001
C2T									-	<0.001	<0.001	<0.001	<0.001	<0.001	<0.001	<0.001	<0.001	<0.001	<0.001	<0.001
C3										-	<0.001	<0.001	<0.001	0.352	0.113	<0.001	<0.001	0.052	<0.001	0.169
P1											-	<0.001	<0.001	<0.001	0.145	<0.001	<0.001	<0.001	<0.001	<0.001
P2												-	1.000	<0.001	<0.001	<0.001	<0.001	<0.001	<0.001	<0.001
P2M													-	<0.001	0.439	<0.001	<0.001	<0.001	<0.001	<0.001
P3														-	<0.001	<0.001	<0.001	<0.001	<0.001	<0.001
P4															-	<0.001	<0.001	<0.001	<0.001	<0.001
P5																-	<0.001	<0.001	1.000	<0.001
P6																	-	<0.001	<0.001	<0.001
PP1																		-	<0.001	0.439
PP1M																			-	<0.001
PP2																				-

[a]Comparison to effects of base at 95% confidence interval and *p-value* <0.05.

(b) impoundment depths

Figure 2-14. Two-Sample Means Test

2.4 ENCASEMENT

After fabric evaluations, the top four modified fabrics were evaluated as an encasement material with excelsior fiber fill material and compared to traditional heavy-duty synthetic plastic netting used on excelsior wattles. Excelsior wood fiber was selected due to its high flow-through rate and low impoundment performance across multiple slopes and flow rates as reported by Whitman et al. (2021a). The objective of this assessment was to examine how various encasement material types with low percent open areas impact a wattle's impoundment abilities. This evaluation was

conducted in a hydraulic flume where each wattle type underwent three replicate tests using a new wattle. Each test series included four incremental flow rates over three-channel slopes for a total of 36 experiments per wattle type.

2.4.1 HYDRAULIC FLUME TESTING APPARATUS

The flume system used in the Iowa State University's Larry Buss Hydrology Lab is shown in Figure 2-15. The steel flume measures 38.0 ft (11.6 m) in length, with a uniform 4.00 ft (1.22 m) width by 2.00 ft (0.610 m) height cross-section. The rectangular open-channel flume consists of tempered glass walls and floor to allow for almost any angle to be observed. The flume has the capability to ability to adjust between a 0% and 5.0 % slope through an actuated tilting jack mechanism. An adjustable tailgate allows for variable flow depths to be achieved. Whitman et al. (2021a) provides additional details on the steel flume specifications.

(a) flume side profile (b) cross-section locations

Figure 2-15. Testing apparatus: (a) Iowa State University flume; and (b) cross-sectional data acquisition locations

2.4.2 CHANNELIZED FLOW WATTLE TEST REGIME

Wattles were evaluated using the same method and measurement techniques as Whitman et al. (2021a)2021a) for direct data comparison. Flow was sequentially increased using 0.25, 0.750,

1.25, and 2.00 ft^3/s (0.01, 0.02, 0.04, and 0.06 m^3/s) at slope grades of 3.50%, 4.25%, and 5.00%. Measurements were taken approximately 2.5 min after beginning of each test or until the flow reached equilibrium. This process involved measuring the upstream subcritical flow length and depth at the wattle face. These measurements were analyzed with respect to slope and flow rate. Prior to testing, nine cross-sectional locations were created for data gathering. Each cross-section was spaced 3.00 ft (0.914 m) apart, measuring from the wattle face. The cross-sections were utilized to measure the water depth along the channel using the same methodology as the encasements. At each cross-section site, incremental scales were fastened to the tempered glass sidewalls to visually measure the water depth readings throughout each experiment.

2.4.3 WATTLE INSTALLATION

The flume located at Iowa State University has an adaptable design for accommodating a wide assortment of testing scenarios. This can be accomplished by a recessed sample tray that is located along the flume bottom, approximately 20 ft (6.10 m) downstream of the flume head. Allowing for custom inserts to be constructed and remain flush with the bottom of the flume to meet a wide variety of testing demands. For this study, a custom insert constructed for research conducted by (Whitman et al. 2021) was reused to maintain similar methodology. This custom insert allowed wattles to be installed and secured using a staggered rope securement system, alternating from upstream to downstream on the installed wattle, as shown in Figure 2-16. Stainless steel eyelets were secured to a high-density polypropylene sheet and were spaced 57.2 cm (22.5 in.) on the center with a 0.950 cm (0.375 in.) natural fiber rope was threaded through the eyelets to secure the wattles in place. The natural fiber rope was tensioned by hand to secure the wattles in place. The tension was not measured during installation. Visual observations during testing were made that indicated rope tension did increase due to the water absorption expansion.

The securement method mimics field installation methods that create contact between the wattle and the ground face – allowing for flow bypass underneath the wattle during testing to be minimized. Flow bypass along the tempered glass sidewalls was minimized by cutting wattle specimens approximately 12.0 in. (30.5 cm) longer than the width of the flume to ensure sufficient fill material would be available within the wattle encasement ends.

Figure 2-16. Wattle securement system.

2.4.4 CONTROL TEST: EXCELSIOR WATTLE WITH PLASTIC NETTING ENCASEMENT

A 12.0 in. (30.5 cm) diameter, 20.0 ft (6.10 m) long excelsior wattle was cut to length and served as the control in a plastic netting encasement with a 92% POA. The wattle's impoundment properties were unaffected by the encasement's POA, creating a baseline for the performance of fill material, independent from the encasement. This experiment compared various encasements to the plastic netting to improve lower-performing fill materials. Donald et al. (2013) observed thathe wattle performance is optimized as the upstream subcritical flow length is maximized and the energy grade line slope is minimized. This is typically achieved with an impervious weir. Whitman et al. (2021a) defined the PTW as the optimum hydraulic performance range achievable.

Whitman et al. (2021a) indicates excelsior fill material lack in reaching the PTW, making it suitable for this experiment to demonstrate any potential improvements encasement material may provide. Subcritical flow lengths and depths recorded during control testing revealed the baseline to improve upon.

2.4.5 WATTLE PACKING FOR VARIOUS ENCASEMENTS

Each encasement fabric was packed with excelsior fill material using the same method. Excelsior wattles, with a heavy-duty synthetic plastic netting encasement, used as the control were ordered from one manufacturer and fill material was transferred to the various fabric encasements. The plastic netting encasement was cut and removed from the excelsior fill material. The excelsior fill material was then placed on a scale and weighed to ensure each wattle was filled at the desired density. Next, the fill material was pushed through in a 30.5 cm (12.0 in.) concrete tube form (Figure 2-17) while maintaining the original fill packing intact. The encasement fabric was either knotted or zip tied, depending on the encasement thickness, at one end and placed over the outside of the concrete tube form. The excelsior fill material was then pushed through the tube form and into fabric encasement. Once all the aliquoted excelsior was in its new fabric encasement, the wattle was packed to ensure it was 5.00 ft (1.53 m) in length to fit in the flume and knotted or zip tied closed with excess fabric removed. This packing method mimicked a manufactured packing method. By ensuring that the manufactured wattle packing was left intact when transferring the fill material to the fabric encasement minimized additional density variation in the fill material.

Figure 2-17. Wattle Packing Method

2.4.6 EVALUATED WATTLES FOR ENCASEMENT TESTS

This study assessed five encasements, including a plastic netting ("Control"), two cotton fabrics ("C2M" and "C2MT"), polypropylene ("PP1M"), and polyester-polypropylene mix ("P2M"). Top-performing fabrics analyzed in Phase I of this study determined the selected fabrics used in wattle application. Not all fabrics were strong enough to be woven for a 12.0 in. (30.5 cm) diameter, and supply demands limited material options. Table 2-6 describes the five examined wattles' physical properties.

Table 2-6. Tested Wattle Properties for Encasement Tests

Wattle Evaluated	Test	POA (%)	Measured diameter, ft (m)	Installed height, ft (m)	*Weight, lbs. (kg)	Dry density, lbs./ft^3 (kg/m^3)
Control	1	92.03	0.88 (0.27)	0.71 (0.22)	9.50 (4.32)	3.89 (62.27)
	2	92.03	0.97 (0.30)	0.67 (0.20)	9.50 (4.32)	3.23 (51.67)
	3	92.03	0.94 (0.29)	0.67 (0.20)	9.50 (4.32)	3.44 (55.09)
C2M	1	29.04	0.87 (0.26)	0.65 (0.20)	9.50 (4.32)	4.01 (64.19)
	2	29.04	0.86 (0.26)	0.65 (0.20)	9.50 (4.32)	4.07 (65.18)
	3	29.04	0.84 (0.26)	0.68 (0.21)	9.50 (4.32)	4.26 (68.29)
C2MT	1	2.45	0.85 (0.26)	0.63 (0.19)	9.50 (4.32)	4.20 (67.23)
	2	2.45	0.92 (0.28)	0.69 (0.21)	9.50 (4.32)	3.61 (57.84)
	3	2.45	0.90 (0.27)	0.68 (0.21)	9.50 (4.32)	3.72 (59.55)
P2M	1	37.24	0.85 (0.26)	0.65 (0.20)	9.50 (4.32)	4.20 (67.23)
	2	37.24	0.88 (0.27)	0.69 (0.21)	9.50 (4.32)	3.95 (63.22)
	3	37.24	0.87 (0.26)	0.69 (0.21)	9.50 (4.32)	4.01 (64.19)
PP1M	1	37.73	0.88 (0.27)	0.75 (0.23)	9.50 (4.32)	3.95 (63.22)
	2	37.73	0.88 (0.27)	0.69 (0.21)	9.50 (4.32)	3.95 (63.22)
	3	37.73	0.92 (0.28)	0.69 (0.21)	9.50 (4.32)	3.56 (57.01)

*Values per 4.00 ft (1.22 m) long wattle

2.4.7 WATTLE ENCASEMENT EVALUATION CRITERIA

Ideal wattles maximize subcritical flow length to minimize channelized flow velocity. Whitman et al. (2021a) used the impoundment length and depth ratio as an evaluation criterion and was followed for this study. An MLR model compared three slopes, four flow rates and four fabric encasements against the control for kinetic energy reduction in the channel. A regression equation

shows how each independent variable (i.e., slope, flow rate, and encasement) influences the dependent variable (i.e., impoundment length and/or depth) and the significance of that effect. Model findings reveal the optimal slope, flow rate, and wattle encasement for reducing kinetic energy. Equation (8) shows the MLR model equation,

$$f(x) = \beta_0 + \beta_1 x_1 + \beta_2 x_2 + \ldots + \beta_n x_n \quad (2\text{-}4)$$

where $f(x)$ = dependent variable (i.e., impoundment length and/or depth); β_0 = intercept coefficient; β_i = least squares coefficients; x_i = inclusion/exclusion of independent variables (i.e., slope, flow rate, or encasement - represented as a 1 or 0).

2.4.8 ENCASEMENT RESULTS AND DISCUSSION

Three installations per wattle type were subjected to the incremental flow and slope testing regime for the five wattle types. Whitman et al. (2021a) used an impermeable weir to identify a PTW threshold which was utilized in this study. This study focused on how wattle encasements affect hydraulic performance relative to a plastic netting encasement and how they function at varied flow rates and slopes.

Each test series consisted of three slopes and four flow rates and was replicated three times, resulting in 36 tests per wattle type. The length and depth ratios of each test were plotted to determine the overall performance of each wattle. The PTW represents the optimum hydraulic performance range achievable. As more data points land within the PTW, the more effective the wattle is at impounding water, maximizing the possible amount of subcritical flow upstream. This study was conducted in a controlled environment with minimal flow bypass and no undermining or scouring. To achieve the given findings in the field, improved installation methods beyond manufacturer recommendations would be needed.

2.4.8.1 ENCASEMENT RATIO ANALYSIS

When analyzing hydraulic performance using impoundment length and depth ratios, it's easy to see each product's strengths and shortcomings. The fabric's ability to impound high flow [0.25, 0.75, 1.25, and 2.00 ft^3/s (0.01, 0.02, 0.04, and 0.06 m^3/s)] had little influence, but there was a significant difference in low flow [0.25 ft^3/s (0.01 m^3/s)] circumstances. Table 2-7 shows the average depth and length ratios for low-flow scenarios.

Table 2-7. Encasement Experimental Results for Low Flow

Wattle Evaluated	Average low flow depth ratio[a]	Low Flow depth ratio percent change[b]	Average low flow length ratio[a]	Low flow length ratio percent change[b]
Control	66.2%	N/A	52.1%	N/A
C2M	81.8%	19.1%	67.7%	23.1%
C2MT	93.9%	29.5%	79.0%	34.0%
P2M	68.5%	3.3%	54.0%	3.4%
PP1M	61.8%	-7.2%	48.2%	-8.1%

Note: N/A = not applicable
[a]Percent of theoretical design obtained during testing
[b]Percent change between control and evaluated wattle

Table 2-8 shows the average depth and length ratios for high flow scenarios.

Table 2-8. Encasement Experimental Results for High Flow

Wattle Evaluated	Average high flow depth ratio[a]	High Flow depth ratio percent change[b]	Average high flow length ratio[a]	High flow length ratio percent change[b]
Control	117.0%	N/A	77.4%	N/A
C2M	130.9%	10.6%	78.6%	1.5%
C2MT	127.8%	8.5%	74.6%	-3.8%
P2M	119.4%	2.0%	79.4%	2.5%
PP1M	122.6%	4.6%	72.9%	-6.2%

Note: N/A = not applicable
[a]Percent of theoretical design obtained during testing
[b]Percent change between control and evaluated wattle

The percent change from the control wattle that are plotted in Figure 2-18.

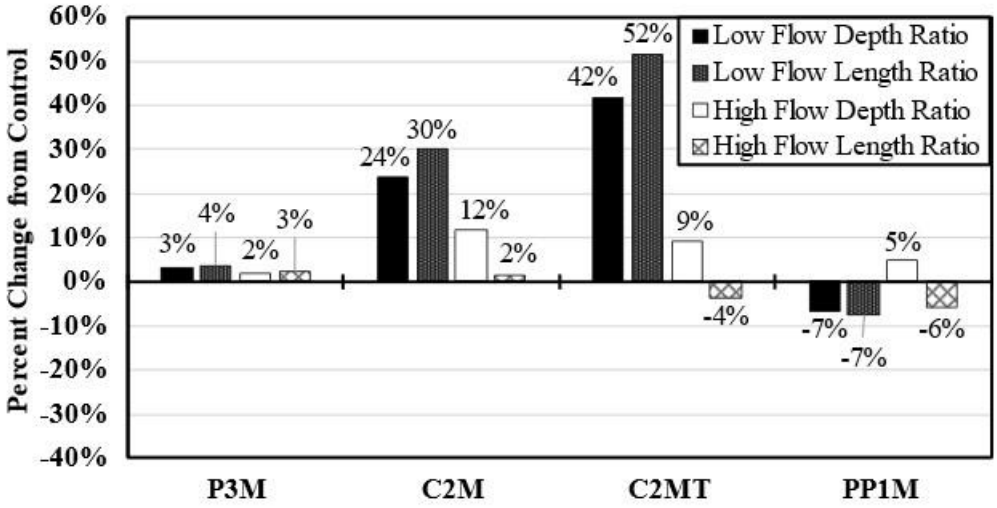

Figure 2-18. Wattle Impoundment Ratio Encasement Variations When Compared to the Control (i.e., Excelsior Wattle with a Standard Plastic Netting)

Figure 2-19 graphically illustrates the distribution of data points and averaged values for low and high flow from Table 2-7 and Table 2-8. PTW is the light gray window in each plot's upper right corner. All wattles performed similarly in high flow conditions, with average depth ratios above 100% and length ratios nearing 80%. However, in low-flow situations, all wattles are far from the PTW except for the cotton-encased wattles.

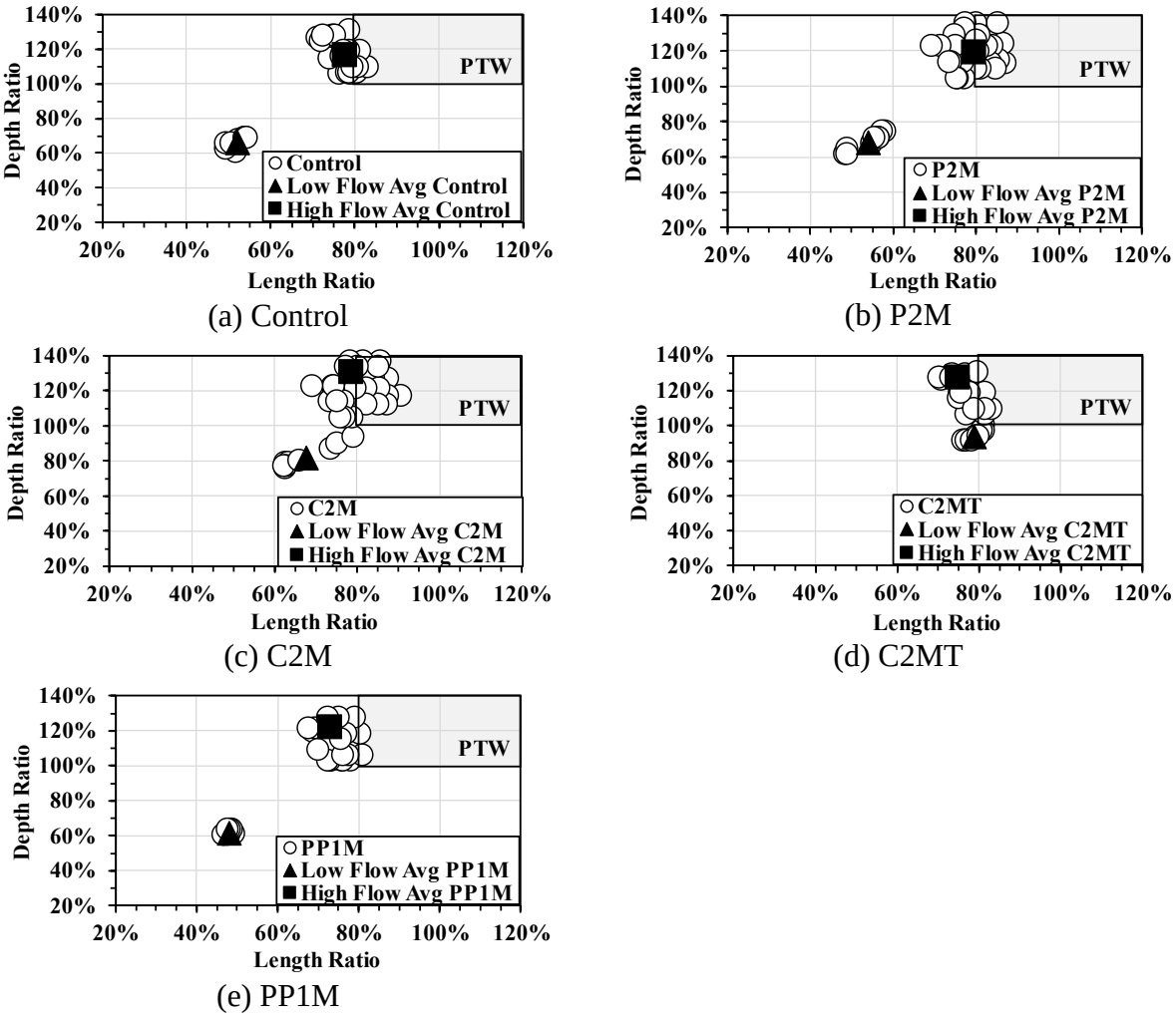

Figure 2-19. Comparison of depth ratio to length ratio for various encasements

Figure 2-20 compares impoundment depths for each examined wattle at 0.25 ft^3/s (0.01 m^3/s) flow rate and 5% longitudinal slope.

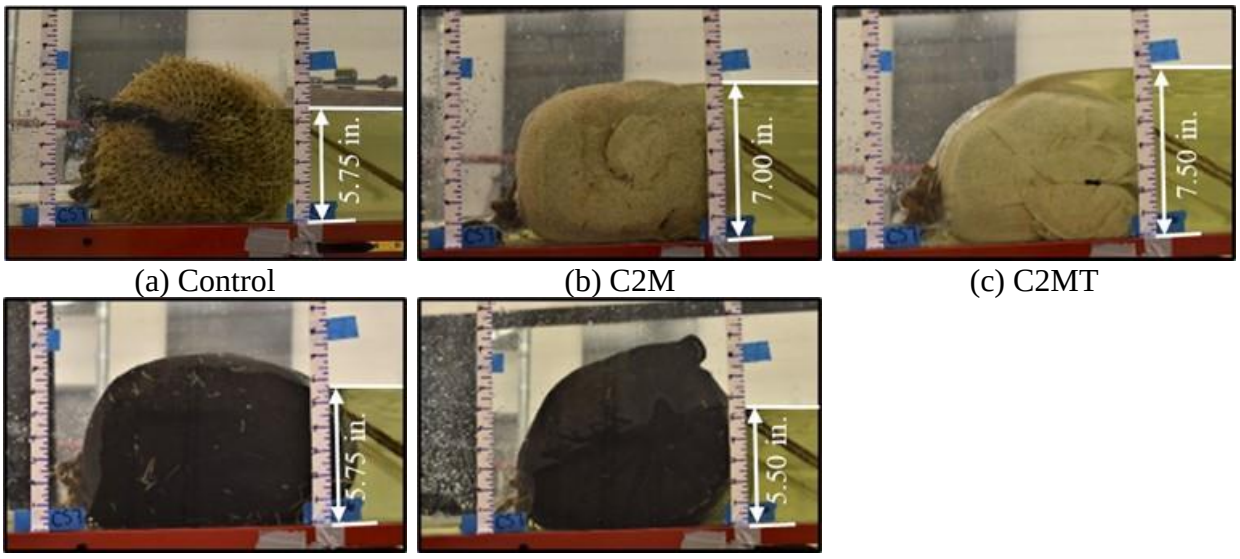

(a) Control (b) C2M (c) C2MT

(d) P2M (e) PP1M

Figure 2-20. Wattle Impoundment for Encasement Tests, Tests With a 0.25 ft^3/s (0.01 m^3/s) Flow Rate and 5% Slope (*Note: 1.00 in. = 2.54 cm*)

2.4.8.2 WATTLE ENCASEMENT STATISTICAL ANALYSIS

Four multiple linear regressions were estimated to evaluate the effectiveness of the different wattles. The first two regressions determined the relative impacts of five different wattle types and three slopes on (a) depth ratio and (b) length ratio for low flow conditions [0.25 ft^3/s (0.01 m^3/s)] using 15 experimental records. The second two regressions determined the relative impacts of five different wattle types, three slopes, and three flow rates on (a) depth ratio and (b) length ratio for high flow conditions [0.75, 1.25, and 2.00 ft^3/s (0.02, 0.04 and 0.06 m^3/s)] using 45 experimental records.

Estimation results of the four models can be seen in Table 2-9, including R^2 values with very high measures of fit. Results highlight how different wattle types significantly influence the depth and length ratios, compared to the excelsior with standard heavy-duty synthetic plastic netting (control). Specifically, under high and low flow conditions, wattles with smaller POA (e.g., P2M, C2M, and C2MT) increase both depth and length ratios, relative to Excelsior, resulting in improved effectiveness. Additionally, under low and high flow conditions, wattles with larger

POA (e.g., PP1M) decrease the depth and length ratios, relative to the control, leading to reduced effectiveness.

Interestingly, increasing the slope under low flow conditions led to increased impoundment ratios, whereas increasing the slope under high flow conditions led to decreased length impoundment ratios (there was no impact on high flow depth ratios). Regardless of the wattle type, as the flow rate increased for high flows, depth ratios increased while length ratios decreased.

Table 2-9. Wattle Multiple Linear Regression Analysis for Low Flow Conditions

	Low Flow Rate 0.25 ft³/s (0.01 m³/s)				**High Flow Rates 0.75 to 2.00 ft³/s (0.02 to 0.06 m³/s)**			
	Length Ratio		**Depth Ratio**		**Length Ratio**		**Depth Ratio**	
	Coeff	***p*-value[a]**	**Coeff**	***p*-value[a]**	**Coeff**	***p*-value[a]**	**Coeff**	***p*-value[a]**
Constant	0.517	<0.001	0.650	<0.001	0.821	<0.001	1.075	<0.001
Wattle Type (Base: Excelsior with Standard Plastic Net)								
P2M	0.018	0.021	0.023	0.070	0.020	<0.001	0.024	<0.001
C2M	0.156	<0.001	0.156	<0.001	0.036	<0.001	0.038	<0.001
C2MT	0.269	<0.001	0.277	<0.001	0.000	0.916	0.008	0.027
PP1M	-0.039	<0.001	-0.044	0.003	-0.027	<0.001	-0.038	<0.001
Slope (Base: 3.50%)								
4.25%	0.004	0.461	0.015	0.106	-0.029	<0.001	-0.001	0.763
5.00%	0.010	0.089	0.021	0.033	-0.048	<0.001	-0.003	0.258
Flow Rate [Base: 0.750 ft³/s (0.0212 m³/s)]								
1.25	-	-	-	-	-0.018	<0.001	0.094	<0.001
2.00	-	-	-	-	-0.045	<0.001	0.196	<0.001
R^2	0.997		0.997		0.964		0.994	

[a]Comparison to effects of base at 95% confidence interval and *p*-value <0.05.

2.5 DENSITY

Following the same procedure as the encasement study, excelsior wattles were evaluated by changing their fill density to evaluate how increasing the density of the wattles affected the hydraulic performance. This study was conducted in the 4.00 ft (1.22 m) wide hydraulic flume located at Iowa State University's Larry Buss Hydrology Lab. The channelized flow testing regime, wattle installation techniques, and control tests all remained the same for this density evaluation from the previous encasement section.

2.5.1 INCREASED DENSITY WATTLE PACKING

Each wattle density variation was packed with excelsior fill using the same method. The manufactured wattle's weights were averaged to determine the average control density. Excelsior wattles were dissected to contain equal fill material portions at shorter lengths to fit in the flume. The wattles were shortened to be 5.00 ft (1.53 m) in length to fit in a 4.00 ft (1.22 m) wide flume. Wattles were cut to be an extra foot in length as it was difficult to pack the material that tight by hand, and to ensure the wattle would snugly compress against the flume sidewalls to ensure a water-tight fit. Fill material was inserted using a 12.0 in (30.5 cm) concrete tube form while maintaining the original excelsior packing to imitate commercial production. Each wattle was compacted to a length of 5.00 ft (1.53 m) to fit in the flume snugly. Leaving the manufactured wattle packing intact when transferring fill material to the fabric encasement reduced density variation. All density calculations and measurements were taken for 4.00 ft (1.22 m) sections.

2.5.2 EVALUATED WATTLES FOR WATTLE TESTS

Three replicated tests were conducted for each wattle density evaluated. Three different density wattles were evaluated as part of this study. The encasements consisted of the standard heavy-duty synthetic plastic netting that was used as the control netting in the encasement section previously. The densities were increased by 1.00 lb/ft (1.49 kg/m) for each wattle from the control which was the average density of a wattle from one manufacturer. The wattles with increased densities were notated as "C-10.5" and "C-11.5" in this experiment. The physical property descriptions of each of the three wattles tested are in Figure 2-7.

Table 2-10. Tested Wattle Properties for Density Tests

Wattle Evaluated	Test	POA (%)	Measured diameter, ft (m)	Installed height, ft (m)	*Weight, lbs. (kg)	Dry density, lbs./ft^3 (kg/m^3)
Control	1	92.03	0.88 (0.27)	0.71 (0.22)	9.5 (4.32)	3.89 (62.27)
	2	92.03	0.97 (0.30)	0.67 (0.20)	9.5 (4.32)	3.23 (51.67)
	3	92.03	0.94 (0.29)	0.67 (0.20)	9.5 (4.32)	3.44 (55.09)
C-10.5	1	92.03	0.94 (0.29)	0.73 (0.22)	10.5 (4.77)	3.82 (61.24)
	2	92.03	0.95 (0.29)	0.81 (0.25)	10.5 (4.77)	3.72 (59.53)
	3	92.03	0.90 (0.27)	0.69 (0.21)	10.5 (4.77)	4.11 (65.82)
C-11.5	1	92.03	0.92 (0.28)	0.77 (0.24)	11.5 (5.23)	4.37 (70.02)
	2	92.03	0.96 (0.29)	0.73 (0.22)	11.5 (5.23)	3.96 (63.42)
	3	92.03	0.92 (0.28)	0.79 (0.24)	11.5 (5.23)	4.37 (70.02)

*Values per 4.00 ft (1.22 m) long wattle

2.5.3 WATTLE DENSITY EVALUATION CRITERIA

The wattle evaluation criteria remained the same as the easement study where ideal wattles maximize subcritical flow length to minimize channelized flow velocity. Once again, the impoundment length and depth ratio, developed by Whitman et al. (2021a), was used as an evaluation criterion and was followed for this study. An MLR model compared three slopes, four flow rates and two densities against the control for kinetic energy reduction in the channel. A regression equation shows how each independent variable (i.e., slope, flow rate, and density) influences the dependent variable (i.e., impoundment length and/or depth) and the significance of that effect. Model findings reveal the optimal slope, flow rate, wattle density for reducing kinetic energy. Equation (2-5) shows the MLR model equation,

$$f(x) = \beta_0 + \beta_1 x_1 + \beta_2 x_2 + \ldots + \beta_n x_n \quad (2\text{-}5)$$

where $f(x)$ = dependent variable (i.e., impoundment length and/or depth); β_0 = intercept coefficient; β_i = least squares coefficients; x_i = inclusion/exclusion of independent variables (i.e., slope, flow rate, or density- represented as a 1 or 0).

2.5.4 DENSITY RESULTS AND DISCUSSION

For each of the three different types of wattle densities, three individual installations per wattle were subjected to the incremental flow and slope testing regime. The performance target window threshold was identified by Whitman et al. (2021a) through the use of an impervious weir and was used in this study as a target area for each wattle density test. This study focused on how the various wattle densities affected the overall hydraulic performance across various flow rates and slopes when compared to the average standard excelsior wattle fill density from one manufacturer.

2.5.5 WATTLE DENSITY RATIO ANALYSIS

For each type of wattle, there were 36 tests conducted, each consisting of three slopes and four flow rates, with three replications. The length and depth ratios of each test were plotted to evaluate the overall performance of the wattles. The PTW represents the range of hydraulic performance that can be achieved optimally. A wattle is more effective at impounding water and maximizing subcritical flow upstream if more data points fall within the PTW. This study was carried out in a controlled environment with minimal flow bypass, no undermining, and no scouring. To replicate these results in the field, installation methods beyond the manufacturer's recommendations would be required.

The impoundment length and depth ratios, when looking at the hydraulic performance, point out how the products performance changed. The fill densities' ability to impound high flow [0.750, 1.25, and 2.00 ft^3/s (0.0212, 0.0354, and 0.0566 m^3/s)] had predominantly a negative influence. Table 2-11 shows the average depth and length ratios for low-flow scenarios.

Table 2-11. Density Experimental Results for Low Flow

Wattle Evaluated	Average low flow depth ratio[a]	Low Flow depth ratio percent change[b]	Average low flow length ratio[a]	Low flow length ratio percent change[b]
Control	66.2%	N/A	52.1%	N/A
C-10.5	53.7%	-23.3%	40.8%	-27.6%
C-11.5	55.3%	-19.8%	43.1%	-20.8%

Note: N/A = not applicable
[a]Percent of theoretical design obtained during testing
[b]Percent change between control and evaluated wattle

Table 2-12 shows the average depth and length ratios for high flow scenarios.

Table 2-12. Density Experimental Results for High Flow

Wattle Evaluated	Average high flow depth ratio[a]	High Flow depth ratio percent change[b]	Average high flow length ratio[a]	High flow length ratio percent change[b]
Control	117.0%	N/A	77.4%	N/A
C-10.5	120.3%	2.7%	73.5%	-5.2%
C-11.5	122.8%	4.7%	77.8%	0.5%

Note: N/A = not applicable
[a]Percent of theoretical design obtained during testing
[b]Percent change between control and evaluated wattle

The percent change from the control wattle are plotted in Figure 2-21.

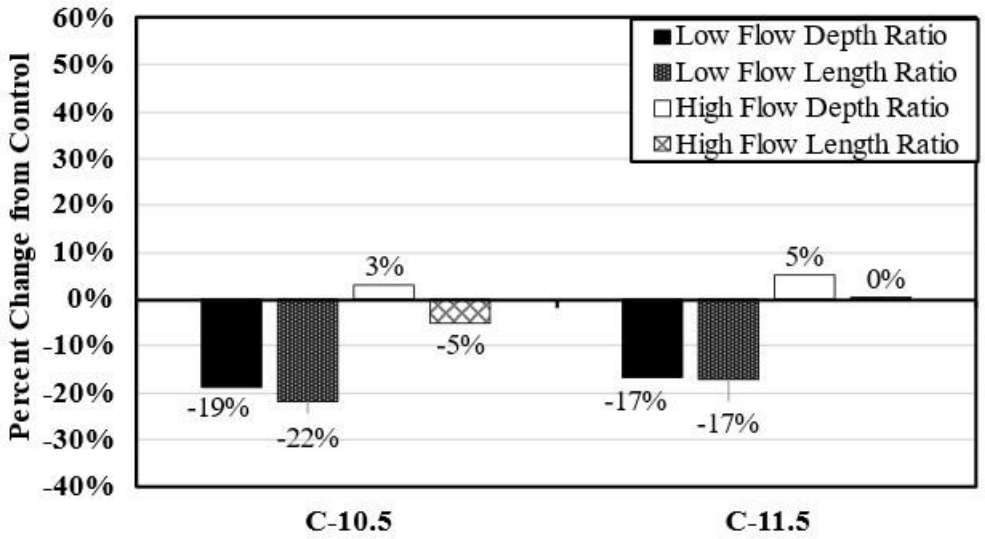

Figure 2-21. Wattle Impoundment Ratio Density Variations When Compared to the Control (i.e., Excelsior Wattle with a Standard Plastic Netting)

The distribution of data points and averaged values for low and high flow from Table 2-11 and Table 2-12 is shown in Figure 2-22. The light gray window in the upper right corner of each plot represents the PTW, making it easy to visualize the relationship between the data points and the PTW for each wattle evaluated. In high flow conditions, all the wattles performed similarly, with average depth ratios exceeding 100% and length ratios approaching 80%. However, in low-flow situations, all the wattles, except for the cotton-encased wattles, were far from the PTW.

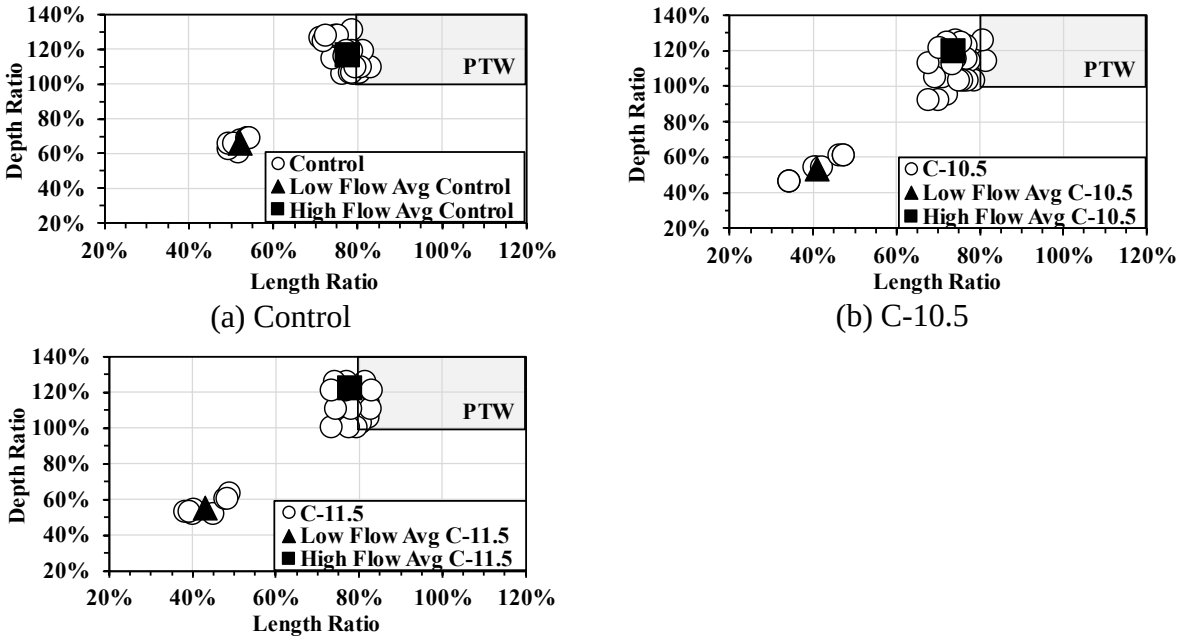

(a) Control (b) C-10.5

(c) C-11.5

Figure 2-22. Comparison of Depth Ratio to Length Ratio for Various Fill Densities

Figure 2-23 compares the impoundment depths for each wattle at a flow rate of 0.25 ft^3/s (0.01 m^3/s) and a longitudinal slope of 5%.

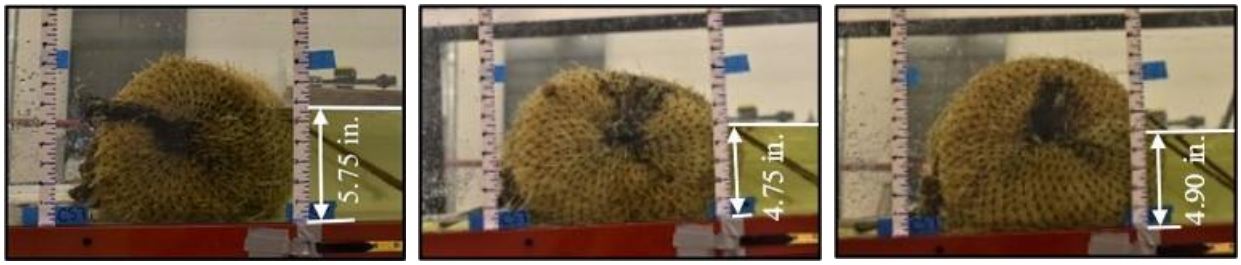

(a) Control (b) C-10.5 (c) C-11.5

Figure 2-23. Wattle Impoundment During Density Tests, Tests With a 0.25 ft^3/s (0.01 m^3/s) Flow Rate and 5% Slope *(Note: 1.00 in. = 2.54 cm)*

2.5.5.1 WATTLE DENSITY STATISTICAL ANALYSIS

Four multiple linear regressions were estimated to evaluate the effectiveness of the different wattles. The first two regressions determined the relative impacts of five different wattle types and three slopes on (a) depth ratio and (b) length ratio for low flow conditions [0.25 ft^3/s (0.01 m^3/s)] using 15 experimental records. The second two regressions determined the relative impacts of five different wattle types, three slopes, and three flow rates on (a) depth ratio and (b)

length ratio for high flow conditions [0.75, 1.25, and 2.00 ft^3/s (0.02, 0.04, and 0.06 m^3/s)] using 45 experimental records.

Estimation results of the four models can be seen in Table 2-13, including R^2 values with very high measures of fit. Results highlight how different wattle densities significantly influence the depth and length ratios, compared to the manufactured density of excelsior wattles with a standard heavy duty synthetic plastic netting (control).

Specifically, under high and low flow conditions, wattles with increased densities from the control (C-10.5 and C-11.5) decreased both impoundment lengths and depth ratios significantly across low and high flow conditions, resulting in reduced hydraulic performances relative to the manufactured packing density, with the exception of C-11.5 for impoundment length during high flow conditions which had no significant change.

The slope and flow results remained the same as what was presented in the encasement section previously where, increasing the slope under low flow conditions led to increased impoundment ratios, whereas increasing the slope under high flow conditions led to decreased length impoundment ratios (there was no impact on high flow depth ratios). Regardless of the wattle density, as the flow rate increased for high flows, depth ratios increased while length ratios decreased.

Table 2-13. Wattle Multiple Linear Regression Analysis for Low Flow Conditions

	Low Flow Rate 0.25 ft³/s (0.01 m³/s)				High Flow Rates 0.75 to 2.00 ft³/s (0.02 to 0.06 m³/s)			
	Length Ratio		Depth Ratio		Length Ratio		Depth Ratio	
	Coeff	*p*-value[a]	Coeff	*p*-value[a]	Coeff	*p*-value[a]	Coeff	*p*-value[a]
Constant	0.516	<0.001	0.650	<0.001	0.810	<0.001	1.072	<0.001
Wattle Type (Base: Excelsior with Standard Plastic Net)								
C-10.5	-0.113	<0.001	-0.125	<0.001	-0.032	<0.001	-0.066	<0.001
C-11.5	-0.090	<0.001	-0.109	<0.001	0.009	0.122	-0.044	<0.001
Slope (Base: 3.50%)								
4.25%	0.008	0.135	0.014	0.155	-0.031	<0.001	-0.005	0.134
5.00%	0.007	0.206	0.014	0.159	-0.053	<0.001	-0.007	0.040
Flow Rate [Base: 0.750 ft³/s (0.0212 m³/s)]								
1.25	-	-	-	-	-0.002	0.748	0.103	<0.001
2.00	-	-	-	-	-0.020	0.003	0.203	<0.001
R^2	0.994		0.986		0.885		0.996	

[a]Comparison to effects of base at 95% confidence interval and *p*-value <0.05.

2.6 WATTLE CONCLUSIONS

Recent studies involving wattles have explored the ideal installation methods to prevent product failure, developed a standardized evaluation method, and compared the hydraulic performance of various wattle fill materials. However, there was a gap in research on modifying wattle encasing. This research aimed to assess how the hydraulic performance of wattles.

Product evaluations can be done on wattles in a small-scale setting to help product designers create innovative designs. Using a 15.0 ft (4.57 m) long fiberglass hydraulic flume with a 1.00 ft (0.30 m) width and 1.50 ft (0.457 m) deep rectangular open channel was sufficient in comparing manufactured wattles and an impervious barrier to an innovative wattle product. Conducting a small-scale impoundment test can be a quick and cost-effective way to provide product insight to those looking to improve their design before moving forward with investments. However, it is important to ensure communication with the product designer to agree on products that should be tested and compared, evaluate manufactured products from different manufacturers

to ensure fair product comparison, and explain the results and their meanings to the product designer so they can get the most out of the results.

Fabrics chosen for wattle applications were selected based on impoundment abilities. Top-performing fabric encasement per fabric type, identified in Phase I, were modified for a tighter weave and utilized in the wattle application tests, Phase II. Polypropylene, cotton, bamboo cotton mix, and polyester-polypropylene mix encasement fabrics were evaluated. By scanning each cloth and computing the POA, hydraulic performance and wattle applications could be compared. Additionally, this study methodology used for Phase II was replicated from Whitman et al. (2021a) to allow for direct comparison and expansion of the results.

The encasement selection portion of the study found that decreasing the POA by 97.3% more than the control, obtained a maximum impoundment length of 139 in. (354 cm) and depth of 8.42 in. (21.3 cm). Additionally, cotton fabrics with larger POA performed equally to polyester and polyester-polypropylene mix fabrics with smaller POA [e.g., C3, PP1, and P4 had POA values of 49.1, 39.9, and 29.1%, respectively, but yielded similar impoundment lengths of 24.7, 21.9 and 27.2 in. (62.7, 55.7, and 69.0 cm) and depths of 3.38, 3.30, and 3.45 in. (8.59, 8.38, and 8.76 cm), respectively].

Impoundment length and depth ratio plots show that during high flow, nearly every wattle evaluated was successful at impounding water within or close to the PTW. High impoundment capabilities were likely related to the volume of water traveling down the channel, as the water had less time to pass through the wattles before overtopping. During low flow, evaluated wattles were more likely to inadequately impound water. This difference in performance depends greatly on the material type and density (Donald et al., 2015). This deficient performance during low flow conditions is the target area to seek improvement.

Low flow [0.25 ft^3/s (0.01 m^3/s)] and high flow [0.75, 1.25, and 2.00 ft^3/s (0.02, 0.04, and 0.06 m^3/s)] were used to evaluate the wattles' hydraulic performance. The MLR showed that C2M improved length and depth ratios the most for low and high flow. C2MT performed similarly to C2M but did not improve enough to justify the extra expense. P2M enhanced impoundment length and depth in low and high flow, but not as much as C2M. P2M has better hydraulic performance than the control, but C2M outperforms P2M and is more environmentally friendly.

Only PP1M consistently lowered hydraulic performance significantly for length and depth impoundment ratios and low and high flow conditions, suggesting that materials utilized may play a crucial factor in affecting impoundment. The MLR investigation comparing encasement POA with impoundment length and depth ratios showed no direct association, confirming the hypothesis that fabric type mattered more than POA when boosting wattles' hydraulic performance. A material made of only polypropylene had an adverse effect on the hydraulic performance than when polyester is mixed with polypropylene.

Increasing fill density appeared to significantly diminish the overall hydraulic performance, regardless of the flow conditions, which is contrary to previous research performed. One variable that could not be accounted for was the repacking of the two denser wattles. This process may not have been representative of how the control wattle was packed, opening additional pore passages throughout the media, or altering the packing density distribution of the fill material. Future research that can account for this variable may lead to different results.

It is important to note that this study was conducted using clean water. Future research should include soil introduction in analyzing the hydraulic performance relationship with POA, as encasement blinding and soil buildup will likely affect performance. POA was investigated with dry encasement fabrics. Investigating how the fabric's POA changes when saturated may help

understand its hydraulic performance. Due to a global supply shortage, obtaining materials to evaluate was limited. Therefore, investigating the hydraulic performance of additional biodegradable encasement options – for example, bamboo cotton blend (i.e., B1), performed well in the encasement evaluation phase of this study but could not be woven to the required dimensions due to its age and fragility. Looking into the hydraulic performance of additional biodegradable materials would also be favorable as the industry is pushing towards reducing plastic in E&SC practices. A life cycle cost analysis of the various encasement material options would also be worth exploring to identify the difference in overall costs. Lastly, this study could be expanded by performing longevity testing, field applications, and quantifying flow-through rates of various fill materials.

CHAPTER THREE: FLOCCULANTS

3.1 IMPLEMENTATION CONCERNS

Construction site practitioners are gradually moving towards implementing the use of flocculants on their sites to aid in maximizing sediment retention on their sites. However, flocculants are a controversial item to implement as there are limited studies that have explored optimizing flocculants on sites where there are so many uncontrolled factors. Kazaz et. al. (2021) surveyed 51 departments of transportation (DOTs), including the District of Columbia, inquiring about flocculant usage. This study reported 39% of state agencies actively utilizing flocculants in E&SC practices; however, 54% of those state agencies that utilize flocculants rely on manufacture guidance on dosage and application rates. Manufacturer guidelines are not intended for universal applications (Kazaz et al., 2021). For example, wastewater management and construction sites have drastically different environments and variables that can or cannot be controlled. Meaning they are intended more of suggestions for temporary starting points. Kazaz et. al. (2021) found that only 23% of the DOTs that utilize flocculants require monitoring downstream of receiving water bodies for residual flocculant. State agencies that do not use flocculants listed reasons being the potential risk of polluting waterbodies downstream, regularity restrictions on flocculant usage, and additional costs and efforts to E&SC plans (Kazaz et al., 2021). When selecting the proper flocculant type for settling soil out of suspension, the soil type is a crucial consideration that needs to be made. This is because flocculants are soil-specific as each soil type has different charges and minerals that can affect flocculants abilities to react and bind with the particles (Kazaz, 2022).

When flocculants are implemented on construction sites, strategic placement and routine maintenance checks should be conducted to ensure proper usage over time. There is a wide range of methods to apply flocculants and differ by state standards; however placement to ensure

sufficient agitation and maintenance needs are universal. Figure 3-1 depicts two examples of poor flocculant block implementations. Figure 3-1(a) is a flocculant block installation in a storm drain that has not been maintained. Sediment has accumulated and covered all sides of the block, restricting it from being able to come in contact with flow, which activates the flocculant, therefore, hindering the block from effectively treating any flow. This problem can be solved by removing the sediment layer or replacing the flocculant blocks before the next flow event. Figure 3-1(b) shows another flocculant block that was installed after triangular silt dike ditch check that had not been adequately maintained. The block is once again covered in sediment; however, this block has no protection from the sun. So, the block has dried out and formed a hard sediment shell. Flocculants need to be protected from the sun to prevent them from drying out and hardening. Dosing is only able to occur when the flocculant is hydrated and in a gelatinous form. The solution for Figure 3-1(b) would be to replace the flocculant block and provide a method of sun protection. The dried flocculant block may be able to be recovered by soaking it in a tub of water for some time until the sediment can be removed, and the block is no longer hard.

(a) sediment layer covering flocculant (b) dried block from sun exposure

Figure 3-1. Poor Flocculant Block Implementations

Note: photo credit Barry Fagan

Assuming flocculates are implemented in ideal locations where sufficient mixing is provided and proper maintenance is maintained, the primary concern with flocculant use is based on toxicity. Australia and New Zealand use flocculants throughout their stormwater BMPs. However, due to these chemicals having potential to be highly toxic if improperly used, the Australian and New Zealand Environment and Conservation Council (ANZECC) and Agriculture and Resource Management Council of Australia and New Zealand heavily regulate and monitor flocculant treatment to minimize the possibility of contaminating downstream waterbodies, resulting in the loss of aquatic organisms (ANZECC et al. 2000). For example, the hemoglobin in fish gills has a negative charge, therefore cationic flocculants bind to fish hemoglobin, causing them to suffocate (Colen et al., 2012; Duggan et al., 2019; Kazaz et al., 2021; USEPA 2022b). Safety data sheets (SDS) require manufacturers to include toxicology limits for available products (Occupational Safety and Health Administration 1910.1200, 2012). These toxicology limits are identified by acute toxicity tests that represent dose-response information in terms of lethal concentrations (LC_{50}) or lethal dose (LD_{50}) that kill 50% of experimental subjects (Stephan, 2009). LC_{50} is used to refer to concentrations in air or water and is often reported in concentrations over

volume. Alternatively, LD_{50} refers to an amount of a material that is given to the test subject all at once, often expressed in concentrations over body weight (Canadian Centre for Occupational Health and Safety, 2023). The most common administration methods are by any route of entry, oral (given by mouth) or dermal (applied to the skin).

Acute toxicology limits are summarized in Table 3-1 for aquatic organism test subjects and Table 3-2 for mammal test subjects. Buczek et al. (2017) evaluated five different anionic and one nonionic PAM products on early-life-stage freshwater muscles. LC_{50} values were determined after 24, 48, and 96-hours using concentrations two to three times greater than the recommended concentration for turbidity removal (<5 mg/L). The longer the time exposure, the lower the LC_{50}; therefore, values in Table 3-1 represent the 96-hour exposure time. Fort & Stover (1995) focused on effects on freshwater fleas from cationic polymers, aluminum sulfate ($Al_2(SO_4)_3$), and ferric chloride ($FeCL_3$) and found acute toxicity at very low concentrations after 48-hours of exposureClick or tap here to enter text.. Another study looking at freshwater fleas dealt with anionic PAM, cationic and nonionic polymers and found that after 96-hours, flocculants were a new class of micropollutants since they were found to be highly toxic to water organisms (Beim & Beim, 1994). Beim & Beim (1994) goes on to emphasize the necessity for controlling for residual flocculants from discharging effluents and the need for identifying a Maximum Permissible Concentration (MPC) for flocculant types. Duggan et al. (2019) evaluated zebrafish embryos over the course of 7-days with cationic PAM and cationic starch. They found no statistical difference from the number of deaths for embryos exposed to cationic starch compared to the embryo medium (control), thus encouraging switching cationic PAM with cationic starch.

Table 3-1. Summary of Aquatic Acute Toxicology Studies with Various Flocculants

Research Study	Flocculant Type	Aquatic Organism	Results (LC_{50})
Buczek et al. 2017	Anionic and Nonionic PAM	Freshwater mussel (Lampsilis cariosa)	≥ 127 mg/L
		Freshwater mussel (Alasmidonta raveneliana)	≥ 330 mg/L
		Freshwater mussel (Mehalonaias nervosa)	≥ 706 mg/L
Fort & Stover, 1995	Cationic polymers	Freshwater fleas (Ceriodaphnia dubia)	< 0.025 mg/L
	$Al_2(SO_4)_3$	Freshwater fleas (Ceriodaphnia dubia)	< 0.025 mg/L
	$FeCL_3$	Freshwater fleas (Ceriodaphnia dubia)	< 0.025 mg/L
Beim & Beim, 1994	Anionic PAM	Freshwater fleas (Daphnia magna)	14.1 mg/L
		Planaria (Baicalobia guttata)	> 100 mg/L
		Grmmaridae (Eulimnogammarus verrucosus)	2,100 mg/L
		Minnows (Phoxinus phoxinus L.)	> 1,000 mg/L
	Nonionic polymer	Freshwater fleas (Daphnia magna)	≥ 13.2 mg/L
		Planaria (Baicalobia guttata)	≥ 65 mg/L
		Grmmaridae (Eulimnogammarus verrucosus)	≥ 2,050 mg/L
		Minnows (Phoxinus phoxinus L.)	≥ 407 mg/L
	Cationic polymers	Freshwater fleas (Daphnia magna)	≤ 2.1 mg/L
		Planaria (Baicalobia guttata)	≥ 1.6 mg/L
		Grmmaridae (Eulimnogammarus verrucosus)	≥ 70 mg/L
		Minnows (Phoxinus phoxinus L.)	≥ 2.2 mg/L
Duggan et al. 2019	Cationic PAM	Zebrafish embryos (Danio rerio)	17.4 mg/L
	Cationic Starch	Zebrafish embryos (Danio rerio)	3.8 mg/L

Rats and dogs were orally subjected to nonionic and anionic PAM to determine acute toxicity (Table 3-2). The maximum single dose that was accepted by the animals was 464 mg/kg (1023 mg/lb.) of body weight over the course of 90-days to which both animals showed no signs of toxicity but altered liver weights for female rats and depressed weight gain, increased organ weight, and abnormal stomach contents for dogs when fed concentrations above 10,000 mg/L (Christofano et al., 1969). ThisClick or tap here to enter text. 2-year study found no significant observed adverse effects for both rats and dogs that were fed diets containing 2,000 mg/L PAM.

As PAM has larger molecules, it is not able to penetrate skin, thus making itself not significantly toxic (Anderson, 2005). Acrylamide, however, is capable of penetrating skin and is far more lethal as it is classified as a neurotoxin (Erkekoglu & Baydar, 2014). Erkekoglu & Baydar (2014) emphasizes that low and high doses of acrylamide yield the same neurotoxic effects. Toxicity studies have evaluated effects of acrylamide on mice, rats, guinea pigs, rabbits, and cats via oral, dermal and/or injection. Results showed that there was no significant difference between exposed mammalian species (Anderson, 2005; Erkekoglu & Baydar, 2014; International Programme on Chemical Safety, 1985). These results indicate that PAM is less of a concern than its acrylamide monomer (Anderson, 2005; Beim & Beim, 1994; King & Noss, 1989; Liebert, 1991; McCollister et al., 1965; Rawat et al., 2012; Uthra et al., 2017). Although studies have indicated that PAM products contain residual acrylamide that ends up being released in the environment as the polymers untangle, the degradation of PAM leading to additional acrylamide release remains unclear from literature (Caulfield et al., 2003; Guezennec et al., 2015; King & Noss, 1989; Seybold, 1994; Smith et al., 1997).

Table 3-2. Summary of Mammal Acute Toxicology Studies

Research Study	Toxicity Study	Flocculant Type	Test Organism	Results (LD_{50})
Christofano et al. 1969	Oral	Nonionic PAM	Rats	was not reached with maximum dose of 464 mg/kg body weight
			Beagle Dogs	> 2,000 mg/L
		Anionic PAM	Rats	was not reached with maximum dose of 464 mg/kg body weight
			Beagle Dogs	> 2,000 mg/L
IPCS, 1985	Oral	Acrylamide	Rats	≥ 107 mg/kg body weight
			Mice	≥ 107 mg/ kg body weight
			Guinea Pigs	≥ 150 mg/ kg body weight
	Dermal	Acrylamide	Rats	400 mg/ kg body weight
			Rabbits	1148 mg/ kg body weight
	Intravenous Injection	Acrylamide	Cats	85 mg/kg body weight
	Intraperitoneal Injection	Acrylamide	Rats	≥ 90 mg/kg body weight

Note: 1.00 mg/kg = 2.20 mg/lb.

The concern of polluting downstream waterbodies is a result from improper implementation of flocculants by overdosing. Manufacturers provide toxicology information as it differs between flocculant types. However, limited studies have been done on monitoring and detecting residual concentrations. Depending on the flocculant type, adding too much can have serious negative repercussions on the aquatic ecosystems (Al Momani & Örmeci, 2014) which would require a substantial amount of funding and effort to remedy. Kazaz et al. (2021) breaks down the various flocculant types by their charge and drawbacks for individuals to easily see the difference between each type. Only natural starch, calcium sulfate (gypsum), and polyaluminum chloride (PAC) have not been reported as toxic in high concentrations (Mclaughlin & Zimmerman, 2008). PAM has also been suspected to have carcinogenic properties because the single compound acrylamide, when present in high enough concentrations, is known to cause cancer (Al Momani & Örmeci, 2014; Besaratinia & Pfeifer, 2007; Carere, 2006). The U.S. Food and Drug Administration (FDA), USEPA, and the National Resources Conservation Service (NRCS) all

regulate acrylamide concentrations in commercial PAM products (Code of Federal Regulations, 2023; Sojka & Lentz, 1996; Touzé et al., 2015; USEPA 2023). As polymer chains disentangle during flocculation, trapped acrylamide molecules in the chain can be released, which is the leading reason why U.S. drinking water treatment methods maintain PAM concentrations below 1 mg/L (Aguilar et al., 2005; Guezennec et al., 2015; Touzé et al., 2015; Xiong et al., 2018). However, wastewater treatments are not held to the same stringent regulations.

Too much PAM can have negative impacts on not only the treatment efficiency, but also the environment (Al Momani & Örmeci, 2014; Glover et al., 2004; Mikulec et al., 2015). Wastewater treatments typically use high molecular weight PAM as it can serve several purposes other than flocculating particulates, however, an accidental spill can result in significant environmental challenges for surface and groundwater as associated acrylamide monomers become present through degradation process like chemical, mechanical, thermal, photolytic, and biological processes (Howard et al., 1978; Xiong et al., 2018). Although many studies have evaluated the impacts of flocculant spills or overdosing, mitigation methods lack research. Research on naturally occurring microbes in sediment have been found to convert acrylamide into ammonia and acrylic acrid by-products that are nontoxic (Kay-Shoemake et al., 1998; K.Labahn et al., 2010; Shanker et al., 1990; Shukor et al., 2009; Smith et al., 1997; Xiong et al., 2018). These microbes were found to degrade acrylamide at a rate of 90 mg/L/day (Shukor et al., 2009). Although microbes can be one method of mitigation, their ability to use up PAM has not been explored, nor is their mitigation rate fast enough to prevent a spill or overdose from expanding into other waterbodies. One discussed solution to mitigate a PAM spill or overdose quickly would be to add sediment to the contaminated area until the PAM is used up by forming flocs that can be

later dredged out. However, literature was not found to support the idea of capturing PAM with sediment.

3.2 RESEARCH PURPOSE

Although there is a plethora of research that has dealt with flocculants, an abundance of questions still remain with regard for best management practices with flocculants on construction sites where environmental factors cannot be controlled. This research explores possible detection methods for quantifying flocculant concentrations in the field, expanding on settling velocity residual detection method from Kazaz et al.(2022), and performing large-scale test evaluations with granular/powder and block/log form PAM that use the expanded settling velocity residual detection method to quantify dosing rates over time. The results from large-scale test evaluations provide insight on the rate at which flocculant is being dosed in a channel during flow, when reapplication for granular PAM should be performed, guidance on the number of flocculant blocks should be placed in a channel at a time, placement of flocculant in a channel to achieve proper dosing, and observed floc size during channel flow. These testing methodologies performed in this study are intended to serve as a baseline testing methodology that can be used to evaluate other flocculant products to provide guidance on optimum flocculant implementation for construction sites.

3.3 FLOCCULANT DETECTION METHODS

There are several ways to detect polymers; however, reproducing consistent results in complex environments has been found challenging (Dente et al., 2000). Spectrophotometry has been used by Lentz et. al. (1994) and Al Momani and Örmeci (2014) to estimate residual concentrations of PAM. The method performed by Lentz et. al. (1994) looked at combining kaolinite mineral standard with PAM and correlated transmittance variations of PAM concentrations with the settling. Light absorbance was measured and correlated with known PAM concentrations by Al

Momani and Örmeci (2014). PAM has also been evaluated using turbidimetry (Kang et al., 2013) and viscometry (Jung et al., 2016).

This study describes the methods and experimental procedures of the various detection methods and bench-scale evaluation phase of this research. Due to the low concentration range of PAM that was targeted for large-scale detection, multiple detection methods were explored as possible alternative methods. All flocculant detection methods were used to estimate concentrations above and below 5.0 mg/L of anionic granular H30 PAM flocculant from Manufacturer A (G-PAM) and anionic block H30 PAM flocculant from Manufacturer A (B-PAM). This target concentration was selected as it was the manufacturer's recommended dosage for this product. The following sections describes how the viscosity and particle charge of water was explored as a possible alternative to the settling velocity method that was used for large-scale testing using two different viscosity detection methods and one particle charge analyzer.

3.3.1 VISCOSITY

Since PAM is highly water-absorbent and will form a soft gel when hydrated, it influences the viscosity when diluted in water (Rawat et al., 2012). Several researchers have explored these influencing characters to predict PAM viscosity for various applications better. Shin and Cho (1993) developed an equation for viscosity of PAM solutions that accounts for shear-thinning of non-Newtonian characteristics and temperatures. This study used 1,000 mg/L of granular PAM diluted with distilled water to create a 0.1% solution PAM solution. A falling needle viscometer and Brookfield viscometer were used to quantify the viscosity of the samples. Results indicated that 1,000 mg/L PAM solution viscosity at shear rates below 0.001 s^{-1} was found to be most sensitive to temperatures between 20 to 60°C (68 to 140°F), whereas shear rates between 10.0 to 200 s^{-1} were nearly uninfluenced by temperature.

Other studies reported that PAM degradation impacts viscosity as it is influenced by application techniques. Viscosity changes were measured using a granular PAM application method for agricultural use. Superfloc A836, that is commonly used irrigation furrow, and Pristine, an inverse oil emulsion PAM, were selected for this study conducted by Bjorneberg (2013). The study reported that for every 10 mg/L increase for both PAM solutions, it resulted in an approximate 5% increase in viscosity, relative to water. These viscosity measurements were performed using a no. 50 and a no. 150 Cannon-Fenske kinematic viscometer. This study continued to report that temperature, concentration, and flow conditions all significantly varied PAM viscosities and had been backed by Jung et al. (2016). Even though Bjorneberg (2013) evaluated flow conditions that have high shear stresses, the report details the significant 15 to 20% reduction in viscosity from one pass through a centrifugal pump was likely a result of broken PAM chains. Indicating the fragility of PAM molecules would need to be considered in any PAM viscosity analysis.

Time is another factor that can influence the viscosity of PAM solutions. Narkis and Rebhun (1966) evaluated PAM viscosity over time with an aqueous emulsion and granular form PAM. The two respective flocculant types, Cyanamer P-26 and Cyanamer P-250, have different molecular weights, ranging from 2.24×10^5 and 1.95×10^6, respectively. Narkis and Rebhun (1966) found that over 57 days, PAM undergoes an osculating process of disentanglement and re-entanglement of the polymer chains. This osculation eventually reaches equilibrium over time, but higher concentrations and molecular weights lead to more time required to reach equilibrium. Narkis and Rebhun (1966) found that viscosity is based on the entanglement of PAM molecules. Therefore, viscosity readings will continue to change for a solution until equilibrium is achieved.

Finding detection methods that are portable, fast, and easy to perform while likely containing sediment to some degree within the sample poses as a challenge. As mentioned in the literature review previously, the viscosity of PAM is highly influenced based on the temperature, concentration, flow, and system conditions, and how long the PAM agent has been diluted. However, as many studies that evaluate viscosity look at solutions without sediment, this study focused on the ability to measure viscosity from field samples to determine if concentrations below 20 mg/L were capable of being quantified. If the desired range was capable of being quantified, further evaluations would investigate accounting for the known factors that can influence sample variability. A Cannon-Fenske Routine Viscometer and Brookfield Digital Viscometer two detection methods that were evaluated and are detailed in the following sections.

3.3.1.1 CANNON-FENSKE ROUTINE VISCOMETER

A Cannon-Fenske Routine Viscometer, or Cannon-Fenske tube, shown in Figure 3-2, is a glass "U" liked shaped tube used to measure the kinematic viscosity of a transparent Newtonian fluid (Cannon Instrument Company, 2023) by measuring the time it takes for a fluid to travel from point A to point B, known as the efflux time. This method was tested due to its low cost and simplicity of use, making it an ideal possibility for companies and state DOTs to invest and adopt the method. Cannon-Fenske tubes are hand-made glass tubes which differ by size depending on the volume and expected viscosity range that is being measured.

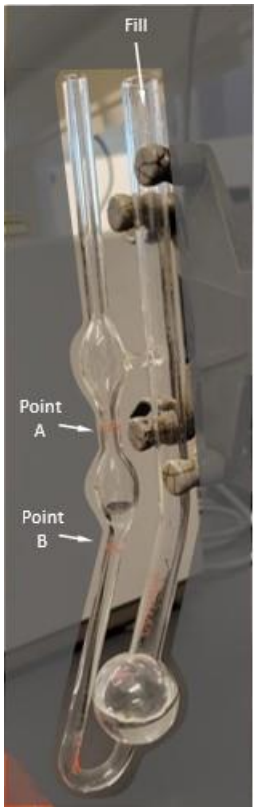

Figure 3-2. Cannon-Fenske Tube

3.3.1.1.1 CANNON-FENSKE ROUTINE VISCOMETER TESTING METHODOLOGY

For this evaluation, two size 50 Cannon-Fenske tubes (notated as Tube 1 and Tube 2), with a viscosity range of 0.8 to 4.0 mm^2/s, were used to measure the viscosity of samples with G-PAM concentrations ranging from 1.0 mg/L to 20 mg/L, with the control being 0 mg/L of flocculant.

Cannon-Fenske tubes were held up with a burette clamp and placed so the upper half of the tubes were level and vertical. City of Auburn, AL tap water was used for these experiments. The test was conducted by creating a stock solution of each desired G-PAM concentration. For each test, the pH and temperature of the sample was recorded, then 0.33 fl oz (10 mL) of the evaluated solution was transferred into the Cannon-Fenske tube. Solutions are poured into the larger, back tube, labeled "Fill" in Figure 3-2, and siphoned up the front, smaller tube, until the solution head is above "Point A." Efflux time started when the solution passed "Point A," and

stops when it passed “Point B.” This process was repeated three times per sample concentration. Between samples, the Cannon-Fenske tube was flushed with deionized water.

When all data collection was completed, each tube was flushed with deionized water again and placed in a base bath for a minimum of 24 hours to ensure the vial was completely free of any possible contaminants. The tubes were rinsed well with deionized water once more to remove the base bath solution. Tubes were then flushed with a 90% Ethanol solution and blown dry with compressed air to ensure no residual fluids were left in the tube before storage.

3.3.1.1.2 CANNON-FENSKE ROUTINE VISCOMETER RESULTS AND DISCUSSION

Both Cannon-Fenske tubes were tested using the same stock solution. The average measured values for this test are shown in Table 3-3.

Table 3-3. Cannon-Fenske Tube Measured Values

			Avg. Efflux Time, sec.	
Concentration, mg/L	**pH**	**Temperature, °F (°C)**	**Tube 1**	**Tube 2**
0.0	7.2	72.6 (22.6)	243.3	264.8
1.0	7.2	75.7 (24.3)	245.8	264.8
2.0	7.2	75.7 (24.3)	245.7	269.0
5.0	7.2	75.0 (23.9)	244.3	268.0
10.0	7.2	75.0 (23.9)	245.3	271.3
20.0	7.2	75.4 (24.1)	266.3	412.7

All data points from Table 3-3 are plotted in Figure 3-3.

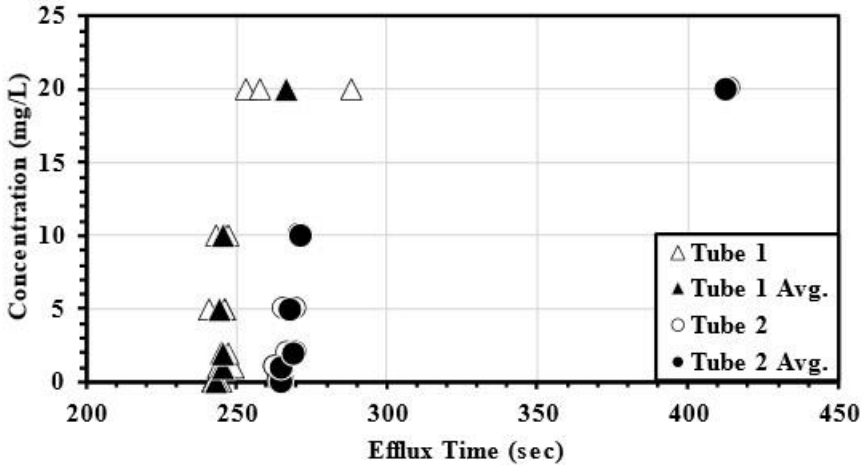

Figure 3-3. Cannon-Fenske Tube Test Results

Figure 3-4 displays the percent change plot where the average efflux time for each concentration is compared to the tap water average efflux time. This plot makes it easier to visualize how similar the low-concentration efflux times are to tap water with no PAM.

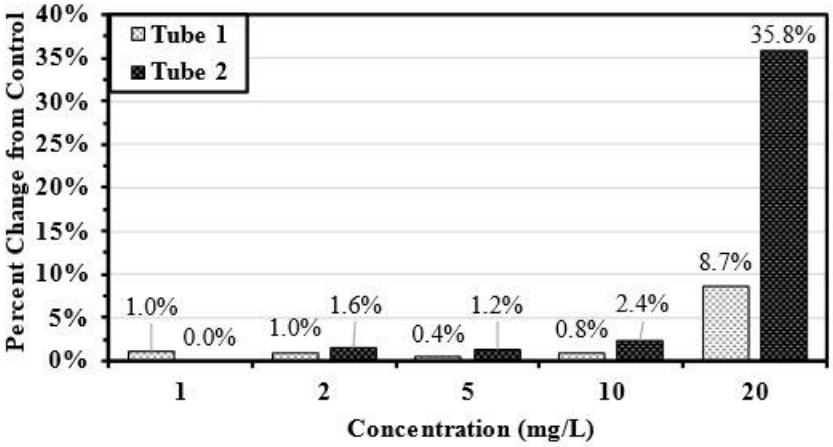

Figure 3-4. Cannon-Fenske Tube Percent Change Plot

A categorical MLR was also run to determine what concentrations significantly differed from the control (tap water with no PAM) between the two Cannon-Fenske tubes. Results for both tubes produced results that could measure change in concentrations above 5 mg/L by the sample's viscosity. Tube 2 results reported a significant change in efflux time with concentrations of 10 mg/L and 20 mg/L, while Tube 1 only had a significant change in efflux time with 20 mg/L.

Indicating that this method is not sensitive enough to measure the manufacturer's recommended dosage concentrations and would only provide insight if increased dosing is already occurring. Additionally, the difference in readings between Tube 1 and Tube 2 suggests that sensitivity results may vary with different Cannon-Fenske tubes. Note that this test used the second smallest tube size of 50 with a viscosity range of 0.8 to 4.0 mm^2/s. The smallest Cannon-Fenske tube size is 25 with a viscosity range of 0.5 to 2.0 mm^2/s. So, there is a possibility that the size 25 tube would be capable of measuring changes in viscosity at lower concentrations. However, it is important to note that Cannon-Fenske tubes require samples to be purified of all any possible solids that may clog the tubing. Since this method was evaluated for the possibility of large-scale applications, field samples would likely contain small amounts of sediment that would need to be completely removed before placing in the Cannon-Fenske tube. Thus, adding an additional source of possible error in readings and an additional challenge to mitigate in the field.

Table 3-4. Cannon-Fenske Tube Multiple Linear Regression Analysis

	Tube 1		Tube 2	
Variables	**Coefficient**	**p-value[a]**	**Coefficient**	**p-value[a]**
Intercept	243.250	<0.001	264.750	<0.001
1.0 mg/L	2.750	0.647	-0.750	0.756
2.0 mg/L	2.417	0.687	4.250	0.095
5.0 mg/L	1.083	0.856	3.250	0.192
10.0 mg/L	2.083	0.728	6.583	0.015
20.0 mg/L	23.083	0.002	147.917	<0.001
R2	0.608		0.998	

[a]Comparison to effects of base at 95% confidence interval and p-value <0.05

Cannon-Fenske Routine viscometers measure a solution's efflux time between two points, which needs converted to into units that describe viscosity. For this experiment, values were not converted into viscosity units as the results did not produce significant results within the desired range of 5 mg/L and the calibration certificates for the Cannon-Fenske Routine viscometers used were not located, which contain necessary information to conduct constant calculations. The process to convert efflux time results into viscosity is done with a viscometer constant. This constantly changes with each temperature. Cannon-Fenske Routine viscometer's calibration must be done using 0.33 fl oz (10 mL) of a standard at 77°F (25°C) (Cannon Instrument Company, 2018). Using the ASTM standard for kinematic viscometers (ASTM International D446-12, 2009), Eq. 3-1 can be used to determine the viscometer constant at other temperatures.

$$C = C_0\left(1 - \left[\frac{4V(\rho_f - \rho_t)}{\pi d^2 h \rho_t (T_t - T_f)}\right][T_t - T_f]\right) \quad \text{Eq. 3-1}$$

Where C is the constant of the viscometer being calibrated; C_0 is the constant of the calibrated viscometer; V is the volume of charge, cm3, given value on the Cannon calibration certificate for that particular Cannon-Fenske Routine viscometer; ρ_f is the fill density, g/cm^3; ρ_t is the test density, g/cm^3; d is the average diameter of the meniscus in the upper reservoir, cm, given value on the Cannon calibration certificate for that particular Cannon-Fenske Routine viscometer; h is the average driving head, cm, given value on the Cannon calibration certificate

for that particular Cannon-Fenske Routine viscometer; T_t is the test temperature, ℃; and T_f is the fill temperature, ℃. Since flocculants differ in density by type and manufacturer, it is recommended to use a pycnometer to determine the density of the solution at each concentration for accurate calculations (ASTM International D789-19, 2008).

Eq. 3-2 would be used to convert the measured efflux time to kinematic viscosity (ASTM International D446-12, 2009).

$$v = tC \quad \text{Eq. 3-2}$$

Where v is the kinematic viscosity is in mm^2/s; t is the efflux time, sec; C is the viscometer constant.

Eq. 3-3 would be the last step used to convert the kinematic viscosity to viscosity (Cannon Instrument Company, 2018).

$$\mu = vd \quad \text{Eq. 3-3}$$

Where μ is the viscosity, cP; $nu{:}\, v$ is the kinematic viscosity is in mm^2/s; and d is the density, g/mL.

3.3.1.2 BROOKFIELD DIGITAL VISCOMETER

The second instrument that was tested for measuring viscosity was the Brookfield Digital Viscometer (Figure 3-5). It is a type of rotational viscometer where it measures the viscosity of a fluid by measuring the torque required to rotate a spindle at a constant speed inside a fluid (Brookfield Engineering Laboratories, 1985). Users can select the desired spindle size, depending on the expected viscosity range of the fluid. The selected spindle is attached to a rotating shaft and lowered into a fluid. When the spindle reaches a constant speed, the percent torque value is displayed. Newer machines have the capability to calculate and display the viscosity units, however, the machine used for this testing only displayed the percent torque, which was then

converted into viscosity units. This method was tested due to its low cost and simplicity of use, making it an ideal possibility for companies and state DOTs to invest and adopt the method.

Figure 3-5. Brookfield Digital Viscometer Testing Apparatus

3.3.1.3 BROOKFIELD DIGITAL VISCOMETER TESTING METHODOLOGY

For this study, a #2 spindle was used on the Brookfield Digital Viscometer, model RVTD. Samples with G-PAM concentrations ranging from 1.0 mg/L to 20 mg/L, with the control being 0 mg/L of flocculant were evaluated. One liter stock solutions of each sample were created using tap water from the City of Auburn, Alabama. Each stock solution was then poured into three 6.76 fl oz (200 mL) beakers for three replicates of each measured concentration. The #2 spindle was then placed at a constant depth for each sample. Next, the machine was switched on, and the percent torque reading was set to zero. The motor was then switched on to allow the spindle to begin spinning. The rotational speed and spindle used for each sample was recorded. After about 30 seconds, the percent torque reading would stabilize, and the value was recorded. Once the data for the sample was collected, the spindle was removed and rinsed with deionized water and wiped clean with a one percent Alconox® Liquinox cleaning solution. Operating manuals contain pertinent information regarding how to convert the percent torque reading to viscosity, depending

on the viscometer model, spindle shape and size used, and rotational speed chosen. All tests in this study were conducted using a RV series viscometer, #2 spindle, at 50 rpm, which gives a constant factor of 8 used in the calculations (Brookfield, 2014).

Eq. 3-4 is the formula needed to convert the percent torque output value to viscosity,

$$\mu = \%torque * Factor \quad \text{Eq. 3-4}$$

where μ is the viscosity, cP; $\%torque$ is the output value given by the viscometer; and $Factor$ is the factor constant found in the operating manual that is dependent on the spindle size and rotational speed used.

3.3.1.4 Brookfield Digital Viscometer Results and Discussion

The viscometer readings fluctuated between 0.9 and 1.0% torque, which translated to 7.2 to 8.0 cP. When the results were averaged, samples that fluctuated between those two values can be found with values of 7.7 cP. Table 3-5 displays the average of three readings for each concentration.

Table 3-5. Brookfield Digital Viscometer Measured Values

Concentration, mg/L	pH	Temperature, °F (°C)	% Torque	Viscosity, cP
0.0	7.2	72.6 (22.6)	0.9	7.2
1.0	7.2	75.7 (24.3)	1.0	8.0
2.0	7.2	75.7 (24.3)	1.0	7.7
5.0	7.2	75.0 (23.9)	1.0	7.7
10.0	7.2	75.0 (23.9)	1.0	8.0
20.0	7.2	75.4 (24.1)	1.0	7.7

Figure 3-6 plots all data points with the averaged data from Table 3-5. Making it easier to see which concentrations produced consistent readings.

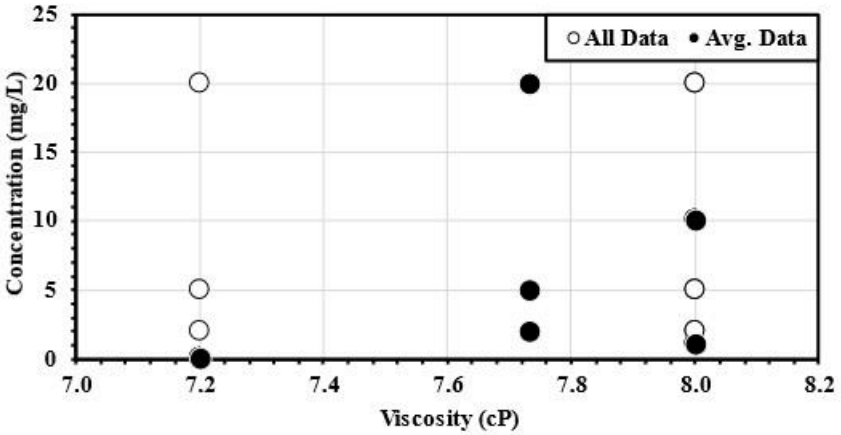

Figure 3-6. Brookfield Digital Viscometer Test Results

Figure 3-7 displays a percent change plot where each concentration of PAM tested is compared to the control (tap water with no PAM).

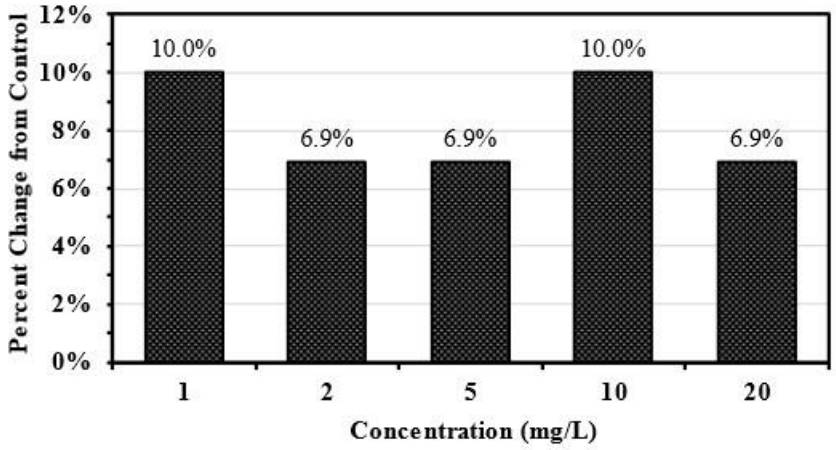

Figure 3-7. Brookfield Digital Viscometer Percent Change Plot

The concentrations with a 10% change significantly differed from the control when the results were run through a categorical MLR (Table 3-6). Indicating that only the samples which produced consistent readings through all three replicates were found to be significant. However, these concentrations were 1.0 mg/L and 10 mg/L. Since the viscometer used was not capable of producing readings between 0.9 and 1.0% torque, and the values between those concentrations were found to produce inconsistent results between the three replications, it suggests the significant

results were produced more by chance, rather than by the characteristics of the fluids tested. With addition to that, the manual states that values under 10% torque are considered inaccurate as the machine has a ± 1% error. Since all readings were well below the 10% torque threshold, it confirms that the viscosity of PAM flocculant solutions at concentrations below 20 mg/L are not capable of being measured using the Brookfield Digital Viscometer.

Table 3-6. Brookfield Digital Viscometer Multiple Linear Regression Analysis

Variables	Coefficient	p-value[a]
Intercept	7.200	<0.001
1.0 mg/L	0.800	0.011
2.0 mg/L	0.533	0.069
5.0 mg/L	0.533	0.069
10.0 mg/L	0.800	0.011
20.0 mg/L	0.533	0.069
R2	0.500	

[a]Comparison to effects of base at 95% confidence interval and p-value <0.05

3.3.2 LABORATORY CHARGE ANALYZER

A Laboratory Charge Analyzer (LCA) (Figure 3-8), also referred to as Streaming Current Detector or Particle Charge Analyzer, is a type of streaming current device which is used to determine the net charge in a sample via the streaming current detection method (Bachand et al., 2010; Bhatia et al., 2014; Chmtrac Systems Inc., 2017). This technology is commonly used in research and development, as well as industrial applications for a variety of applications, including flocculant use.

Figure 3-8. Laboratory Charge Analyzer Testing Apparatus

The product used for this study was an LCA-02 from Chemtrac Systems, Inc. A streaming current device (SCD) identified by its reciprocating plastic piston inside a cylindrical measuring cell, equipped with two electrodes on opposite ends of the cell. An aqueous sample flows freely through the circular orifice above the piston and electrodes. See Figure 3-9(a) for location of each described feature. The reciprocating piston sits between the two electrodes and displaces the liquid inside, forcing it to move rapidly inside the cylindrical measuring cell with each up- and down-stroke. Creating an alternating current, which uses Van Der Waals attraction forces to causes select counter-ions to move to the cylinder walls, generating a tiny current which is detected via the electrodes positioned in the measuring cell (Bhatia et al., 2014; Chmtrac Systems Inc., 2017). The SCD measures the existing charge on suspended particles (Muzi Sibiya, 2014), which is different from pH that is measured by determining the electrical potential (Xylem, 2023). There is currently no ASTM standard for a SCD method (Bhatia et al., 2014). For optimal readings, the probe depth is based on the sample level relative to the open orifice. Figure 3-9(b) shows the two acceptable iterations to achieve consistent results. Users should consult the product manual for the specific make and model. A magnetic stir bar is used to keep the sample continuously moving.

Failure to use the stir bar will result in inaccurate readings. The LCA machine has the capability to be equipped with a temperature and pH probe if desired.

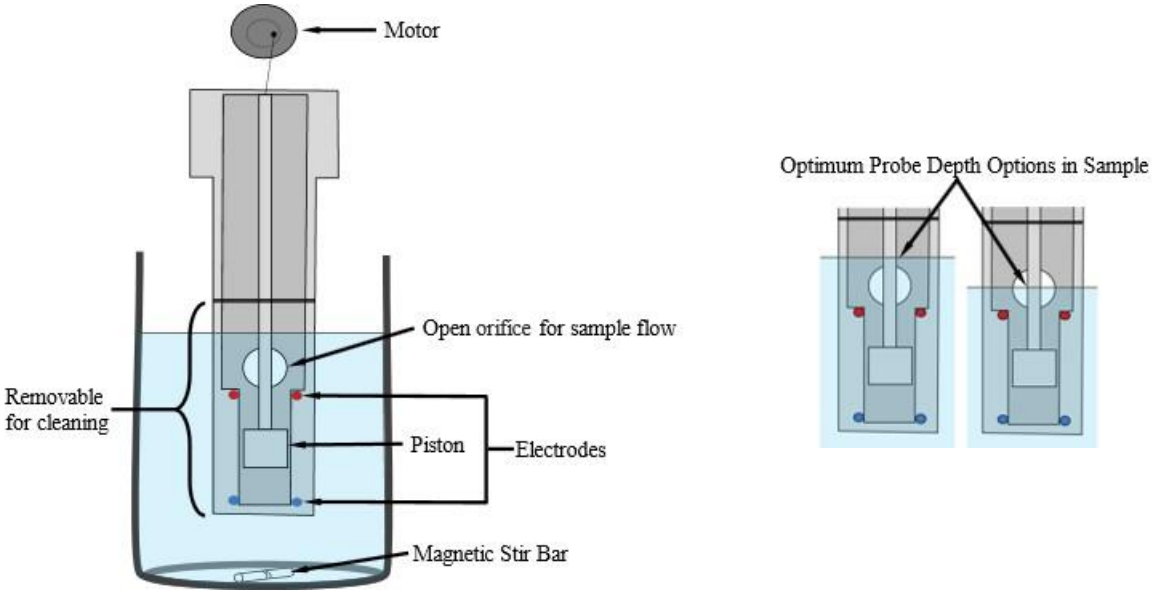

(a) sensor schematic (b) optimum probe depth

Figure 3-9. Streaming Current Device

The LCA has been found to be a quick and effective way of measuring a variety of cationic residual flocculant concentrations (Bachand et al., 2010; Bhatia et al., 2014). However, the exploration of evaluating its performance with anionic flocculants is minimal. This is lack of research is because the machine is not designed for measuring negative concentrations (Chmtrac Systems Inc, 2017). Nevertheless, this study investigated evaluating the use of anionic PAM flocculants using the LCA. The decision was justified as the LCA machine was capable of detecting a small range of negative values. Since this study focused on detecting concentrations above and below 5 mg/L, this study aimed to see if the charge streaming current value (SCV), or also referred to as the particle charge or ionic charge, was within the accurately measurable range.

3.3.2.1 LABORATORY CHARGE ANALYZER TESTING METHODOLOGY

The LCA was used to evaluate three different flocculant forms at various concentrations. Both G-PAM and B-PAM forms were evaluated at concentrations ranging from 0.125 to 7.00 mg/L and 0.250 to 7.00 mg/L, respectively. One cationic flocculant, chitosan, was also evaluated to compare negative and positive residual flocculant detection trends. Chitosan was evaluated in concentrations ranging from 20.0 to 200 mg/L. Both anionic flocculants used have a 5.0 mg/L manufacturer dosage recommendation, and chitosan's manufacturer dosage recommendation was set to 100 mg/L. Values below and above the manufacturer dosage recommendations were evaluated.

A stock of tap water from the City of Auburn, Alabama was used to ensure that all samples were at the same initial pH and similar water temperatures. Beakers with a maximum volume of 50.72 fl oz (1,500 mL) were used to hold each 30.81 fl oz (1000 mL) sample. The LCA machine was equipped with a probe to measure the temperature of the sample and the pH was recorded with a hand-held pH meter separately. Concentrations of 1, 3, 5, and 7 mg/L of G-PAM was used for this calibration test. The same concentrations were evaluated for B-PAM. Chitosan was evaluated in concentrations of 20, 40, 80, 100, and 200 mg/L of Product J from Manufacturer IV was added to each of the respective beakers when the next sample was ready and was flash mixed at 120 rpm for 1 minute with the paddle mixer. Sample was then transferred to the LCA machine, and a magnetic stirrer was placed in the sample and set on high. The SCD requires constant monitoring to ensure the sample continues to stir continuously. Stagnant samples will result in inaccurate readings. After the SCD was lowered into the sample to depths previously mentioned in Figure 3-9(b), the pH meter was propped to sit in the sample and obtain an accurate pH reading while the machine obtained a stable reading. Once the pH meter and SCD had stabilized, results were

recorded. The machine was flushed with deionized water between each sample and wiped down with a clean shop towel to remove any extra debris. Once a sample set was completed, the SCD was disassembled and scrubbed clean with a pipe cleaner brush and Alconox® Liquinox cleaning solution and rinsed thoroughly with deionized water to ensure all soil and flocculant were removed as best as possible. The next sample was placed on the magnetic stirrer and this process was repeated. Each sample was replicated three times to identify inconsistencies. Once all samples clean tap water samples (notated as No Sediment) were run through the LCA, 20g of sandy clay loam AU-SRF soil, located in East Alabama, was sieved through #200 sieve was added to each beaker and flash mixed at 120 rpm for 1 min. The sample was then given 15 min to settle, and the supernatant was separated and ran through the SCD again (notated as Sediment) to see how the pH and increased turbidity impacted the same readings. Supernatant samples had turbidity values between 5.00 to 100 NTU. Samples that did not contain any flocculant for both the No Sediment and Supernatant samples were used as the control.

Some important thing to note is that the flocculant in each sample must be completely dissolved to obtain accurate readings. During testing, the includes the average time taken to ensure each sample was fully aqueous and time to obtain a stable reading were recorded and included in Table 3-7.

Table 3-7. Brookfield Digital Viscometer Multiple Linear Regression Analysis

Flocculant Type	Time to Fully Dissolve, hr	Time for LCA to Obtain a Stable Reading, min
G-PAM	~0.5	10-20*
B-PAM	2-3	10-20*
Liquid Chitosan	N/A	3-10

N/A = sample is already in liquid form and thus only needs to be adequately mixed
*Samples <1.0 mg/L took between 30-45 min

The term “fish eyes” is used to describe a water/polymer gelatinous mass present in water which originated from a dry flocculant application that was insufficiently hydrated after application and

before water introduction (Druschel, 2014; Mainland Machinery, 2023; Mclaughlin & Zimmerman, 2008; WATERTECH of America Inc., 2023). Figure 3-10 displays an example of when 'fish eyes' are present in a sample. G-PAM and B-PAM form flocculants were considered fully aqueous when 'fish eyes' were no longer visible in the sample. Lastly, the supernatant sample, after sediment introduction into each sample, still contained small amounts of sediment. This sediment could build up in the piston area of the SCD and cause readings to take longer. If the signal health on the LCA display remained above 95%, the machine is in acceptable condition to continue processing the sample. If the signal health reading dropped below 95%, the user would need to remove the sample, disassemble, and clean the SCD before completing the sample reading or continuing with further sample processing.

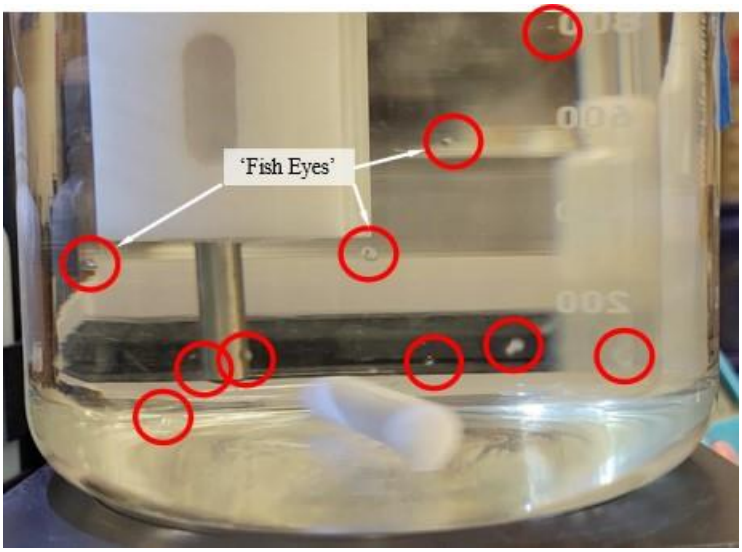

Figure 3-10. Flocculant 'Fish Eyes'

3.3.2.2 Laboratory Charge Analyzer Testing Results and Discussion

This analysis broke the data up by flocculant type and compared the SCV readings produced from the LCA to the measured concentration and pH value. Figure 3-11 displays the SCV readings against the flocculant concentration. Note that Figure 3-11(a) and (b) have the same

x- and y-axis units and Figure 3-11(c) is drastically different. This is because the manufacturer's recommended dosage of the G-PAM and B-PAM forms was the same, while the chitosan was much higher. Additionally, G-PAM and B-PAM form flocculants are both anionic, while chitosan is cationic.

Figure 3-11(a), G-PAM, presents a separation of two linear plots, No Sediment and Supernatant samples, for concentrations below 1 mg/L where the trend is rapidly decreasing in SCV, concentrations above 1 mg/L, the trend flattens out. Meaning that anionic G-PAM can be detected using a SCD; however, it would not serve as an accurate approximation for concentration of flocculant present at concentrations above 1 mg/L. Making it difficult to know if increased dosing is occurring.

Figure 3-11(b), B-PAM, yielded less consistent results. For Supernatant samples, concentrations below 1 mg/L increased in SCV with a logarithmic trend and the trend for greater than 1 mg/L rapidly decreased in SCV linearly when soil is present. Making it difficult to predict low concentrations. However, it could be used for predicting higher concentrations to know if increased dosing is occurring. Interestingly, the inverse relationship with the increase and decrease of SCV values occurred with No Sediment samples. Meaning that this relationship may change with different soil types and would need to be evaluated further.

No Sediment sample presented in Figure 3-11I, anionic chitosan, displayed a power function trend between 0 mg/L to 80 mg/L, where values above 80 mg/L form a linear trend with a slightly increasing slope. The Supernatant samples presented a logarithmic relationship where the lowest concentration evaluated (20 mg/L) was presented as the point where the logarithmic trend flattens out. Meaning that the use of an LCA to estimate Chitosan concentrations in the field

could be used to estimate the presence of flocculant but not accurately estimate the concentration present or if increased dosing is occurring.

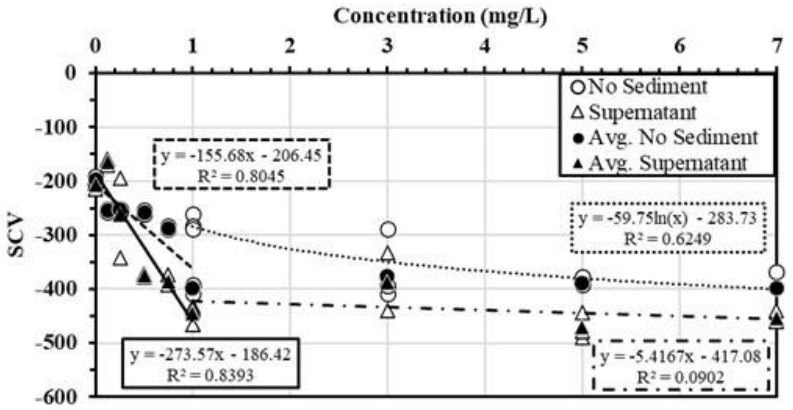

(a) G-PAM

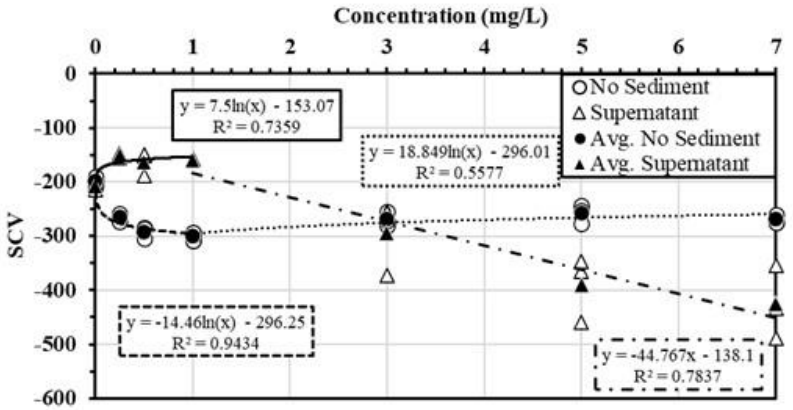

(b) B-PAM

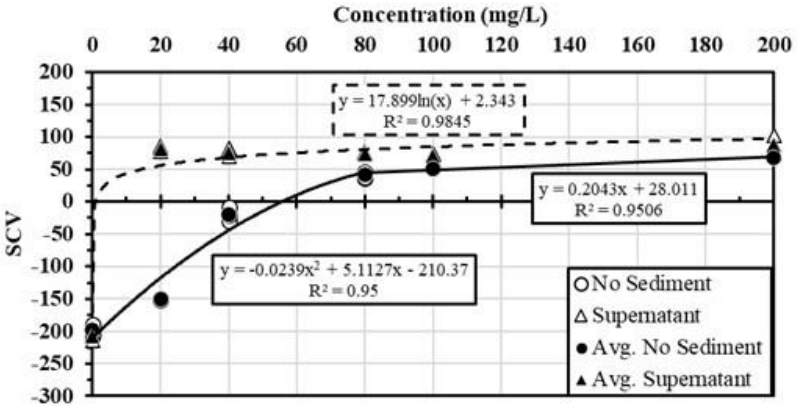

(c) chitosan

Figure 3-11. Flocculant Concentration Trends Against Their Streaming Current Value

Figure 3-12 displays the percent change from the control (no flocculant for both No Sediment and Supernatant samples) for each flocculant evaluated. For both anionic flocculant forms, Figure 3-12(a) and Figure 3-12(b), all No Sediment samples had a negative percent change compared to the control. Meaning that anionic flocculant indeed decreased the water's SCV, whereas the cationic flocculant had reverse results.

In Figure 3-12(a), G-PAM had a relatively similar percent change values for No Sediment and Supernatant samples. Meaning that the addition of sediment leads to similar results at concentrations above 1.00 mg/L.

In Figure 3-12(b), B-PAM indicates that sediment introduction from the Supernatant samples has a drastic impact on the SCV value. Showing the same trend is displayed in Figure 3-11(b) where concentrations below 1.00 mg/L increased the SCV and above 1.00 mg/L decreased it.

Chitosan flocculant, Figure 3-11(c), increased the SCV across all concentrations for No Sediment and Supernatant samples. While the No Sediment samples increased in SCV with concentration, the Supernatant samples at all concentrations had roughly the same percent change.

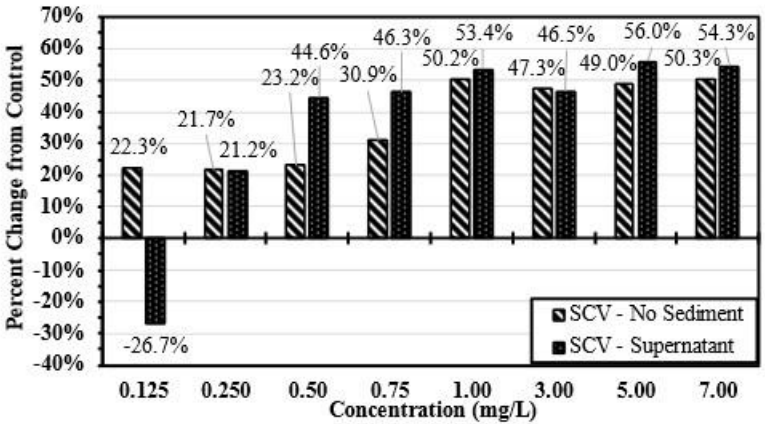

(a) G-PAM

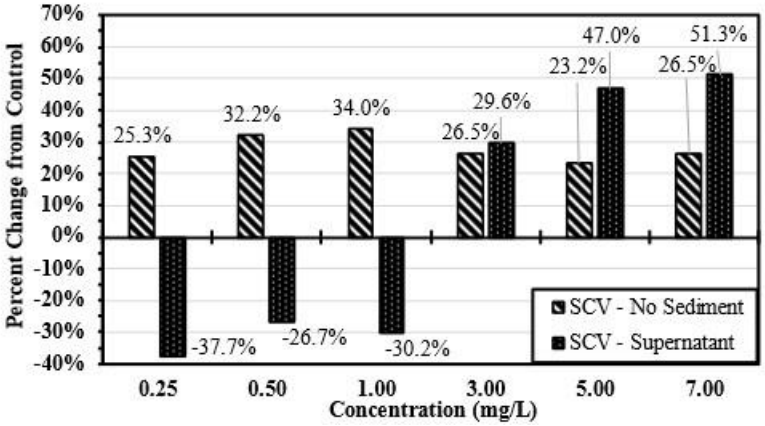

(b) B-PAM

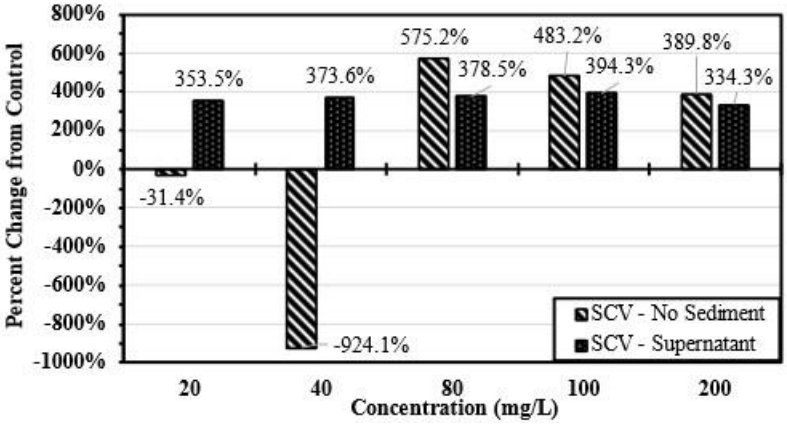

(c) chitosan

Figure 3-12. Streaming Current Value Percent Change from Control (no flocculant) Across Concentrations

Figure 3-13 displays how the SCV and pH compared to each other show data groupings at low and high flocculant concentrations. Presenting as another method for estimating flocculant

presence for each evaluated flocculant type. Note that Figure 3-13(a) and (b) have the same y-axis, while Figure 3-13(c) changes, due to the anionic and cationic properties of the evaluated flocculants. This evaluation shows the relationship between the SCV value from a variety of flocculant concentrations and water pH. Showing that the use of any flocculant type can influence the overall pH of water. When sediment is introduced to flocculated water, depending on the soil type, it can help counteract the pH changes made. Note that conclusions made is from data collected from sample temperatures between of 70.2 to 72.0 °F (21.2 to 22.2°C) and a pH of 7.3. Further testing should be done to explore the relationships across various temperatures and pH ranges to see if data patterns persist.

Figure 3-13(a), G-PAM, Supernatant results show that concentrations above and below 0.25 mg/L can be easily distinguished through data. The same claim can be made with above and below 1 mg/L of G-PAM in No Sediment samples. Figure 3-13(b), B-PAM groupings can be seen for concentrations between 0.25 to 1.00 mg/L and above 5.0 mg/L in Supernatant samples. No Sediment samples yielded two distinct tight groupings with and without flocculant. Figure 3-13(c), shows that in Supernatant samples, samples without flocculant started with a negative SCV value. When chitosan flocculant was added, all SCV readings were positively charged and formed a data cluster where concentrations above 20 mg/L can be easily identified. Whereas No Sediment samples show groupings at 0, 25, 40, and above 80 mg/L.

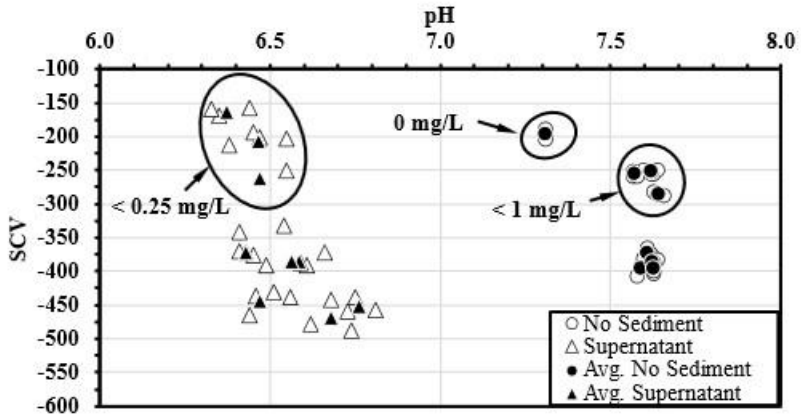

(a) G-PAM

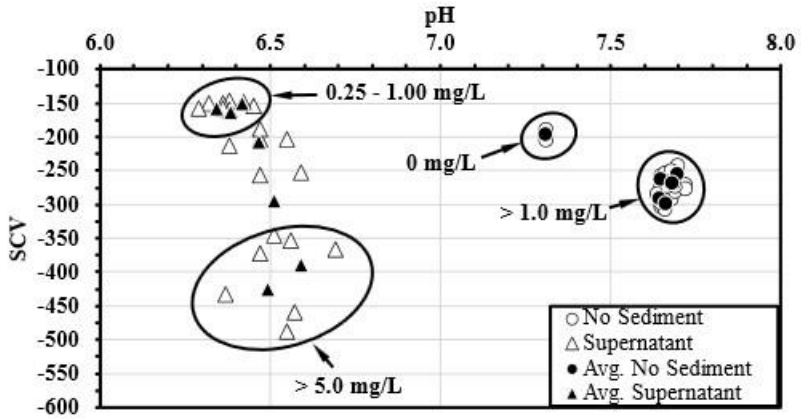

(b) B-PAM

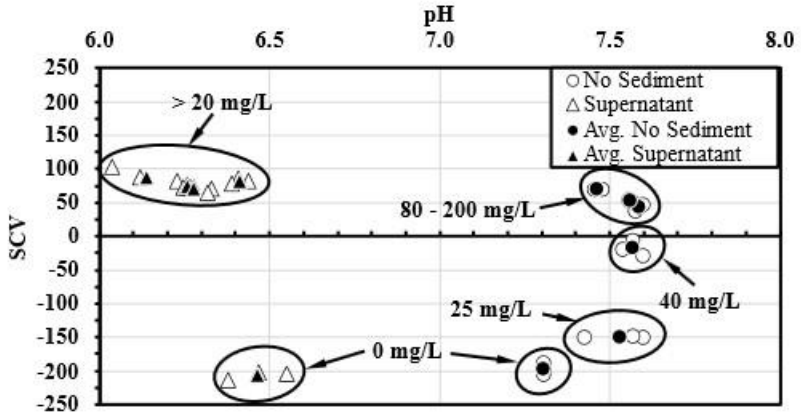

(c) chitosan

Figure 3-13. pH Trends Against Their Streaming Current Value

A categorical MLR, Table 3-8, was ran to identify the concentrations of each flocculant type significantly influenced the SCV. Both G-PAM and B-PAM form flocculants significantly

lowered the SCV while chitosan significantly increased for No Sediment samples at every concentration. Although, after sediment was introduced, the Supernatant samples showed that G-PAM and B-PAM forms only significantly decrease the SCV after 0.5 mg/L and 3.0 mg/L, respectively. While chitosan continued to display a significant increase in SCV readings at all concentrations for Supernatant samples. Meaning that concentrations with significant differences in SCV are, at minimum, distinguishable from the control and can indicate the presence of flocculant. In other words, concentrations above 20 mg/L of cationic flocculant have significant changes in SCV compared to the control of no flocculant, so this testing method is capable of distinguishing chitosan concentrations between 20 to 200 mg/L. Between 0.5 to 7.0 mg/L of G-PAM and 3.0 to 7.0 mg/L of B-PAM are predictable concentration ranges for this testing method.

Table 3-8. Streaming Current Value Multiple Linear Regression Analysis

	No Sediment		Supernatant	
	Coefficients	**p-value[a]**	**Coefficients**	**p-value[a]**
Constant	-198.000	<0.001	-207.000	<0.001
G-PAM (Base: 0 mg/L)				
0.125 mg/L	-56.667	<0.001	43.667	0.120
0.25 mg/L	-55.000	<0.001	-55.667	0.052
0.50 mg/L	-59.667	<0.001	-166.667	<0.001
0.75 mg/L	-88.667	<0.001	-178.333	<0.001
1.00 mg/L	-199.333	<0.001	-237.667	<0.001
3.00 mg/L	-177.667	<0.001	-180.000	<0.001
5.00 mg/L	-190.333	<0.001	-263.333	<0.001
7.00 mg/L	-200.333	<0.001	-246.000	<0.001
B-PAM (Base: 0 mg/L)				
0.25 mg/L	-67.000	<0.001	56.667	0.134
0.50 mg/L	-94.000	<0.001	43.667	0.241
0.75 mg/L	-102.000	<0.001	48.000	0.200
3.00 mg/L	-71.333	<0.001	-87.000	0.029
5.00 mg/L	-59.667	<0.001	-183.333	<0.001
7.00 mg/L	-71.333	<0.001	-218.333	<0.001
Chitosan (Base: 0 mg/L)				
20 mg/L	47.333	<0.001	288.667	<0.001
40 mg/L	178.667	<0.001	282.667	<0.001
80 mg/L	239.667	<0.001	281.333	<0.001
100 mg/L	249.667	<0.001	277.333	<0.001
200 mg/L	266.333	<0.001	295.333	<0.001
R2 Values				
G-PAM	0.994		0.940	
B-PAM	0.921		0.900	
Chitosan	0.998		0.997	

[a]Comparison to effects of base at 95% confidence interval and p-value <0.05

Data was also evaluated to see how the pH changes across increasing concentrations of flocculant. Figure 3-14 shows how the pH varies with flocculant concentrations compared to the control (no flocculant present). Data patterns show that when flocculant is added to tap water, the pH increases, regardless of if the flocculant added is cationic or anionic. This trend is also visible in the MLR shown in Table 3-9, where once the flocculant is added, it causes a significant change in pH at all concentrations, compared to the control. The anionic flocculants produced similar coefficients, indicating that the expected pH change when either G-PAM or B-PAM flocculants

are added to water at any concentration will yield comparable results. This pattern persists with a lower coefficient for cationic flocculants.

Though, if AU-SRF sandy clay loam sieved sediment is added and mixed into flocculated water, it lowers the pH back down near the initial tap water pH at lower concentrations. For G-PAM, Figure 3-14(a), as the concentration increases, the sediment added becomes less effective at combatting the pH change. For B-PAM, Figure 3-14(b), the results are less consistent with increasing concentrations. After sediment introduction for chitosan flocculant, Figure 3-14(c), pH continued to decrease as the flocculant concentration increased.

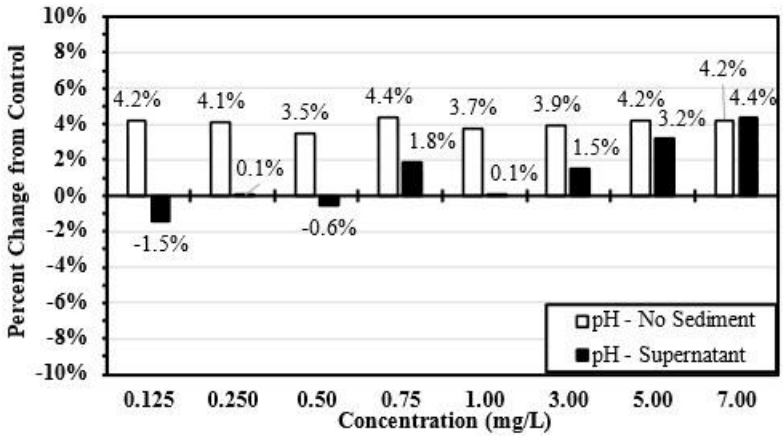

(a) G-PAM

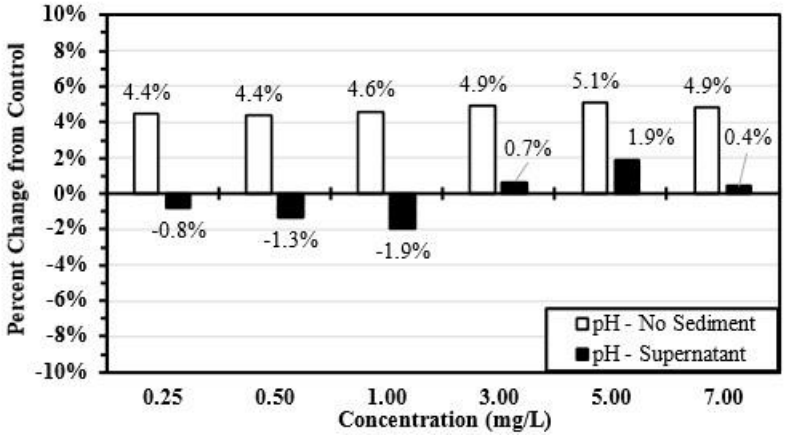

(b) B-PAM

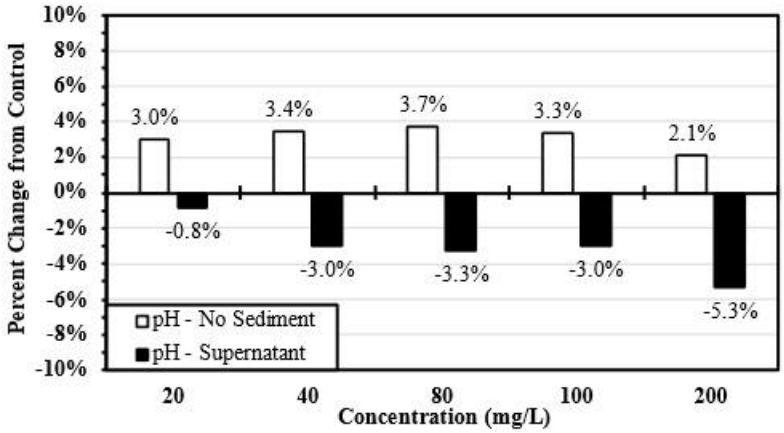

(c) chitosan

Figure 3-14. pH Percent Change from Control (no flocculant) Across Concentrations

Table 3-9 the significant change in pH with Supernatant samples compared to 0 mg/L Supernatant samples. Showing the few concentrations that significantly change the pH with G-PAM and chitosan.

Table 3-9. pH Value Multiple Linear Regression Analysis

	No Sediment		Supernatant	
	Coefficients	**p-value[a]**	**Coefficients**	**p-value[a]**
Constant	7.310	<0.001	6.467	<0.001
G-PAM (Base: 0 mg/L)				
0.125 mg/L	0.317	<0.001	-0.093	0.068
0.25 mg/L	0.310	<0.001	0.003	0.945
0.50 mg/L	0.263	<0.001	-0.037	0.455
0.75 mg/L	0.333	<0.001	0.120	0.022
1.00 mg/L	0.283	<0.001	0.003	0.945
3.00 mg/L	0.300	<0.001	0.097	0.059
5.00 mg/L	0.317	<0.001	0.213	<0.001
7.00 mg/L	0.320	<0.001	0.297	<0.001
B-PAM (Base: 0 mg/L)				
0.25 mg/L	0.340	<0.001	-0.050	0.439
0.50 mg/L	0.337	<0.001	-0.083	0.206
0.75 mg/L	0.353	<0.001	-0.123	0.070
3.00 mg/L	0.380	<0.001	0.043	0.501
5.00 mg/L	0.390	<0.001	0.123	0.070
7.00 mg/L	0.373	<0.001	0.027	0.677
Chitosan (Base: 0 mg/L)				
20 mg/L	0.223	<0.001	-0.053	0.323
40 mg/L	0.260	<0.001	-0.187	0.004
80 mg/L	0.280	<0.001	-0.207	0.002
100 mg/L	0.253	<0.001	-0.187	0.004
200 mg/L	0.157	<0.001	-0.327	<0.001
R2 Values				
G-PAM	0.991		0.859	
B-PAM	0.990		0.921	
Chitosan	0.898		0.810	

[a]Comparison to effects of base at 95% confidence interval and p-value <0.05

However, a separate MLR was ran to determine if pH changed between No Sediment samples and Supernatant samples, Table 3-10, and results found that both G-PAM and chitosan flocculants significantly lowered the pH value.

Table 3-10. Supernatant pH Value Multiple Linear Regression Analysis (Base: No Sediment)

	Coefficients		p-value[a]
Constant	7.412		<0.001
G-PAM	-1.048		<0.001
R2		0.981	
Constant	7.470		<0.001
B-PAM	-1.163		<0.001
R2		0.979	
Constant	7.488		<0.001
Chitosan	-1.199		<0.001
R2		0.975	

[a]Comparison to effects of base at 95% confidence interval and p-value <0.05

3.3.3 SETTLING VELOCITY

The final flocculant concentration detection method used in this study was by measuring the settling velocity of flocs formed in a sample. This technique has been employed in oceanography and metallurgy to evaluate the porosity of large, suspended particles and the thickening capacity of flocculated suspensions, respectively (Kajihara, 1971; Parsapour et al., 2014). Using settling velocity to approximate flocculant concentrations for various flocculant types was developed by Kazaz et al. (2022). The settling velocity method was developed to be an evaluation method that could be easily adopted and performed by state DOTs for flocculant field monitoring. The foundation of settling velocity data was built using Stokes' Law, which highlights the drag fo'ce's resistive impact against the gravitational forces during the settling of a small spherical particle through a fluid medium, (Hunter, 1986; Singh & Adhikari, 2018). Equation (3-5), is used calculate the terminal settling velocity for a small spherical particle in a Newtonian fluid (Hunter, 1986).

$$U_{stokes} = \frac{-2gr^2(\rho_2 - \rho_1)}{9\mu_1} \quad (3\text{-}5)$$

Where U_{stokes} = terminal settling velocity (ft/s [m/s]); g = gravitational acceleration (ft/s^2 [m/s^2]); r = particle radius (ft [m]); ρ_2 = density of the small-sized spherical particle (slugs/ft^3 [kg/m^3]); ρ_1 = density of fluid (lb./ft^3 [kg/m^3]); and μ_1 = fluid viscosity (lb$_f$·s/ft^2 [N·s/m^2]).

Kazaz et al. (2022) evaluated 14 different flocculant products and six different manufacturers. Strong settling velocities correlations were found to fully define roughly 90% of known concentration values for each flocculant type. Although the results proved positive for large-scale application, the study was conducted using tap water in a lab setting. Whereas large-scale applications include an assortment of environmental conditions that influence flocculant efficacy and settling rate, such as soil types, metal salts, water salinity, pH, and temperature (Butler et al., 2021; Forbes, 2011; Kazaz et al., 2022; Labeeuw et al., 2021; O'Shea et al., 2010; Parsapour et al., 2014; Pérez et al., 2016; Roselet et al., 2015, 2017). This testing methodology was adopted and used to expand the settling velocity prediction curves to account for additional conditions present in the field to assist in more precise predictions.

Settling velocity calibration curves were created to account for a range of pH and temperatures at various flocculant concentrations. Soil used to develop the curves was a sandy clay loam from Eastern Alabama, sourced from AU-SRF. Calibration curves were designed with this soil type as later testing would be conducted at this site and the flocculants used were match tested to this specific type. Developing this calibration curve with the same soil type assisted in accounting for the possibility of salts present in the soil that may impact flocculation. This section will go over the testing methodology and results for creating soil and flocculant-specific calibration curves for G-PAM and B-PAM.

3.3.3.1 SETTLING VELOCITY CALIBRATION TESTING METHODOLOGY

A large plastic tub was used to set the pH of the water to the desired range. Smaller volumes are more difficult to set and control the pH range. The tub was filled with tap water from the City of Auburn, Alabama where the water temperature was close to the desired temperature. Low temperatures (50°F [10°C] and below) will require water to be chilled overnight prior to testing). Depending on the desired pH range, add acid or base buffering solution to tap water to raise or lower the pH, respectively. General Hydroponics pH Control acid and base buffering solutions were used to change the pH of tap water. A paint mixer was used to sufficiently mix solution before taking a pH reading. The water pH was set to values between 5.35 to 5.45, 6.35 to 6.45, 7.35 to 7.45, or 8.35 to 8.45 to ensure consistency between samples. Once the pH was within the desired range, the temperature was set by using heat lamps to raise the temperature. If samples needed cooled, 33.81 fl oz (1,000 mL) of pH set water was transferred to 50.72 fl oz (1,500 mL) glass beakers. All samples at each pH, temperature, and concentration were ran in triplicate to identify data inconsistencies. If the temperature needed to cool a couple degrees, samples would be placed in a refrigerator for 10-15 minutes. Samples that needed cooled to temperatures below 50°F (10°C) were placed in a salted ice bath, being careful to not contaminate the pH water with any salt. While the pH water was being set to the desired temperature, a Jar Test Multiple Stirrer machine cleaned prior to any use in case to remove any possible contaminates. This was done by rinsing the stirring rods, paddles, and paddle rest with deionized water, spraying with Alconox® Liquinox cleaning solution, and wiping clean with a paper towel.

Glass graduate cylinders were prepped with ruler tape on the cylinder side, with zero starting at the cylinder base. The cylinders were placed in front of a white poster board to aid in seeing gradients when samples were poured. A GoPro camera was set up in front of the graduated

cylinder and positioned so the top and bottom of the cylinder were visible in the GoPro screen. Ruler tape was positioned to the side of the cylinder in the GoPro screen to ensure it was not obstructing the view of the sample that would be poured. A digital clock - with hours, minutes, and seconds on display - was placed beside the cylinder and in the GoPro frame and used to record the sample settling time. See Figure 3-15 for placement of cylinder and clock in GoPro screen. Sourced sandy clay loam soil was sieved through #200 sieve and weighed out into jars, each containing 20g of sieved soil. A precision scale was used to weigh out flocculant. The scale was calibrated every day before use to ensure accurate weights. Flocculant was weighed with ±0.1 mg accuracy. The B-PAM was weighed out by using a cheese grater to create smaller pieces. Fresh material was grated daily and stored in an airtight jar to prevent it from drying out. Weighed B-PAM was used within 1 hour of weighing to ensure flocculant does not dry out and harden, which could impact results. If B-PAM hardened before use, sample was reweighed out with freshly grated flocculant block.

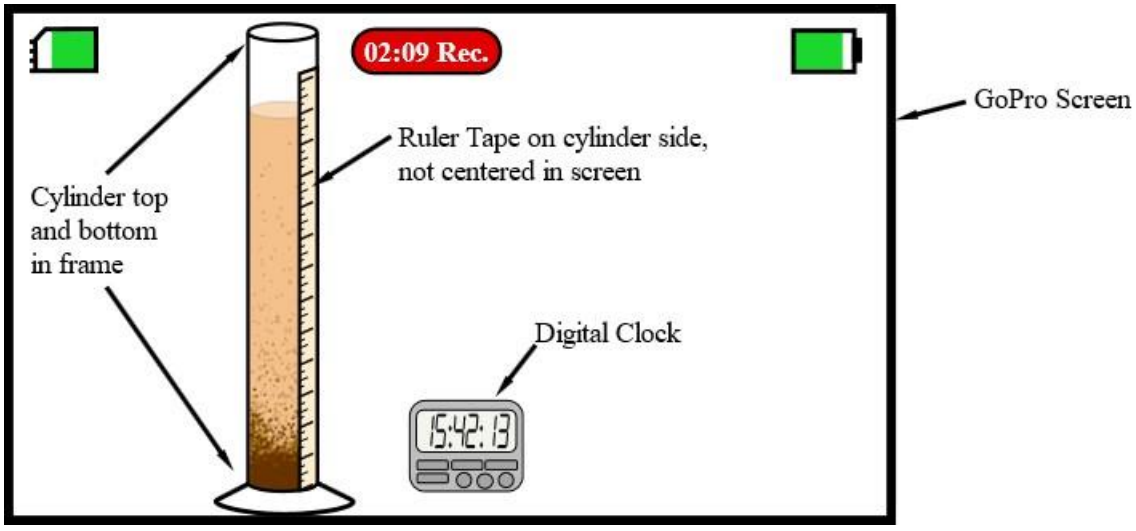

Figure 3-15. Placement of Cylinder and Clock Within GoPro Screen

Once the pH water reached the desired temperature, samples were moved to a jar test multiple stirrer machine and 20 g of sieved testing soil was added to the pH and temperature set

sample. The sample was then flash mixed (120 rpm) for one minute. Sample beakers were then removed from the machine and the weighed flocculant was added to the center of the beaker. Flocculant was never added to the sample was on the stirring machine and stirring rods in sample to prevent the possibility of flocculant sticking to the beaker sidewalls or stirring rod, which would prevent it from being mixed into the sample. GoPro video camera recording was started, and sample beakers were placed back on the stirrer machine and flash mixed (120 rpm) again for one minute. Samples were quickly removed from the machine and poured into the prepped glass cylinder, being sure to pour fast enough so that all sediment in sample remains suspended while pouring. Samples were recorded until sediment was fully settled, or for one hour if gradient was not easily visible. See Figure 3-16 for an example of a visible gradient and settled sample.

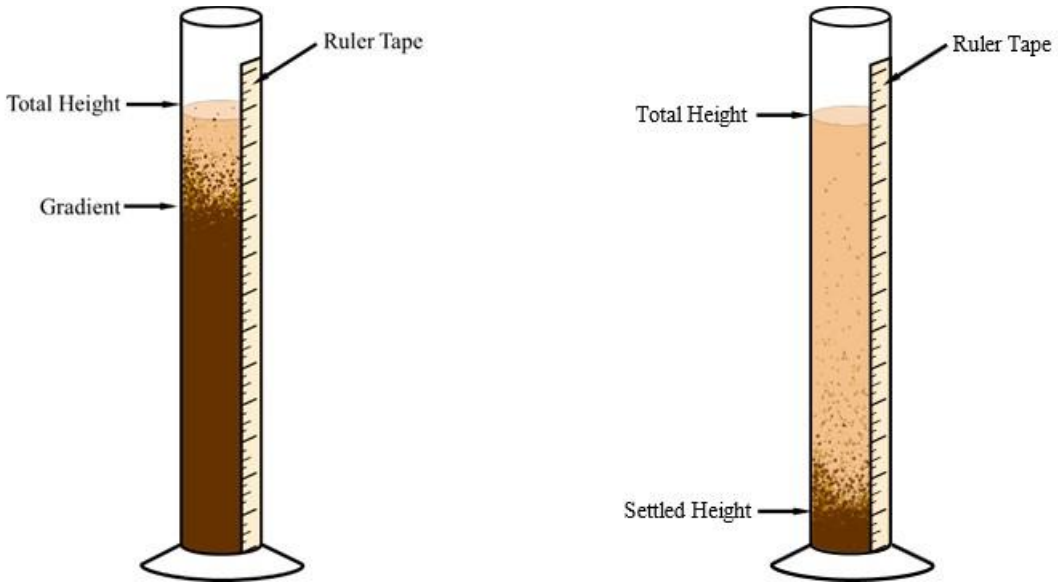

(a) visible gradient (b) settled sample

Figure 3-16. Visible Gradient and Settled Sample Example

After samples were settled, the glassware was cleaned with hot water and scrubbed clean with Alconox® Liquinox cleaning solution. The Jar Test Multiple Stirrer machine was cleaned by rinsing with deionized water, spraying with Alconox® Liquinox cleaning solution, and wipe clean with a paper towel. If sample flocculated under 30 sec, it is recommended to repeat the

cleaning process two or three time to ensure all flocculant is removed. GoPro video recordings of the sample were reviewed to capture the time the sample was poured, total height of the sample in the cylinder using the ruled tape in the cylinder side, settled time, and settled height. This information was then used to calculate the settling velocity by taking the difference in time and height for the soil to settle. Settle time and height varies depending on the floc size. Sample was considered as settled when the lowest gradient point touched the fully settled sediment. The settled height is taken at the same time the settled time is recorded as sediment will continue to compress after suspended sediment settles. See Figure 3-17 to visually understand how to determine when sample is settled. Note that some samples were difficult to determine a gradient. GoPro videos record in 10-minute video clips. If gradients could not distinguish between these video clips, a video editing software was used to stitch multiple video clips together. When moving the scrub bar rapidly back and forth across the entire settling time, a gradient was able to be distinguished. See Appendix B for a step-by-step testing procedure.

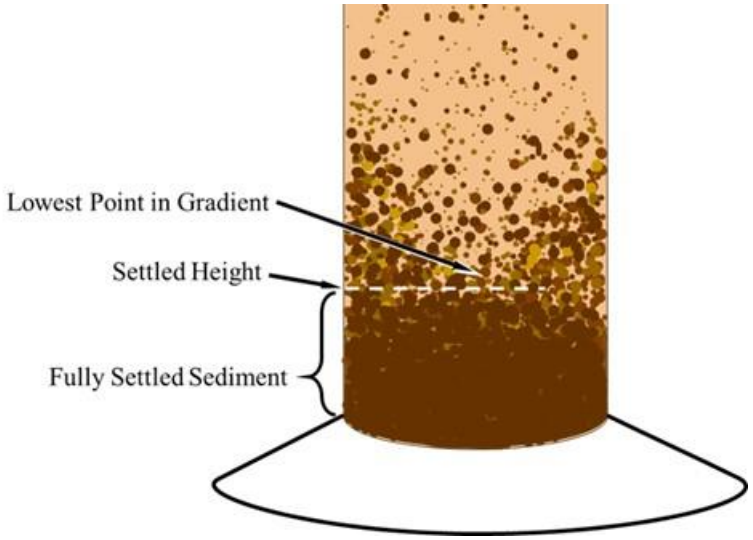

Figure 3-17. Determining Settled Sample Time and Height

This testing methodology has many possibilities for error and contamination. By being as efficient as possible with sample preparations, implementing a GoPro to record setting rates, use

of glassware rather than plastic, and strict cleaning procedures, several possible sources of error and contamination can be accounted for. The GoPro allows samples to be evaluated from the same distance and perspective and more precise sampling start and end times to be captured. Glassware is used rather than plastic to prevent PAM adhesion and cross-contamination. However, weighing out low-weight samples in milligrams, reusing glassware multiple times in one day, and reusing jar testing multiple stirrer machine, there are still possibilities for error and sample contamination. Cleaning glassware with hot water can help dilute and rid PAM from glassware and rinsing with deionized water and wiping the stirring machine multiple times with a cleaning agent can also assist in minimizing cross-contamination.

3.3.3.2 Granular PAM Settling Velocity Calibration Results and Discussion

A total of 80 samples were replicated three times at four pH concentrations between 5.4 to 8.4, four temperatures between 1.0 to 30℃, and five concentrations between 0.0 and 7.0 mg/L, resulting in 240 total samples evaluated to generate the G-PAM settling velocity calibration. A cumulative distribution function of the data (Figure 3-18) was used to determine the acceptable level of variability with the data once each of the initial samples were ran with the three replicates each. The CDF was created by calculating the standard deviation between the three replicates for each sample that was tested at the different pH values, temperatures, and concentrations measured, resulting in 80 total standard deviation values. The standard deviation values were then ranked in ascending order. The probably for the lowest standard deviation sample value was calculated by dividing one by the number of standard deviation values, yielding 1.25%. All subsequent probability calculations were calculated by adding 1.25% to the previous probability value. The largest standard deviation value should have a probability equal to 100%, if properly calculated. The standard deviation and probability values were then plotted on the CDF plot, Figure 3-18.

Here, the variability can be seen that of 90% of the data Is within 500 in./hr for the first 240 samples collected (initial samples). Meaning, the top 10% of the initial samples collected are considered as outliers. This was justified because the top 10% of the data was notably more dispersed. Therefore, any sample replicates that were more than 500 in./hr from the mean of the other two, all three replicates of that sample would be repeated. This process was repeated until all three sample replicates were within the specified range for each of the 80 samples. The final 240 samples that were within the specified range, were then plotted in the CDF plot.

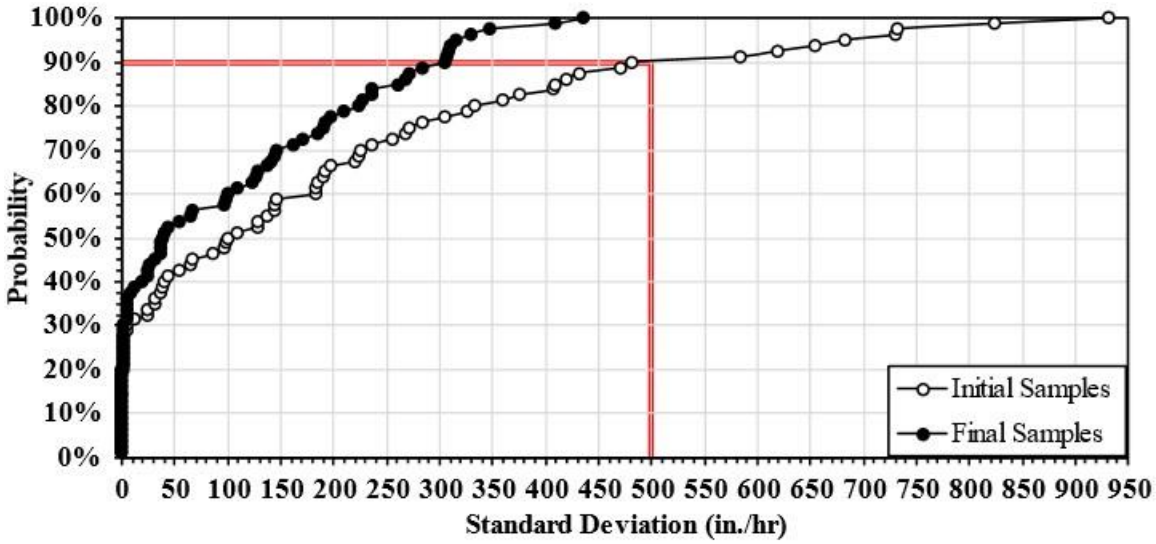

Figure 3-18. G-PAM CDF Plot

Figure 3-19 shows how each temperature, pH, and G-PAM concentration influences the settling rate. As the temperature increases, flocculant settling velocities increase across all pH concentrations, but these settling velocities are fastest at lower pH concentrations. This is because anionic PAM is a negatively charged functional group that is considered as a Lewis base due to its ability to donate electron pairs to a Lewis acid, enabling the formation of flocs through covalent bonds (Brown et al., 1989). A Lewis acid is defined as an atom, ion, or molecule that can accept an electron pair from another atom, while a Lewis base can donate the electron pair (Jensen, 1978).

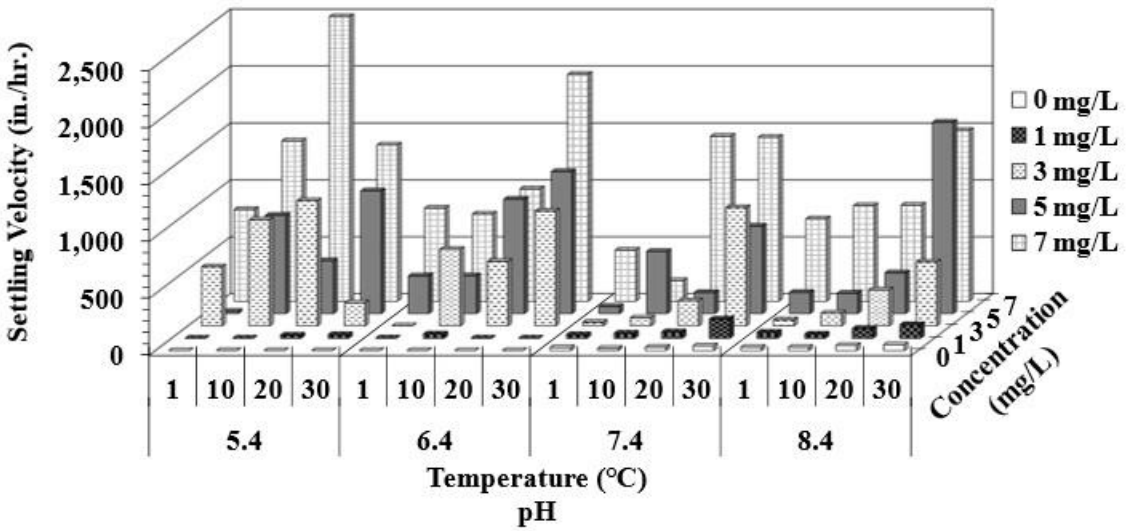

Figure 3-19. Soil Settling Velocity Against Different pH Concentrations, Temperatures, and Increasing G-PAM Concentrations

Table 3-11 shows MLR results that indicate pH, temperature, and G-PAM concentration all significantly influence the settling velocity. The MLR regression equation was rewritten to solve for G-PAM concentration, shown in Eq. 3-6.

Table 3-11. G-PAM Settling Velocity Multiple Linear Regression Analysis

	Coefficients	*p*-value[a]
Constant	153.134	0.305
pH	-68.605	<0.001
Temperature (°C)	17.536	<0.001
G-PAM Concentration (mg/L)	156.184	<0.001
R^2	0.620	

[a]Comparison to effects of base at 95% confidence interval and *p*-value <0.05

$$C_{g-PAM} = \frac{v_{settle} - 153.13 + 68.61pH - 17.54T}{156.18} \quad \text{Eq. 3-6}$$

Where C_{g-PAM} is the G-PAM concentration (mg/L); v_{settle} is the soil settling velocity (in./hr); pH is the pH value of sample before performing residual test; and T is the temperature of sample before performing residual test (°C). Allowing users to enter known pH, temperature, and measured settling velocity data from large-scale test samples to predict G-PAM dosing concentrations in the field during different seasons and geographical locations. Eq. 3-6 can be

rewritten to solve for the soil settling velocity, which can be used for detention pond designing to ensure the treated water has sufficient time to settle out of suspension before being discharged off-site. This equation was based on a concentration calibration range between 1 mg/L to 7 mg/L of G-PAM. High concentrations may not be accurate predictions. Even though data did include flocculant free settling velocities, the lowest flocculant concentration that could be accurately measured was 1 mg/L, thus, this equation is not able to accurately predict concentrations under 1 mg/L. Temperature and pH ranges used for this calibration equation accounted for 1.0 ℃ (34°F) to 30℃ (86°F), and 5.4 to 8.4 pH, respectively.

It is important to note that this equation is flocculant and soil specific. The flocculant used was G-PAM from Manufacturer I. Since flocculants are also soil specific and flocculants differ by manufacturer, a calibration curve for each flocculant type for each manufacturer matched with each soil type.

3.3.3.3 Block PAM Settling Velocity Calibration Results and Discussion

A total of 144 samples were replicated three times at four pH concentrations between 5.40 to 8.40, four temperatures between 1.0 ℃ (34°F) to 30℃ (86°F), and five concentrations between 0.00 and 200 mg/L, resulting in 432 total samples evaluated to generate the B-PAM settling velocity calibration. A cumulative distribution function of the data (Figure 3-20) was used to determine the acceptable level of variability with the data once each of the initial samples were ran with the three replicates each. The CDF was created by calculating the standard deviation between the three replicates for each sample that was tested at the different pH values, temperatures, and concentrations measured, resulting in 144 total standard deviation values. The standard deviation values were then ranked in ascending order. The probably for the lowest standard deviation sample value was calculated by dividing one by the number of standard deviation values, yielding 0.78%.

All subsequent probability calculations were calculated by adding 0.78% to the previous probability value. The largest standard deviation value should have a probability equal to 100%, if properly calculated. The standard deviation and probability values were then plotted on the CDF plot, Figure 3-20. Here, the variability can be seen that of 95% of the data is within 60 in./hr for the first 432 samples collected (initial samples). Meaning, the top 5% of the initial samples collected are considered as outliers. This was justified because the top 5% of the data was notably more dispersed. Therefore, any sample replicates that were more than 60 in./hr from the mean of the other two, all three replicates of that sample would be repeated. This process was repeated until all three sample replicates were within the specified range for each of the 144 samples. The final 432 samples that were within the specified range, were then plotted in the CDF plot.

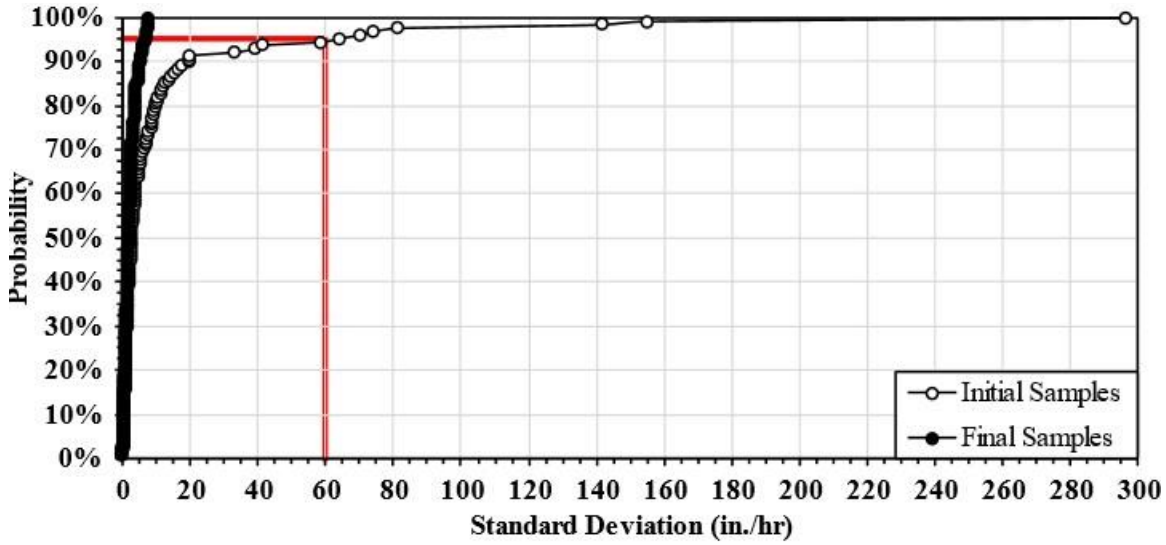

Figure 3-20. B-PAM CDF Plot

Figure 3-21 shows how each temperature, pH, and B-PAM concentration influences the settling rate. As the temperature, pH, and concentration increases, soil settling velocities also increase. This is slightly different from G-PAM where a low pH resulted in increased settling velocities. This data was based on a concentration calibration range between 3.00 to 200 mg/L of B-PAM, and 0.00 mg/L was also evaluated and used as the control. A range of 3.00 to 200 mg/L

of B-PAM was evaluated to see if there would be a correlation with G-PAM concentrations at various pH and temperatures. Since B-PAM and G-PAM contain the same flocculating agent, the concentration range of B-PAM was expanded well beyond the manufacturer's recommendations of 5.00 mg/L to assess if the quantity of flocculating agent could be correlated with the two PAM forms. However, due to the nature of a flocculant block being a gelatinous consistency before being subjected to water, it is challenging to quantify how much flocculant dissolved into the sample. Meaning while this data was collected by weighing out grated pieces of B-PAM and adding the known weights to one liter of water with sediment, it can be said that the turbid water came in contact with the known amount of B-PAM. However, it is unknown how much of the known amount dissolved and became accessible to create flocs. During testing, B-PAM clumps were occasionally observed when graduated cylinders were cleaned. However, due to the scale of B-PAM pieces used for obtaining various weights, recovering B-PAM after the test was not a viable option. Therefore, there is a possibility that even though all samples were ran at different pH values, temperatures, and B-PAM concentrations, only a small amount of the flocculant may have made it in the sample. Which, if the concentration is low enough, would result in settling velocities to be similar across the board.

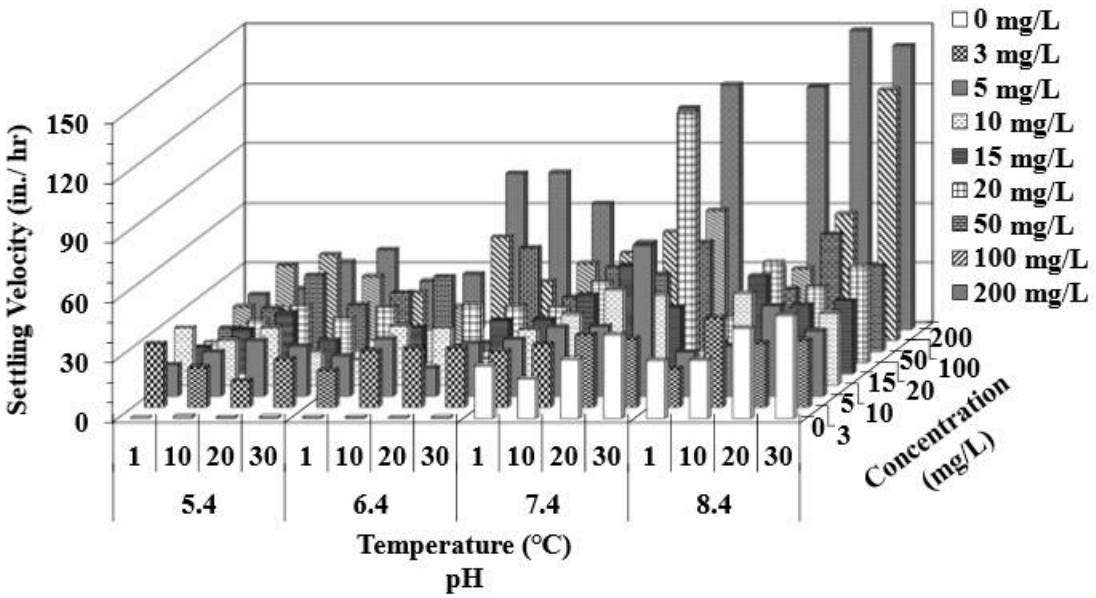

Figure 3-21. Soil Settling Velocity Against Different pH Concentrations, Temperatures, and Increasing B-PAM Concentrations

Samples evaluated at pH 7.4, temperatures above 20°C (68°F), and concentrations above 50 mg/L had the highest variability outside of the acceptable range of 60 in./hr from the mean of the other two sample replications, resulting in these samples being repeated multiple times. The same occurred with pH 8.4, temperatures above 20°C (68°F), and concentrations above 10 mg/L where these samples had the highest variability and required reevaluations. Samples at the highest pH, temperature, and top two concentrations were ran 11 times before obtaining consistent results. Indicating that the higher the pH, temperature, and concentration, the less consistent the results were and required multiple runs. Suggesting the possibility that the wide range of variability was due to more of the flocculating agent dissolved into the sample. Since the flocculant block was grated and small pieces were used to weigh out the samples, there was no consistency with each gelatinous piece. Thus, the high variability could have been a result of smaller pieces of B-PAM dissolving and forming flocs where the larger pieces only partially dissolved. Therefore, the ASTM jar testing methodology (ASTM International D2035-19, 2008) may be ideal for G-PAM but not B-PAM. It is recommended for future evaluations to change the testing methodology for

block form flocculants to allow for additional time for the block to dissolve where it can create flocs and correlate those results to settling velocities collected in large-scale testing.

Table 3-12 shows MLR results that indicate pH, temperature, and B-PAM concentration all significantly influence the settling velocity.

Table 3-12. B-PAM Settling Velocity Multiple Linear Regression Analysis

	Coefficients	*p*-value[a]
Constant	-54.422	<0.001
pH	9.841	<0.001
Temperature (°C)	0.784	<0.001
B-PAM Concentration (mg/L)	0.215	<0.001
R^2	0.524	

[a]Comparison to effects of base at 95% confidence interval and *p*-value <0.05

The MLR regression equation was rewritten to solve for B-PAM concentration, shown in Equation Eq. 3-7.

$$C_{b-PAM} = \frac{v_{settle} + 54.42 - 9.84pH - 0.78T}{0.22} \quad \text{Eq. 3-7}$$

Where C_{b-PAM} = B-PAM concentration (mg/L); v_{settle} = soil settling velocity (in./hr); pH = pH value of sample before performing residual test; and T = temperature of sample before performing residual test (°C). Same as the prediction equation for G-PAM, this equation allows users to enter known pH, temperature, and measured settling velocity data from large-scale test samples to predict B-PAM dosing concentrations in the field during different seasons and geographical locations. Again, Eq. 3-7 can be rewritten to solve for the soil settling velocity, which can be used for detention pond designing to ensure the treated water has sufficient time to settle out of suspension before being discharged off-site.

It is important to note that this equation is flocculant and soil specific. The flocculant used was B-PAM from Manufacturer I. Since flocculants are also soil specific and flocculants differ by manufacturer, a calibration curve for each flocculant type for each manufacturer matched with each soil type.

3.4 LARGE-SCALE APPLICATION TESTING

Current state DOTs that use flocculants on construction sites each have different methods for guiding application rates. These methods were found to be either following dosage and application rates from manufacturer recommendations without downstream monitoring, having no guidance but require downstream monitoring, they have their own standards, or refer to toxicology limits to guide application rates (Kazaz et al., 2021). The differences in application methods can result in inconsistent usage across the country. Flocculant detection method tests were conducted for the possibility of large-scale application evaluations for determining residual flocculant concentration used on a construction site. Initial large-scale testing using the settling velocity method developed by Kazaz et al. (2022) indicated additional environmental conditions affected results and would need to be accounted for. These environmental factors that are known to influence flocculant efficacy are soil types, metal salts, water salinity, pH, and temperature (Butler et al., 2021; Forbes, 2011; Kazaz et al., 2022; Labeeuw et al., 2021; O'Shea et al., 2010; Parsapour et al., 2014; Pérez et al., 2016; Roselet et al., 2015, 2017). This section will describe the AU-SRF testing facility, detail initial large-scale testing performed which prompted the need to accounting additional factors in residual velocity plots by Kazaz et al. (2022), explain large-scale testing and sample processing methodology, and results for granular and block form flocculant large-scale testing.

3.4.1 AU-SRF OVERVIEW

Large-scale testing took place at AU-SRF which is an outdoor research facility that is capable of simulating storm conditions on construction sites with the goal of improving various stormwater technologies used throughout all construction phases. The facility is located at the National Center for Asphalt Technology (NCAT) test track in Opelika, AL. It was originally built in 2009 as a 1.0 ha (2.5 ac) research facility as part of a research partnership between Auburn University and

Alabama Department of Transportation (ALDOT). The research staff oversaw an expansion project in the summer of 2020 which added 3.0 ha (7.5 ac) to the facility's total area, greatly increasing its research capability. Figure 3-22 shows an aerial view of the facility's initial and expanded areas, along with outlines of granular and block form flocculant large-scale testing locations.

Note: 1.0 ft = 0.3 m

Figure 3-22. Ariel View of AU-SRF with Large-Scale Testing Locations

Initial and expanded areas both contain upper and lower retention ponds that are used to supply and capture water used during testing simulations. The facility has the capability of testing various channelized flow conditions, simulating rainfall on slopes, a sediment basin, inlet protection, surface skimmers, slope drains, stockpile management, various forms of ditch check testing, vegetation establishment, ground stabilization, infiltration swale, and training opportunities.

Large-scale testing methodologies in the following sections detail the individual testing locations used for granular and block form flocculant large-scale testing. Note, over the duration of this study, when water from the upper pond in the initial area was too low to supply enough water during testing, water was pumped from the upper pond in the expanded area to refill water in the in the initial area upper pond.

3.4.2 INITIAL FAILED LARGE-SCALE TESTS

Initial large-scale testing using G-PAM and B-PAM was conducted in the expanded area at AU-SRF. Testing started with B-PAM where three silt fence ditch checks were installed in the 222 ft (67.7 m) long channel shown in Figure 3-23. The average channel top width was 16 ft (5 m). The three silt fence ditch checks were spaced 130, 59, and 46 ft (40, 18, and 14 m) apart, respectively, moving downstream the channel, beginning from measuring the distance from the end of the sediment mixing trough. The silt fence ditch checks were spaced by placing the third ditch check towards the end of the channel. The third silt fence ditch check weir was cut to 16 in. (41 cm) to accommodate two additional ditch checks upstream. Then, using a string and bubble line level, one end of the string was placed held at the lowest point of the weir, while the other end of the string was walked up the channel until the string and ground intersection point yielded a straight, level line. This level line represented a standing pool impoundment length. The subsequent upstream silt fence ditch check was then installed at the end of the predicted standing pool impoundment length to ensure maximum impoundment was achieved during flow conditions. The second weir was then cut to 8 in. (20 cm) and the first weir was cut to 16 in. (41 cm). Samples were collected upstream (U in figures and tables) when water overtopped the ditch check (DC in figures and tables), before coming in contact with the flocculant blocks, between the first and second ditch check, and after ditch check two and three. Two flocculant blocks were installed

directly after the first silt fence ditch check so that overtopping water would fall directly onto the blocks. The blocks were secured in place with rope to ensure consistent dosing throughout the duration of the test. Samples were collected as the silt fence ditch checks impounded water at 4, 8, 12, and 16 in. (10, 20, 30, and 41 cm) depths and every 10-minutes for 40-minuts after the channel reached steady state. All silt fence ditch check weirs were cut to be 16 in. (41 cm) from the ground, meaning the 16 in. (41 cm) impoundment depth sample was taken when the weir overtopped. All samples were collected in 33.4 fl oz (1,000 mL) multi-use plastic jars. Sediment was introduced into the channel at 23.3 lb./min (10.6 kg/min) with 1.75 ft^3/s (0.16 m^3/s). Flocculant blocks were hydrated using a watering can prior to channel flow to activate the flocculant and simulate rainfall before channel flow.

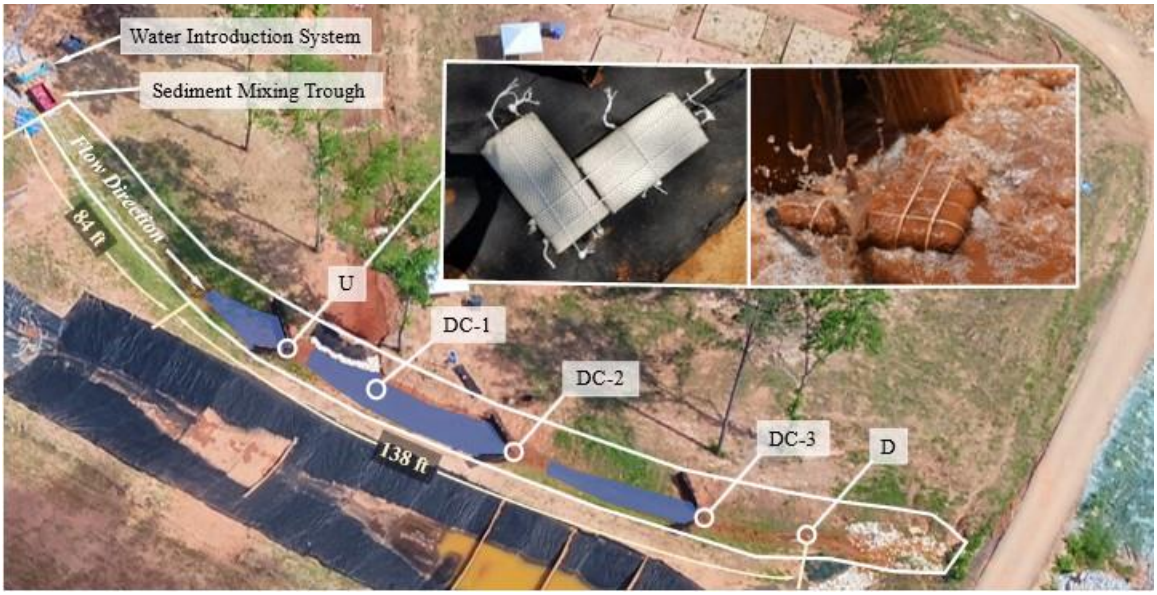

Note: 1.0 ft = 0.3 m

Figure 3-23. Initial B-PAM Testing Channel

All collected samples were processed for residual flocculant within four days after collection. Residual tests were performed by shaking each sample bottle to resuspend all sediment and transferring the samples to 51 fl oz (1,500 mL) glass beakers. The samples were then placed on a jar test multiple stirrer machine and flash-mixed (120 rpm) for 1-minute. Samples were

removed from the machine and set aside to rest for 15 minutes, allowing the sediment to settle out of suspension. After 15-minutes, the settled sediment was separated by slowly pouring the supernatant into a new, clean 51 fl oz (1,500 mL) glass beaker. Next, prepared AU-SRF sediment was added to the supernatant sample. The AU-SRF sediment consisted of 0.71 oz (20 g) of soil sieved through a #200 sieve. Once soil was added, the sample was placed back on the jar test multiple stirrer machine and flash mixed again for 1-minute. The sample was immediately poured into a 34 fl oz (1,000 mL) graduated cylinder where the settling velocity was measured and recorded.

The soil settling velocity curve for B-PAM initially developed was modified to create a better-fit line and used to predict the B-PAM concentration from large-scale tests (Figure 3-24). Three replications were run with block form flocculant and the settling velocity of each sample was measured. Data was averaged across all three replications. Field soil settling velocities from samples were plugged into the respective equation in Figure 3-24, based on the settling velocity range being above or below 80 in./hr (203 cm/hr).

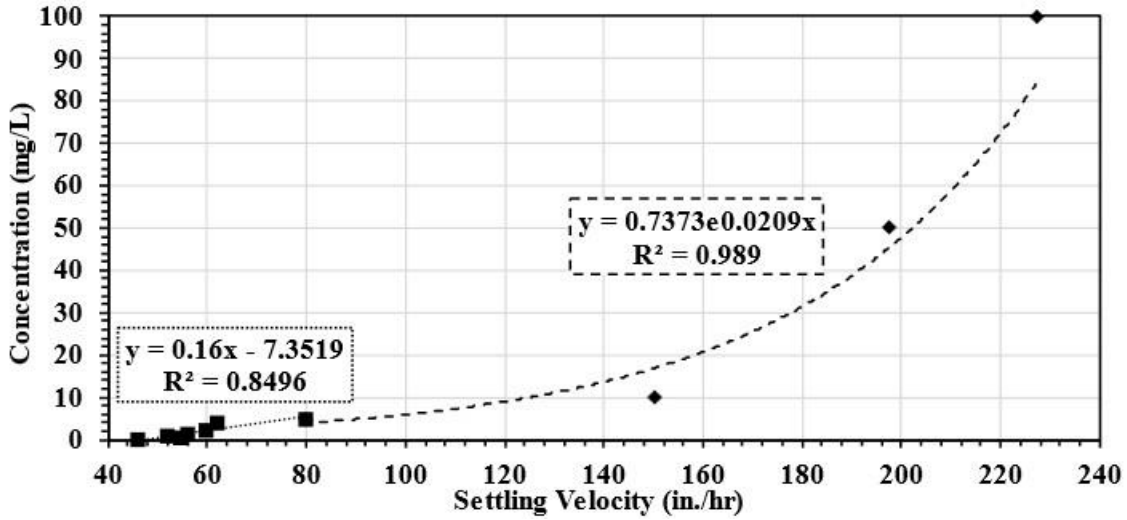

Figure 3-24. Initial B-PAM Soil Settling Velocity Curve

Table 3-13 shows B-PAM predicted concentrations that range between 9 and 352 mg/L. This range indicated brought about concern with accurately predicting concentrations in the field and prompted further investigation into the sampling methods and techniques used. The manufacturer's recommended dosing concentration with B-PAM is 5 mg/L, so 352 mg/L using two blocks indicated substantial overdosing, using the initial prediction equation. Additionally, upstream samples were predicted to contain high flocculant concentrations, indicating cross-contamination between tests in the sample containers.

Table 3-13. Initial B-PAM Predicted Concentrations

Sampling Time	Predicted Settling Concentration (mg/L)				
	U	DC-1	DC-2	DC-3	D
4 in. (10 cm) Impoundment Depth	9	14	19	27	N/A
8 in. (20 cm) Impoundment Depth	22	19	44	51	N/A
12 in. (30 cm) Impoundment Depth	14	30	26	352	N/A
16 in. (41 cm) Impoundment Depth	23	28	71	125	56
10 min	14	26	49	37	23
20 min	37	35	50	38	57
30 min	37	40	42	24	25
40 min	12	72	37	20	51

Observations during large-scale tests indicated that flocs were observed in all samples collected. Further investigations found that PAM adheres to plastic surfaces by forming weak intermolecular bonds via polymer chains (Menter, 2012; Syed et al., 2015). Regardless of how well the plastic containers were cleaned, flocs consistently formed in the sample containers with or without being subjected to flocculant during testing. Alternatively, PAM is much less likely to stick to a glass surface as glass is a relatively inert material with a smooth and nonporous surface, making it difficult for adhesion to occur (Al-Hashmi & Luckham, 2010; Hench & Wilson, 1984). However, as field conditions are not a glass-friendly environment, single-use plastic bags were substituted instead (Figure 3-25).

(a) multi-use plastic containers (b) single-use plastic bags

Figure 3-25. Sample Collection Containers

Since the soil settling velocity curve was developed using tap water, a curve offset was used to assess if predictions improved. Pond water from large-scale tests was sampled and used to measure the soil settling rate, without flocculant. The settling velocity difference from the collected large-scale test samples and pond water was used to create an adjusted settling velocity prediction (Eq. 3-8).

$$Adjusted\ Settling\ Velocity = Field\ Test\ Sample - Pond\ Water \quad \text{Eq. 3-8}$$

Table 3-14 contains the initial adjusted B-PAM predicted concentrations with a range of 0 to 12 mg/L. Although this concentration prediction range is more reasonable, predicting residual flocculant only at DC-3 during the second half of water impoundment was highly unlikely. There would be some degree of residual flocculant needed at the first half of impounding water at DC-3 and subsequent ditch checks prior. Thus, these results indicated this technique was not ideal for predicting residual concentrations of B-PAM.

Table 3-14. Initial Adjusted B-PAM Predicted Concentrations

Sampling Time	Predicted Settling Concentration (mg/L)				
	U	DC-1	DC-2	DC-3	D
4 in. (10 cm) Impoundment Depth	0	0	0	0	N/A
8 in. (20 cm) Impoundment Depth	0	0	0	0	N/A
12 in. (30 cm) Impoundment Depth	0	0	0	12	N/A
16 in. (41 cm) Impoundment Depth	0	0	0	4	0
10 min	0	0	0	0	0
20 min	0	0	0	0	0
30 min	0	0	0	0	0
40 min	0	0	0	0	0

As cross-contamination seemed to be the outstanding issue, single-use plastic bags were then used to replace all sampling containers and large-scale tests started back up with G-PAM testing. The large-scale testing channel configuration for initial G-PAM tests is shown in Figure 3-26. The 70.1 m (230 ft) long channel consisted of three 20 in. (51 cm) diameter straw wattle ditch checks (DC-1, DC-2, and DC-3) and one 20 in. (51 cm) excelsior wattle (DC-4) at the end of the channel. The first three ditch checks were spaced 39, 16, and 27 ft (12, 5, and 8 m) apart, respectively, moving downstream the channel, beginning from measuring the distance from the end of the sediment mixing trough. The wattles were spaced by placing the third ditch check in the channel to allow for sample collection before flow was directed to the underground pipe. Then, using a string and bubble line level, one end of the string was placed held at the lowest point of the wattle, while the other end of the string was walked up the channel until the string and ground intersection point yielded a straight, level line. This level line represented a standing pool impoundment length. The subsequent upstream wattle was then installed at the end of the predicted standing pool impoundment length to ensure maximum impoundment was achieved during flow conditions. The first two ditch checks, labeled DC-1(F) and DC-2(F), each contained 5.1 oz. (145 g) of G-PAM spread according to ALDOT standards – on the top and upstream face

of the wattle (ALDOT 2020), where the "F" indicates flocculant application. Sampling location "U" represents samples collected upstream of flocculated water, "P" is samples collected directly after the underground corrugated pipe, and "G" represents samples collected further downstream the grass channel. The maximum flow the channel could hold was 0.75 ft^3/s (0.07 m^3/s) where 17.8 lb/min (8.07 kg/min) of sediment was mixed with incoming channel flow. Granular flocculant was hydrated using a watering can prior to channel flow to activate the flocculant and simulate rainfall before channel flow. Samples were collected during the first flush and every 10-minutes for 120-minutes after steady state was reached in the channel.

Figure 3-26. Initial G-PAM Testing Configuration

All samples collected were processed the same day, immediately after sample collection with the idea that allowing samples to be processed within four days was one source for inconsistent data. Residual tests were performed same as before with B-PAM samples where samples were shaken, transferred into 51 fl oz (1,500 mL) glass beakers, flash mixed, settled for 15 minutes, supernatant separated, 0.71 oz (20 g) of #200 AU-SRF sieved sediment added, flash mixed again, and poured into a 34 fl oz (1,000 mL) graduated cylinder where the settling velocity was recorded.

The soil settling velocity curve for G-PAM initially developed was modified to create a better-fit line and used to predict the G-PAM concentration from large-scale tests (Figure 3-27). Three replications were run with granular flocculant and the settling velocity of each sample was measured. Data was averaged across all three replications. Field soil settling velocities from samples were plugged into the respective equation in Figure 3-27.

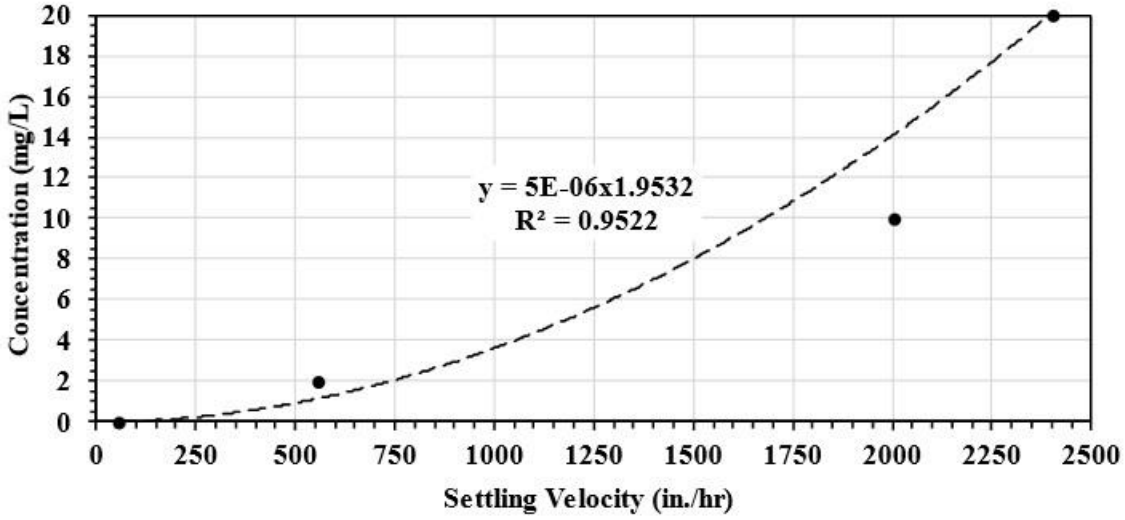

Figure 3-27. Initial G-PAM Soil Settling Velocity Curve

Table 3-15 shows G-PAM predicted concentrations that range between 0 and 56 mg/L. Although G-PAM predicted concentrations were more consistent than B-PAM predictions, they were not consistent enough to rule out the need to continue searching for improved detection methods. Manufacturer's recommended dosing concentration for G-PAM is also 5 mg/L. Meaning, replacing multi-use plastic containers with single-use plastic bags was only one part of the solution. First flush (FF in Tables) samples were expected to contain higher concentrations of flocculant as the flocculant wouldn't have much of an opportunity to mix or dilute. However, fluctuations from 5.0 to 56 and then an unexpected drop to 4.0 mg/L concentrations at DC-2(F), DC-3, and P sampling locations respectively, indicated the prediction equation needed expanded to account for a higher concentration range than 20 mg/L. Additionally, upstream samples still contained

predicted concentrations which suggested a deeper analysis of environmental conditions was still needed.

Table 3-15. Initial G-PAM Predicted Concentrations

Sampling Time	Predicted Residual Concentration (mg/L)						
	U	DC-1(F)	DC-2(F)	DC-3	P	G	DC-4
FF	0	2	5	56	4	9	0
10 min	0	1	3	4	N/A	N/A	0
20 min	0	1	2	2	N/A	N/A	0
30 min	0	1	2	2	N/A	N/A	0
40 min	3	2	1	1	N/A	N/A	0
50 min	1	2	2	3	N/A	N/A	0
60 min	0	1	2	2	0	1	0
70 min	0	2	1	2	N/A	N/A	0
80 min	0	2	2	2	N/A	N/A	0
90 min	0	1	4	3	N/A	N/A	0
100 min	0	0	1	1	N/A	N/A	0
110 min	0	0	1	1	N/A	N/A	0
120 min	1	0	1	1	1	1	0

Adjusting the settling velocity was performed to see how data would change for G-PAM data when the settling velocity difference from the collected large-scale test samples and pond water were used to create an adjusted settling velocity prediction shown in Table **3-16**. The adjusted concentration prediction range maximum was reduced by 2 mg/L, indicating this technique was not sufficient in better predicting residual B-PAM nor G-PAM.

Table 3-16. Initial Adjusted G-PAM Predicted Concentrations

Sampling Time	Predicted Residual Concentration (mg/L)						
	U	DC-1(F)	DC-2(F)	DC-3	P	G	DC-4
FF	0	1	3	54	3	7	0
10 min	0	0	1	3	N/A	N/A	0
20 min	0	0	0	1	N/A	N/A	0
30 min	0	0	0	0	N/A	N/A	0
40 min	1	1	0	0	N/A	N/A	0
50 min	0	0	0	2	N/A	N/A	0
60 min	0	0	0	0	0	0	0
70 min	0	0	0	0	N/A	N/A	0
80 min	0	0	0	0	N/A	N/A	0
90 min	0	0	2	1	N/A	N/A	0
100 min	0	0	0	0	N/A	N/A	0
110 min	0	0	0	0	N/A	N/A	0
120 min	0	0	0	0	0	0	0

Initial B-PAM and G-PAM large-scale tests were conducted prior to expanding on the soil settling velocity detection method. Although the standardized residual settling plots proved positive for large-scale application by Kazaz et al. (2022), this study was used to expand on this technique by applying the residual prediction methodology to large-scale applications to validate field condition applicability. This section detailed cross-contamination sources that can easily be resolved by avoiding multi-use plastic containers when sampling and that the plots developed by Kazaz et al. (2022) with better fit lines still remains inaccurate but shows promise for a good foundation method. Since the residual settling plots developed by Kazaz et al. (2022) were performed using tap water, field conditions include an assortment of environmental conditions that influence flocculant efficacy and settling rate, such as soil types, metal salts, water salinity, pH, and temperature (Butler et al., 2021; Forbes, 2011; Perez, et al., 2022; Labeeuw et al., 2021; O'Shea et al., 2010; Parsapour et al., 2014; Pérez et al., 2016; Roselet et al., 2015, 2017). Meaning the residual settling plots developed by Kazaz et al. (2022) require additional environmental conditions that need to be accounted for when developing standardized residual settling plots. By

creating a calibration curve using the same soil at the testing facility, assumptions of minting similar soil types, metal salts, and salinity were assumed. Salinity would also be accounted for by checking the calibration curves with collected pond water during testing. Leaving pH and temperature as necessary components to be included calibration the soil setting velocity curve.

3.4.3 LARGE-SCALE TESTING METHODOLOGY

The testing methodology is divided into two portions where (1) describes the large-scale testing and sample collecting process and (2) describes large-scale sample processing for granular and block form flocculant tests.

3.4.3.1 COLLECTING LARGE-SCALE TEST SAMPLES FOR GRANULAR PAM

Flocculant dosing was based on previous intermediate-scale testing evaluations conducted in a 40.0 ft (12.2 m) long, 1.5 ft (0.5 m) wide adjustable flume to evaluate various flocculant applications. This comparison was done to see how intermediate-scale testing compared to large-scale applications. For G-PAM flume tests, the channel was subjected to 0.1 ft^3/s (0.003 m^3/s) and 0.85 oz. (24 g) of G-PAM was spread across four rock ditch checks with jute lining. These values for intermediate-scale testing were compared to the large-scale conditions by their flow rates to find the desired G-PAM application rate. Eq. 3-9 shows the formula used to scale up the intermediate-scale testing to large-scale applications.

$$\left(\frac{Q_{flume}}{W_{granular\ flume}}\right) = \left(\frac{Q_{channel}}{W_{granular\ channel}}\right) \qquad \text{Eq. 3-9}$$

Where Q_{flume} is the flow rate used in intermediate-scale flume testing (ft^3/s [m^3/s]); $W_{granular\ flume}$ is the total weight of G-PAM used in intermediate-scale flume testing (oz. [g]); $Q_{channel}$ is the design flow rate for large-scale application testing (ft^3/s [m^3/s]); and

$W_{granular\ channel}$ is the total weight of G-PAM required for large-scale application testing (oz. [g]). This equation was written to solve for $W_{granular\ channel}$ to mimic the application rate used in intermediate-scale testing. Large-scale application testing used a flow rate of 0.75 ft^3/s (0.02 m^3/s). The total calculated weight needed for G-PAM was 6.35 oz. (180 g).

The testing location allowed for three 10 ft (3.1 m) long, 20 in. (51 cm) diameter straw wattles to be installed in the channel between the flow and sediment introduction system and the underground corrugated pipe. The three ditch checks were spaced 39, 16, and 27 ft (12, 5, and 8 m) apart, respectively, moving downstream the channel, beginning from measuring the distance from the end of the sediment mixing trough. The wattles were spaced by placing the third ditch check in the channel to allow for sample collection before flow was directed to the underground pipe. Then, using a string and bubble line level, one end of the string was held at the lowest point of the wattle, while the other end of the string was walked up the channel until the string and ground intersection point yielded a straight, level line. This level line represented a standing pool impoundment length. The subsequent upstream wattle was then installed at the end of the predicted standing pool impoundment length to ensure maximum impoundment was achieved during flow conditions. Figure 3-28 shows the large-scale application setup, along with each sampling location marked with an "O" and the location name. Samples were collected downstream of the wattles, before the next impoundment to allow the flocculant time to be mixed into the water. Each wattle ditch check sampling location was labeled as "DC" with the "(F)" indicating that 2.12 oz. (60.1 g) of flocculant was applied to the upstream wattle. Upstream sampling location is notated as "U," after corrugated pipe is "P," and at the end of the grassed channel is marked as "G." Resulting in six sampling locations throughout the channel.

Figure 3-28. Wattle G-PAM Large-Scale-Testing Setup

Wattles were installed according to ALDOT standards (ALDOT 2020), shown in Figure 3-29.

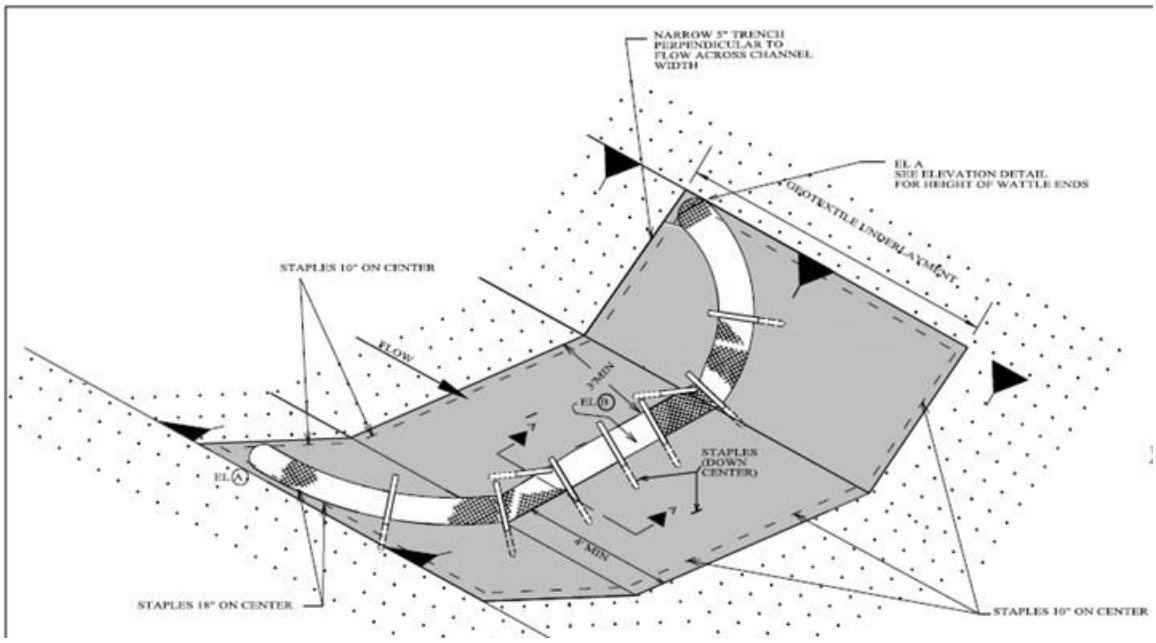

Figure 3-29. Wattle Installation Standards (ALDOT 2020)

The G-PAM was applied considering North Carolina DOT (NCDOT) standards where one-quarter of the G-PAM is applied to the wattle face, half on the wattle top, and a quarter on the wattle back in the lower center portion of the wattle where water will flow to increase surface contact with

applied flocculant (NCDOT 2015). This application is different from ALDOT's method, which recommends flocculant application on the wattle top and face only (ALDOT 2020). Figure 3-30(a) shows ALDOTs granular flocculant application standards. Figure 3-30(b) is a side profile creation of ALDOT standards to better show how flocculant is to be applied.

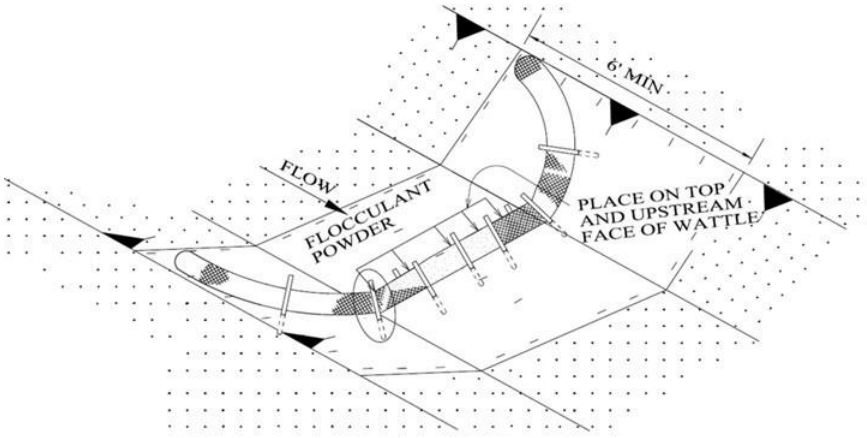

(a) application description (ALDOT 2020)

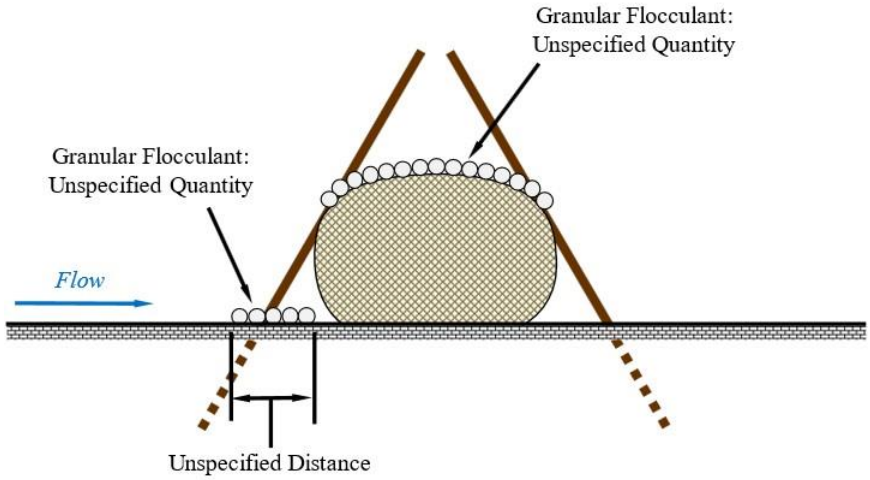

(b) side profile of ALDOT application description

Figure 3-30. ALDOT Granular Flocculant Application

Even though NCDOT indicates granular flocculant should be applied 2.0 ft (0.6 m) minimum upstream and 6.0 ft (1.8 m) minimum downstream of the wattle, flocculant was applied within 1.0 ft (0.3 m) upstream and downstream of the wattle, Figure 3-31(a). This application modification was made to maximize flocculant surface contact without the need for additional

installation materials. Additionally, this application technique is more likely to occur in the field as it is difficult to apply granular flocculant strictly to the wattle top and face. All three wattles had 2.12 oz (60.1 g) applied to each wattle according to Figure 3-31. After G-PAM was applied to the wattle, a watering can was used to saturate and activate the flocculant, simulating rainfall prior to channel flow. This was a crucial step for testing granular PAM flocculant applications to prevent flocculant 'fish eyes' in treated water, which would drastically impact residual flocculant predictions during testing (Druschel, 2014; Mclaughlin & Zimmerman, 2008). Activation occurs during rainfall as dry granular flocculant is saturated prior to runoff commencing.

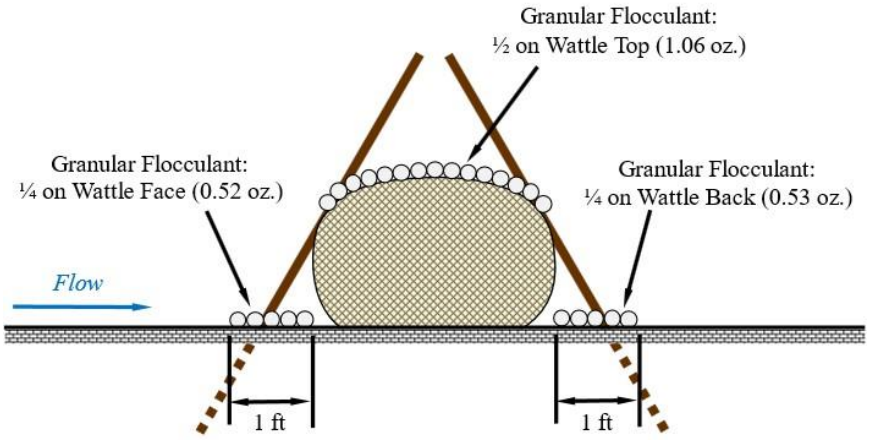

(a) large-scale testing application schematic

Note: 1.0 ft = 0.3 m, 1.0 oz = 28.3 g

(b) large-scale testing application images

Figure 3-31. Large-scale Testing G-PAM Application Method

An equalizing tank system was used to control water inflow rate, Figure 3-32. Figure 3-32(a) shows how pumps with flexible hoses were attached to the equalizing tank where a wood baffle, perpendicular to the inflow in the middle of the tank dissipated water inflow energy. Water exited the tank through a trapezoidal weir. Figure 3-32(b) displays a scaled flow control plate that uses a piezometer to quantify the flow rate of water overtopping the trapezoidal weir. Exit valves located at the tank bottom were used to adjust the flowrate if necessary to achieve the design flow

rate. The equalizing tank system was used to introduce 0.75 ft^3/s (0.02 m^3/s) of flow during each test for 120 minutes. A two-hour test is referred to as a 'longevity test' as it is used to measure the flocculant dosing concentration over time. Allowing enough data to be collected to generate trends that are capable of being used for quantifying how long one flocculant dose will last after application and predict when reapplication would be necessary. Samples were collected at 0, 10, 20, 30, 60, 90, and 120 minutes at each of the six sampling locations and three test replications, resulting in 126 samples. The 0-minute sample represented first flush.

(a) front

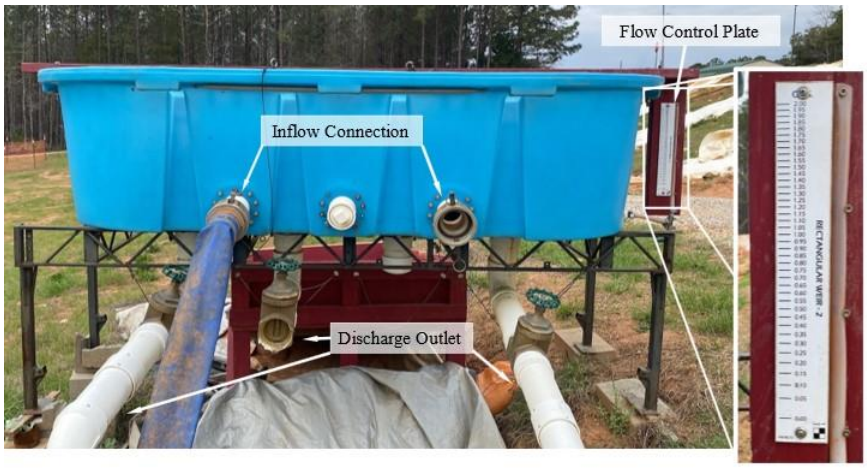

(b) back

Figure 3-32. Water and Sediment Introduction System

Soil was mixed with water introduction in the channel (Figure 3-33) at a rate of 17.8 lb./min (8.09 kg/min). This sediment introduction rate was based on the design flow rate and a 1,500 ± 500 NTU target turbidity. This sediment introduction rate was based on laboratory trial and error testing with scaled flow rates to reach the target turbidity. Due to the length of the test, sediment was only introduced 10 minutes before every sample collected, with the exception to first flush samples. Ensuring that each sample would be taken when the intended turbidity was consistent

throughout the entire channel, allowing for turbidity reduction evaluations to be assessed. Turbidity reduction assessments were used to determine if sufficient mixing was occurring in the channel, which would indicate if the installation configurations were sufficient to maximize flocculant dosing. If sufficient mixing and agitation was not achieved, then other ditch check configurations or installations could be substituted to ensure proper mixing and agitation. Turbidity reduction analysis was conducted by collecting turbidity samples of initial, undisturbed, and disturbed samples.

Figure 3-33. Sediment Introduction Method

Samples were collected in single-use plastic bags to prevent cross-contamination between tests. Since temperature can play a significant role in affecting the efficacy of flocculants, sample bags were placed in coolers with ice and a wooden insert to protect the sample bags from the possibility bags being punctured from the ice (Figure 3-34). This allowed samples to remain in the upright position for easy storage, transport, and most importantly, prevent samples from

heating up during testing so that all sample temperatures remain consistent. Once samples were collected and placed in the cooler, they were left undisturbed for 15 minutes. Once the 15 minutes passed, turbidity subsamples were collected from the top portion of each sample. This undisturbed turbidity subsample represented the mixing that was occurring in the channel. Disturbed samples were collected the next day when samples were processed in the lab where the sample bags were shaken for 1 minute and allowed to settle for 15 minutes. After 15 minutes, a subsample was collected from the top portion of each sample again. The disturbed turbidity subsample represented the best-case scenario mixing to ensure the flocculant has an opportunity to be fully agitated and maximize the contact with any remaining soil. The undisturbed and disturbed samples were compared to initial turbidity samples that were collected at the very end of the large-scale test where each upstream sample, where flocculant was not subjected to, was shaken to resuspend all sediment in the sample. Initial subsamples were collected immediately after agitation and used to represent the initial turbidity of the channel at that time. Each turbidity sample was compared to the initial turbidity at the respective sampling time and used to calculate the percent change in undisturbed and disturbed samples so they could be directly compared to each other.

(a) wooden insert installation (b) wooden insert placement

Figure 3-34. Sample Collection Control Environment

Visual test samples were also collected to confirm the presence of flocculants by visually observing the floc size. Visual samples were collected in 17 fl oz (500 mL) clear plastic jars with 0.35 oz (10 g) of #200 sieved AU-SRF sediment. This amount of sieved sediment quantity was selected as it was the same ratio of sediment to water used for residual testing when measuring settling velocity, allowing for observed floc size testing methodology as in match testing to be maintained. Figure 3-35 shows how visual samples were collected during testing. Visual test samples were only collected at sampling location D as it was after the last dich check with flocculant. It was not collected further downstream at sites P or G, as further locations may have differing flocculant concentrations in the event residual flocculant built up in the underground coregulated pipe between test replications.

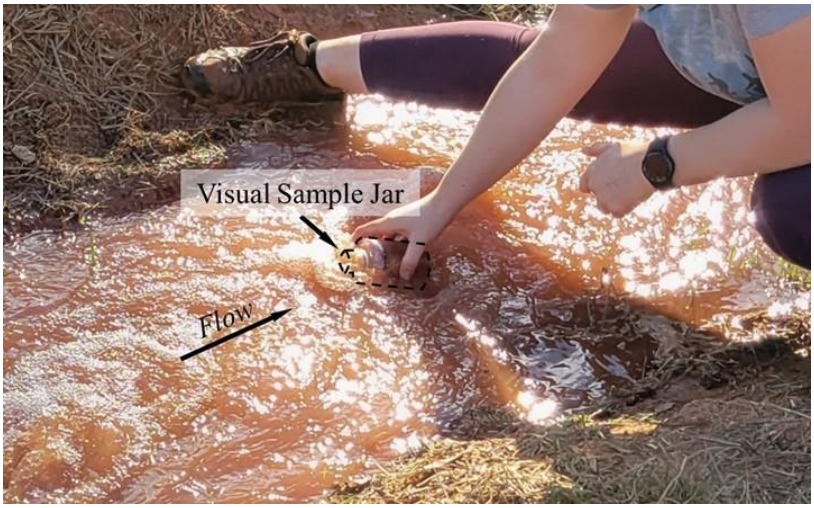

Figure 3-35. G-PAM Visual Sample Collection at Sampling Location D

3.4.3.2 COLLECTING LARGE-SCALE TEST SAMPLES FOR BLOCK PAM

The target flocculant dosing was based on previous intermediate-scale testing evaluations conducted via Flume testing. A 40 ft (12 m) long, 1.5 ft (0.5 m) wide semicircle-shaped, adjustable flume was used to evaluate various flocculant applications. This comparison was done to see how intermediate-scale testing compared to large-scale applications. For B-PAM flume tests, the channel was subjected to 0.1 ft^3/s (0.003 m^3/s) with a flocculant block that was sliced into four equal rectangular pieces. These pieces ended up being 4.5 x 8.0 x 2.5 in. (11.5 x 20.3 x 6.4 cm) length, width, and height respectively. One of the block pieces was used in flume testing and was placed downstream a ditch check where overtopping water would come in contact with the block. These values for intermediate-scale testing were compared to the large-scale conditions by their flow rates to find the desired number of flocculant blocks for large-scale testing. Eq. 3-10 shows the formula used to scale up the intermediate-scale testing to large-scale applications.

$$\frac{\left(\frac{Q_{flume}}{w_{flume\ block}}\right)}{SA_{flume\ block}} = \frac{\left(\frac{Q_{channel}}{w_{wier\ bottom}}\right)}{SA_{block\ total}} \qquad \text{Eq. 3-10}$$

Where Q_{flume} is the flow rate used in intermediate-scale flume testing (ft^3/s [m^3/s]); $w_{flume\ block}$ is the total width of B-PAM used in intermediate-scale flume testing (in. [cm]); $SA_{flume\ block}$ is the surface area of the block used in intermediate-scale flume testing, excluding the bottom face of the block as it is assumed that water would not be flowing underneath the block (in.^{2} [cm^2]); $Q_{channel}$ is the design flow rate for large-scale application testing (ft^3/s [m^3/s]); and $w_{wier\ bottom}$ is the bottom width of the weir for flow introduction (in. [cm]). $SA_{block\ total}$ is the total surface area of all flocculant blocks for large-scale application testing (in.^{2} [cm^2]). This equation was written to solve for $SA_{block\ total}$ where a full block has length, width, and height dimensions of 9.0 x 16 x 2.5 in. (23 x 41 x 6.4 cm), respectively. The number of blocks needed could be deduced by again excluding the bottom face of the blocks as water would not be flowing underneath the blocks and dividing $SA_{block\ total}$ by the water contact surface area of a single block. This was done to mimic the application rate used in intermediate-scale flume testing. Large-scale application testing used a flow rate of 1.80 ft^3/s (0.05 m^3/s). The total calculated number of B-PAM needed was six full-sized blocks. Since flocculant block dosing is much slower due to the gelatinous consistency, the test was set up to evaluate how dosing changed as blocks were added to flow during testing. Therefore, flocculant blocks were added to the channel in sets of two to evaluate how dosing changed between 2, 4, 6, and 8 blocks.

The testing location allowed for one silt fence ditch check installation and multiple flocculant blocks to be installed downstream of the ditch check. Figure 3-36 shows the large-scale application setup, along with the two sampling locations marked with an "O" and the location name. Sampling location A was collected from overtopping water before it came in contact with B-PAM and sampling location B was collected 38 ft (11.6 m) downstream from sampling location A. Resulting in two sampling locations for this test setup. All samples were collected in the same

single-use plastic bags as was used in G-PAM large-scale testing. All collected samples were also placed in a cooler with ice to maintain a constant temperature, just as was done in G-PAM large-scale testing.

(a) upstream sample point (b) downstream sample point

Figure 3-36. B-PAM Sampling Locations

The silt fence ditch check was installed according to ALDOT standards (ALDOT 2020) and is shown in Figure 3-37(a). ALDOT standards use flocculant blocks for sediment basin application where the blocks should be placed in the channel, somewhere between the forebay and sediment basin, Figure 3-37(b).

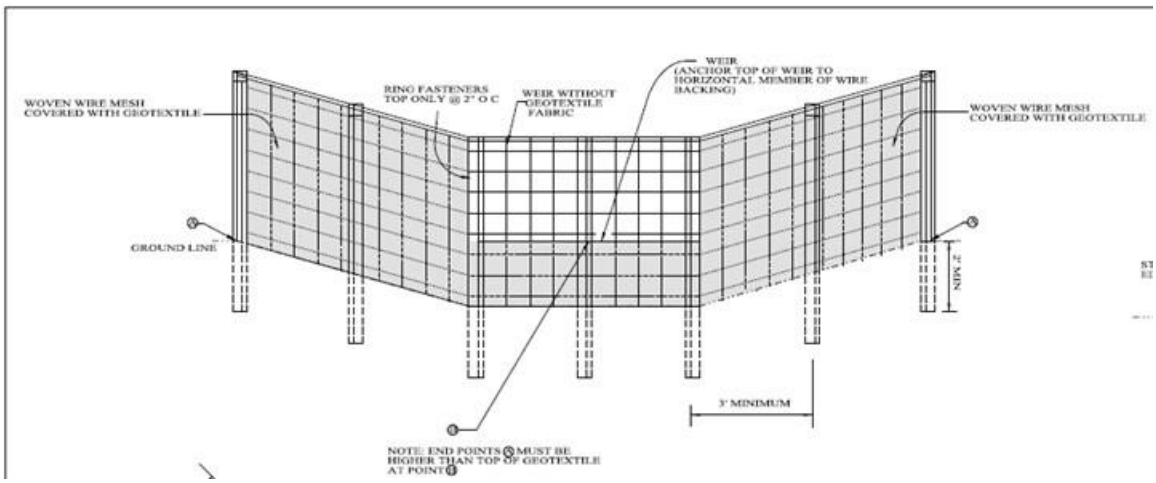

(a) silt fence installation

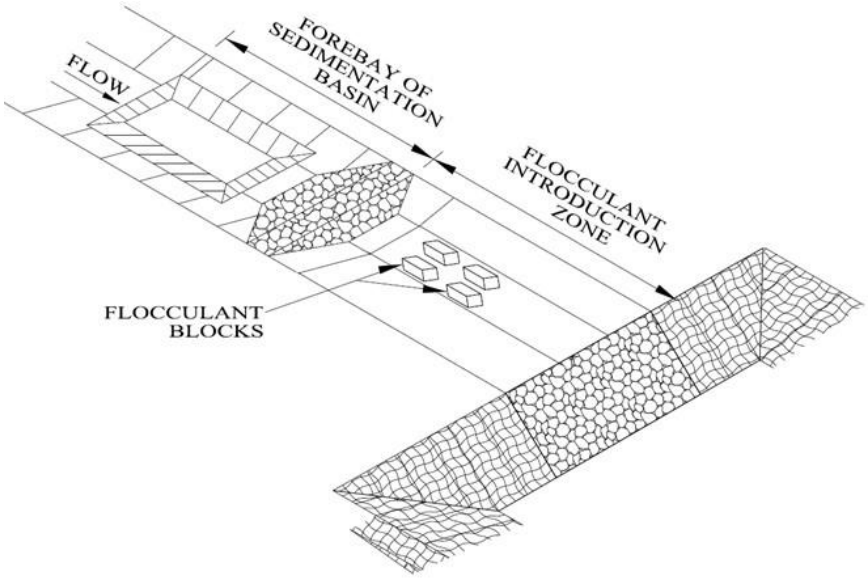

(b) flocculant block standards

Figure 3-37. Silt Fence Installation and Flocculant Block Standards (ALDOT 2020)

Since this study looked to evaluate the use of flocculant blocks with a test apparatus that sought to improve ALDOT standards, a silt fence ditch check was selected to assist in localizing flow, increasing agitation for flocculant mixing, and minimizing sediment buildup on flocculant blocks. Figure 3-38(a) shows flocculant block placement with a silt fence ditch check. Placing blocks directly under the overtopping water from a silt fence ditch check ensures that a majority of the sediment is already captured by the silt fence and the impact of the overtopping water helps

remove sediment that may accumulate on the blocks. This test aimed to evaluate how flocculant dosing changed with the number of blocks in a channel, if the number of blocks installed in the channel exceeded the space available directly underneath overtopping flow from the silt fence ditch check. In this case, only four blocks could fit within this area, subsequent blocks were placed downstream in areas of concentrated flow, Figure 3-38(b).

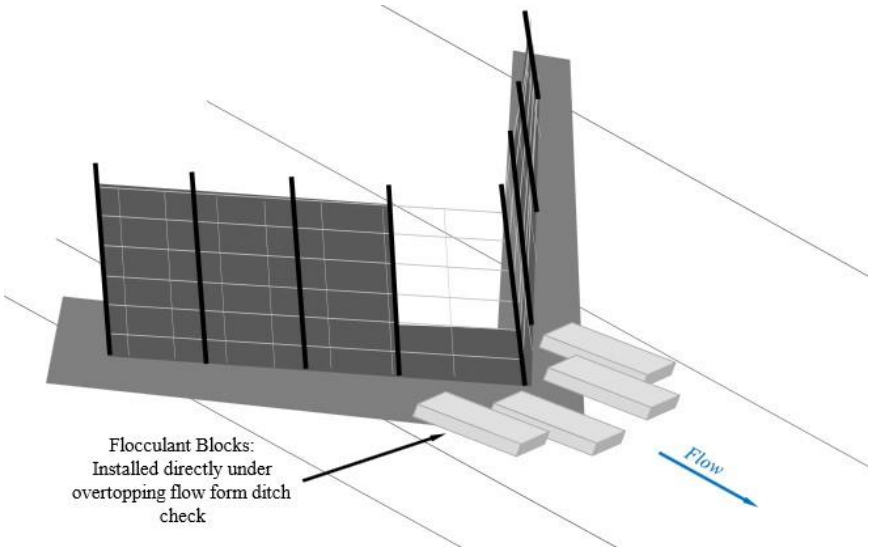

(a) installation schematic

(b) installation zone

Figure 3-38. B-PAM Installation Placement

ALDOT standards do not specify how to secure flocculant blocks as manufacturers have their own recommendations. However, due to the recommended placement of flocculant blocks for silt fence ditch check, Figure 3-39(a) details how to install flocculant blocks with a silt fence ditch check, regardless of if comes with or without a mesh netting. Since B-PAM came with a

mesh netting, Figure 3-39(b) shows how the two sod staples were used to secure blocks during testing.

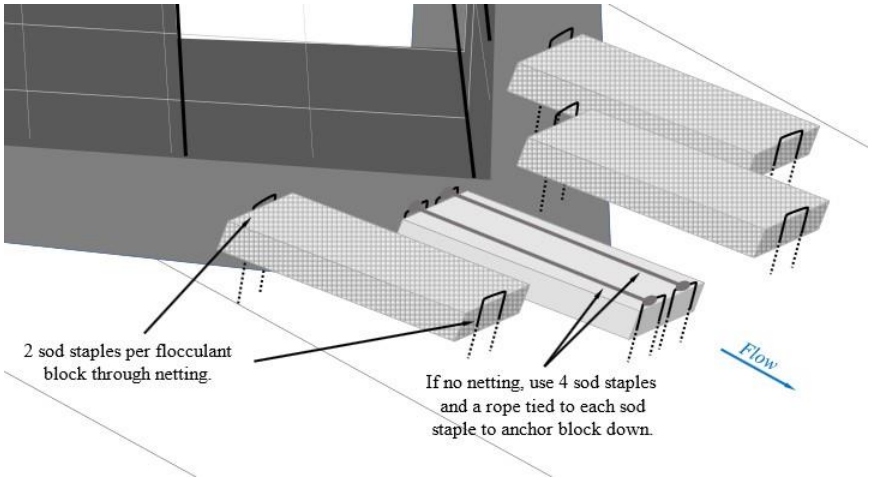

(a) B-PAM securement method

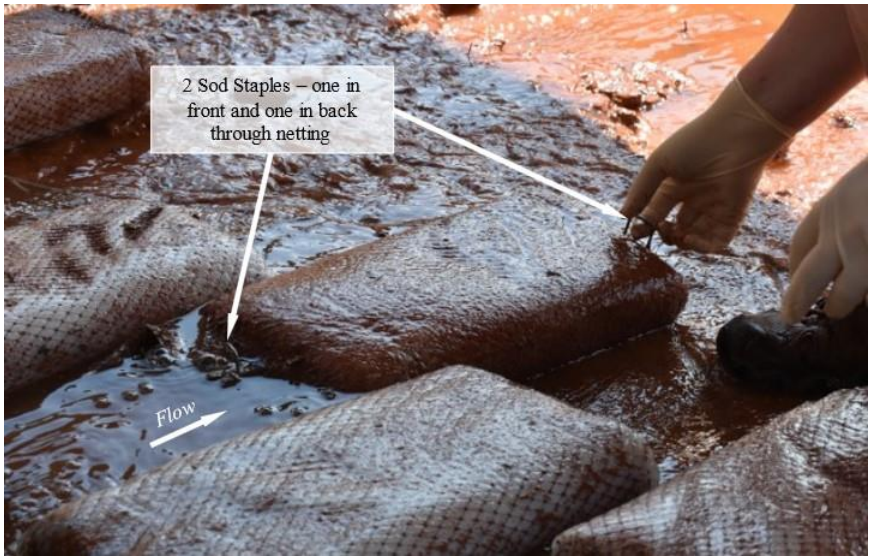

(b) example of B-PAM anchoring

Figure 3-39. B-PAM Installation Securement

Each set of blocks placed in the channel soaked in a tub of water for 10-minutes, prior to installation. This mimicked rainfall activating the blocks prior to the commencement of runoff. The same water introduction system and sediment mixing trough was used to control and monitor flow and create sediment-laden water for G-PAM was used for B-PAM large-scale tests. Sediment was mixed with flow at a rate of 42.8 lb./min (19.4 kg/min). This sediment introduction rate was

based on laboratory trial and error testing with scaled flow rates to reach the target turbidity of 1,500 ± 500 NTU recommended by Manufacturer I to match the target concentration of flocculant. Two blocks were installed in the channel prior to flow and time started once the channel reached steady state. Samples were collected at 3, 6, and 9 minutes. After the last sample was collected, the next two flocculant blocks that were soaking in water were installed in the channel during flow. Samples were collected again at 3, 6, and 9 minutes after the next two blocks were installed and the process was repeated until eight blocks were installed in the channel.

Visual test samples were collected for B-PAM large-scale testing to confirm the presence of flocculants by visually observing the floc size. Clear plastic jars with a 16.9 fl oz (500 mL) volume were used to collect large-scale test samples at sample site B and contained 0.35 oz (10 g) of #200 sieved AU-SRF sediment in each jar. This amount of sieved sediment quantity was selected as it was the same ratio of sediment to water used for residual testing when measuring settling velocity, allowing for observed floc size testing methodology as in match testing to be maintained. Figure 3-40 shows how visual samples were collected during testing at sampling location B. Due to the velocity of the water at sampling location B, water was collected by redirecting water upward and capturing the water as it fell, ensuring that the sediment in the jar was not lost during collection.

Figure 3-40. B-PAM Visual Sample Collection at Sampling Location B

3.4.3.3 PROCESSING LARGE-SCALE TEST SAMPLES

Both G-PAM and B-PAM were subjected to the same sample processing procedure where large-scale tests samples were completed at 4:30 PM on large-scale test days; samples were then brought to the lab where the ice in the coolers was removed and the coolers were left open overnight to reach room temperature before processing all samples the following day, starting at 7:30 AM. This ensured all samples were subjected to the same conditions once collected, minimizing the possibility for data inconsistencies that could result from temperature changes after collection or flocculant degradation over time.

Sample processing began with shaking sample bags vigorously for one minute and poured into three clean 51 fl oz (1,500 mL) glass beakers, each containing more than 34 fl oz (1,000 mL) of the sample. Each collected sample was split into thirds and ran in triplicate to ensure settling velocity readings remained consistent between each replication to identify possible contamination during processing. Samples were given 15 minutes to allow sediment present in the sample to settle out of suspension. After 15 minutes, 1,000 mL of the supernatant was poured into a new clean 1,500 mL glass beaker and the pH, temperature, and turbidity of the sample was taken.

Disturbed turbidity samples taken after sample bags were shaken and set for 15 minutes represented disturbed conditions. Turbidity samples were run through a turbidimeter by filling a small glass vial with the sample water and placing it in the machine. Undisturbed and initial turbidity samples taken during the large-scale test were run by shaking the sample bag until all sediment was suspended and transferring it into glass vial to be placed in the turbidimeter. The jar test multiple stirrer machine was cleaned before use by rinsing the stirring rods, paddles, and paddle rest with deionized water, spraying with Alconox® Liquinox cleaning solution, and wiping clean with a paper towel.

Following the same procedures that were done for the settling velocity tests, ruler tape was placed on glass graduation cylinders with zero at the base. To see gradients when pouring samples, cylinders were put in front of a white poster board. A GoPro camera was placed in front of the graded cylinder to show its top and bottom. To avoid blocking the sample pour, ruler tape was placed on the side of the cylinder in the GoPro screen. A digital clock with hour, minute, and second displays was put beside the cylinder and in the GoPro frame to record sample settling time. Sandy clay loam soil was sieved through #200 sieve and weighed into 0.71 oz (20 g) jars.

Samples were moved to a jar test multiple stirrer machine and 0.71 oz (20 g) of sieved testing soil was added to the sample. GoPro video camera recording was started, and the samples were flash mixed (120 rpm) for one minute. Samples were quickly removed from the machine and poured into the glass graduated cylinder, being sure to pour fast enough so that all sediment in sample remains suspended while pouring. Only two samples were mixed and poured simultaneously as it was important to pour the sample before the sediment settled in the beaker. Samples were recorded until sediment was fully settled, or for one hour if gradient was not easily visible.

Between processing samples for measuring the settling velocity, visual sample jars were shaken to resuspend all sediment and were placed in front of a camera to record the observed floc size. These recordings were done in a studio box where lighting could be maximized, and reflections could be minimized. The videos were recorded in high resolution and the jars were always placed the same set distance from the camera. This allowed for consistency and visual floc size to be later observed when videos were reviewed.

When samples settled, glassware was cleaned with hot water and Alconox® Liquinox. The Jar Test Multiple Stirrer machine was cleaned by rinsing all the paddles with deionized water, spraying with Alconox® Liquinox, and wiping off residual flocculant or sediment with a paper towel. To ensure all flocculant was removed from the paddles of the Jar Test Multiple Stirrer machine, the paddles were sprayed and wiped down two to three times, depending on the amount of residual flocculant observed on the paddles. The sam'le's poured time, total height in the cylinder using the ruled tape on the cylinder side, settled time, and settled height were recorded using GoPro video. The difference in soil settlement time and height was used to compute the settling velocity. The sample was considered settled when the lowest gradient point reached the bottom of the cylinder. As the settled sediment pile continues to compress after all sediment has reached the bottom of the cylinder, it was important to record the time when the base of the gradient reached the settled pile at the base of the cylinder. Video editing software was used to fuse multiple video recordings together if gradients were not distinguishable in shorter clips. After stitching multiple videos together, a gradient was then visible by rapidly rotating the scrub bar throughout the settling time. A step-by-step testing method can be found in Appendix C.

This testing approach is prone to error and contamination. Using glassware instead of plastic, a GoPro to monitor setting rates, and careful cleaning procedures can reduce error and

contamination. The GoPro helps analyze samples from the same distance and obtain more precise sampling start and end times. PAM adherence was prevented by using glassware in the lab and single-use plastic bags for large-scale sample collection. However, reusing glassware and the jar testing multiple stirrer machine can lead to errors and sample contamination. Washing glassware with hot water and cleaning the stirring machine multiple times between uses can assist in preventing sample cross contamination.

3.4.4 RESULTS AND DISCUSSION

Three different evaluations were conducted during G-PAM large-scale tests. The first evaluation focused on dosage and longevity testing. These two tests were conducted by quantifying the residual concentration from collected samples, enabling dosing levels to be evaluated over time to better predict reapplication needs. The second evaluation, turbidity reduction, collected subsamples of each of each sample and compared undisturbed and disturbed sample turbidities differences to assess mixing occurring in the channel. The last evaluation was a visual test which used samples collected in a clear plastic jar at sample site D, downstream of the last flocculant application, where sieved sediment was mixed in the visual test jar and the floc size was visually observed and recorded. Allowing for the observed floc size to be correlated with residual concentrations to confirm flocculation efficacy. B-PAM large-scale tests were also subjected to three different evaluations. The first was dosage and longevity testing, which was done by collecting large sample volumes at each respective sampling location and evaluating the residual concentration from settling velocities to determine the dosing levels over time and determine when reapplication would be necessary. The second two tests were turbidity reduction and visual test. As the testing location was different from G-PAM large-scale tests, the sampling location for

visual tests was at sample site B. The results for each of these three evaluations are described in detail in the following sections.

3.4.4.1 GRANULAR PAM DOSAGE AND LONGEVITY

Once all settling velocity videos were reviewed, the G-PAM concentration equation was used to predict the concentration of G-PAM in each sample. Each sample collected was ran in triplicate to identify irregularities for cross contamination within glassware and mixing equipment. However, all three replicates of each collected sample were kept as no inconsistencies were identified. The 126 samples collected were split into thirds and individually evaluated for its soil settling velocity, resulting in 378 total evaluated samples. Each data point plotted in Figure 3-41(a) and (b) represents nine averaged samples. Since the prediction equation cannot accurately predict concentrations below 1.0 mg/L of G-PAM, the upstream predicted concentration, which was not subjected to any flocculant, had predicted concentrations below 0.9 mg/L. To better represent the predicted concentrations for all samples in Figure 3-41(a) and (b), the upstream sample predicted concentration was used to offset the predicted concentrations of all other flocculated subsequent samples by subtracting the upstream predicted concentration from each subsequent sampling location per sample time.

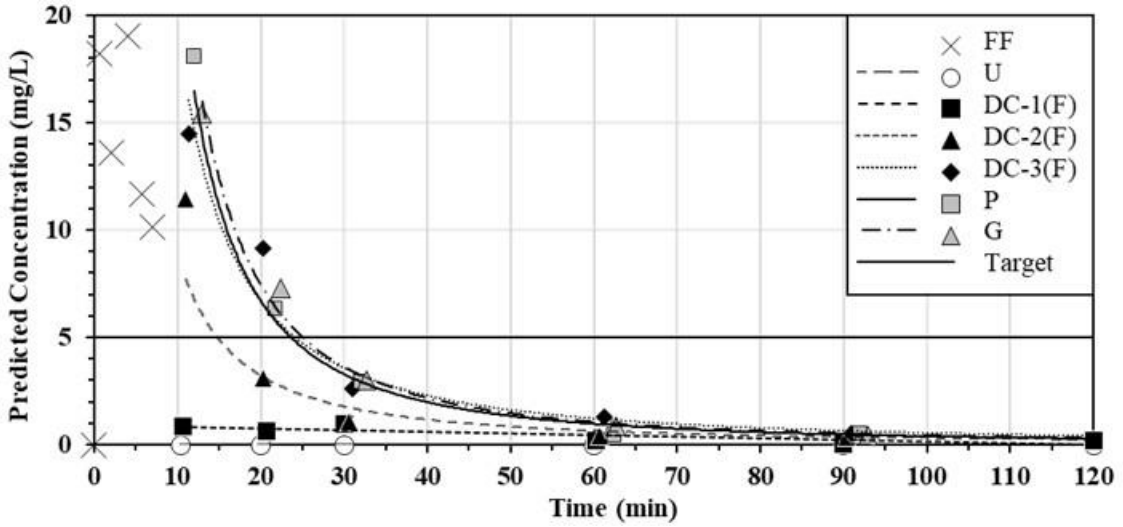

(a) over time

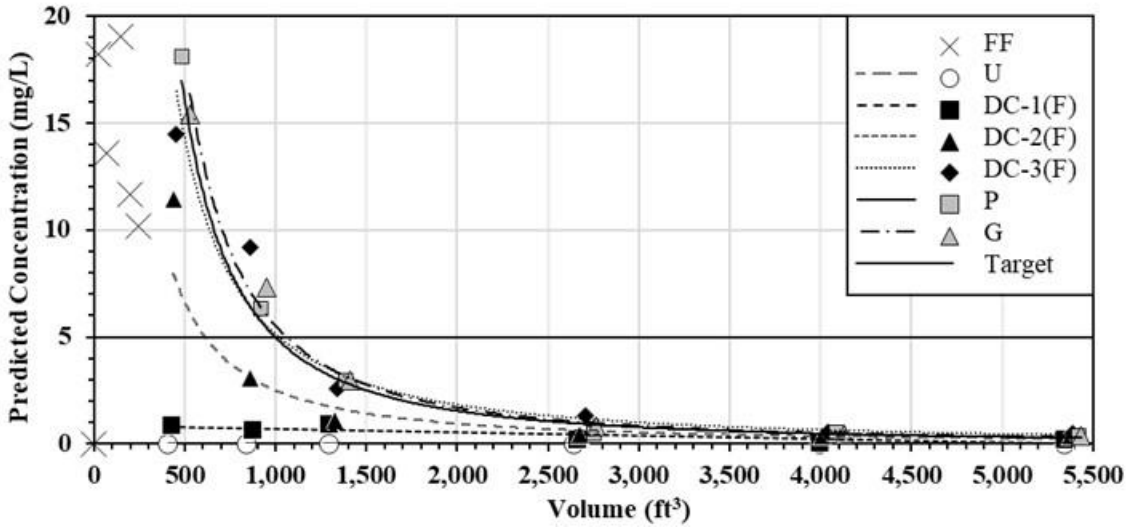

(b) over volume

Figure 3-41. Predicted G-PAM Concentration Trends

Results displaying the predicted concentrations over time are provided in Figure 3-41(a). Figure 3-41(b) shows flocculant concentration predictions based on volume and can provided indication on how concentrations may change based on contact time and rainfall events. In both Figure 3-41(a) and (b), it can be seen that the total 2.12 oz. (60 g) of G-PAM spread each of the three wattles begins dosing at high predicted concentrations of 19 mg/L during the first flush, then rapidly decreases to 3.0 mg/L predicted concentrations over the first 30 minutes or 1,500 ft^3 (42.5

m^3) of flow. Using the regression equations for the last sampling location, G, in Table 3-17, the manufacturer's recommended concentration is predicted to be reached after 25.1 minutes.

Table 3-17. Regression Equations for G-PAM Concentration Trends Over Time

Collection Site	Regression Equation	R^2
U	$y = 0$	N/A
DC-1(F)	$y = -0.0074x + 0.895$	0.704
DC-2(F)	$y = 256.61x^{-1.462}$	0.972
DC-3(F)	$y = 678.58x^{-1.542}$	0.944
P	$y = 1302.5x^{-1.759}$	0.999
G	$y = 1497.4x^{-1.77}$	0.991

When predicting based on flow, looking at predicted based on flow, using Table 3-18, the manufacturer's recommended concentration is predicted to be reached after being subjected to 1,060 ft^3 (30 m^3) of flow.

Table 3-18. Regression Equations for G-PAM Concentration Trends Over Volume

Collection Site	Regression Equation	R^2
U	$y = 0$	N/A
DC-1(F)	$y = -0.0002x + 0.8858$	0.704
DC-2(F)	$y = 41539x^{-1.407}$	0.978
DC-3(F)	$y = 140708x^{-1.479}$	0.937
P	$y = 594191x^{-1.692}$	0.999
G	$y = 724182x^{-1.706}$	0.988

Since increased dosing occurred for the first 25 minutes, it is recommended to balance this by underdosing for a period, especially since flocculant is still found effective at concentrations as low as 20% of the recommended dosage as reported in bench scale testing. Therefore, it is recommended to reapply G-PAM after 3,600 ft^3 (101.9 m^3) or 1.0 in. (2.5 cm) of runoff per acre.

Manufacturer I SDS reports an oral rat toxicity LD_{50} > 5,000 mg/kg body weight with an 'unlikely aquatic toxicity' as G-PAM does not hydrolyze (Carolina Hydrologic, 2019). The rat oral LD_{50} value matches the study performed by Christofano et al. (1969) mentioned in the literature review where an orally administrated LD_{50} for rats was not reached. For aquatic organisms, the maximum predicted concentration of 19 mg/L from G-PAM large-scale tests well

below the toxic range for many aquatic organisms mentioned in the literature review, except freshwater fleas with an LD_{50} = 14.1 mg/L (Beim & Beim, 1994). As the maximum concentration only occurred during the first flush and rapidly decreased below aquatic toxicity limits within the first 20-minutes, this application rate was justified by waiting to reapply flocculant until predicted concentrations fall below 1.0 mg/L. Ensuring high initial concentrations are diluted down below all aquatic organism toxicity limits when effluent leaves the construction site.

3.4.4.2 Block PAM Dosage and Block Quantity

Once all settling velocity videos were reviewed, the B-PAM concentration prediction equation was used to predict the concentration of B-PAM in each sample. Each sample collected was ran in triplicate to identify irregularities for cross-contamination within glassware and mixing equipment; however, all three replicates of each collected sample were kept as no inconsistencies were identified. The 72 samples collected were split into thirds and individually evaluated for their soil settling velocity, resulting in 216 total evaluated samples. Each data point plotted in Figure 3-42(a) represents nine averaged samples. To better represent the collected samples, the difference between the upstream sample, before flocculant introduction, and the downstream sample, after flocculant introduction, was taken after prediction calculations were completed for all B-PAM plots.

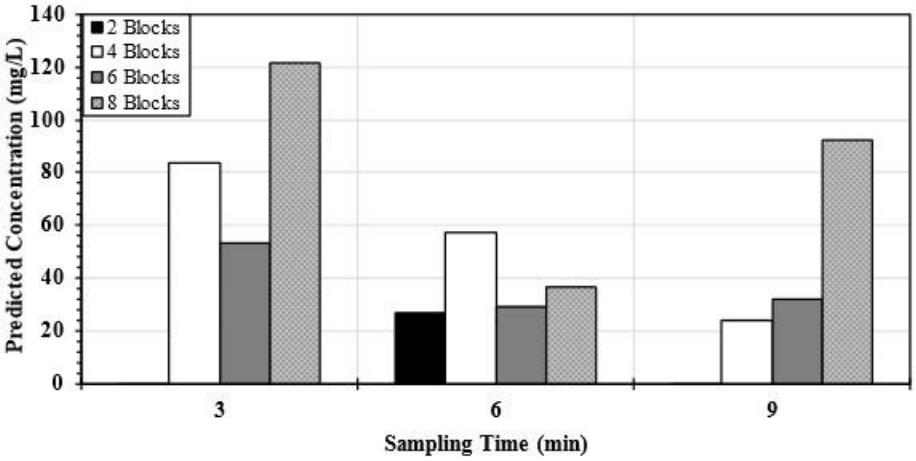

(a) B-PAM prediction equation results

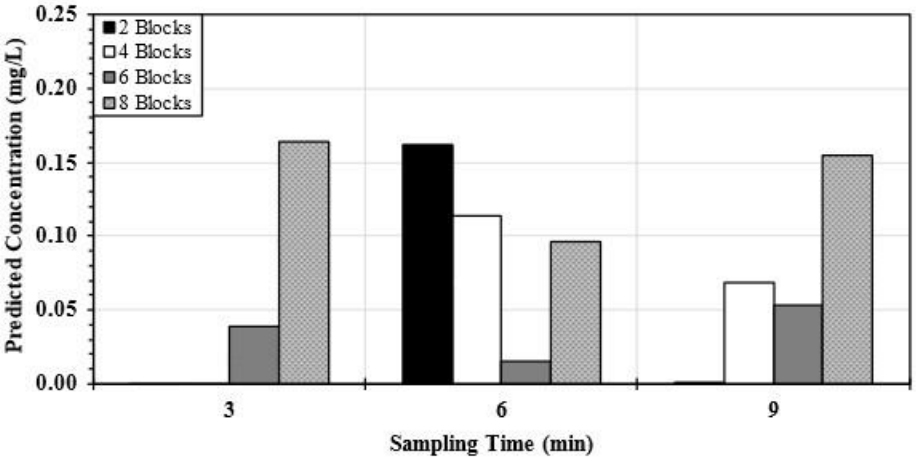

(b) G-PAM prediction equation results

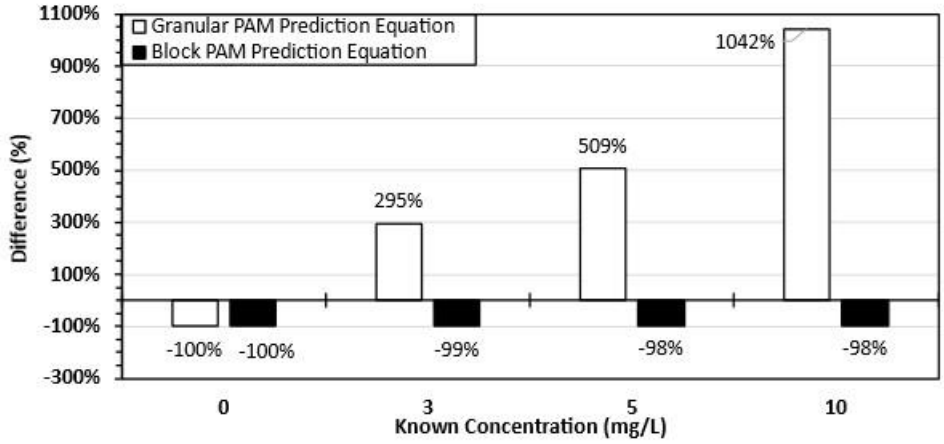

(c) percent difference from known concentration

Figure 3-42. Prediction Equation Results

The flocculant concentration prediction equation for B-PAM shows values between 0 to 122 mg/L. This range of predictions is likely due to the difficulty quantifying flocculant in block forms. Since B-PAM does not dissolve in water easily, and the prediction curve was created by grating a flocculant block, weighing out small pieces, and flash mixing with sediment for one minute, it is impossible to know how much of the gelatinous flocculant pieces actually dissolve into the sample. It can only be said that 1.0 L of water came in contact with the specified amount of flocculant. Therefore, there is a possibility that the B-PAM concentration prediction data could actually contain the same flocculant concentration, regardless of the specified weights. This may result in the prediction equation to be inaccurate.

Since B-PAM and G-PAM forms are both based on the same flocculating agent, G-PAM concentration prediction equation was used to see how results may differ with respect to the PAM flocculating agent, regardless of other additives that may be present, Figure 3-42(b). Here, flocculant concentration predictions were below 1.0 mg/L, which falls outside of the measurable range for this equation; therefore using G-PAM concentration prediction equation was inconclusive.

During each large-scale test, water was collected directly after sediment was mixed with pond water at the time of the test. The purpose of this was to confirm that data created using tap water with measured flocculant concentrations for the prediction curve were representative of samples run with pond water with measured flocculant concentrations. Allowing the accuracy of the prediction curves to be assessed with conditions specific to the test conditions of temperature, pH, soil that was mixed into the water during testing, or any other environmental factors that may be specific to each test run. Figure 3-42(c) shows the percent difference from the measured concentration performed with the sediment-laden pond water collected during large-scale testing

against the predicted B-PAM and G-PAM predicted concentrations. With all concentrations being above 98% different from the measured concentration, it was evident that neither prediction equation obtained reliable results.

With neither of the prediction equations being viable for predicting B-PAM flocculant concentrations, results were plotted by showing the soil settling velocities for the upstream (A in figures), no flocculant, and downstream (B in figures), with flocculant, sampling locations in Figure 3-43. Although the settling velocities do not differ greatly between the two sampling locations, a general trend can be noted that as the number of blocks in the channel increases, the settling velocities at sampling location B increases. Additionally, regardless of how long the blocks were in the channel or the volume of water that ran across them, the settling velocity remains relatively consistent.

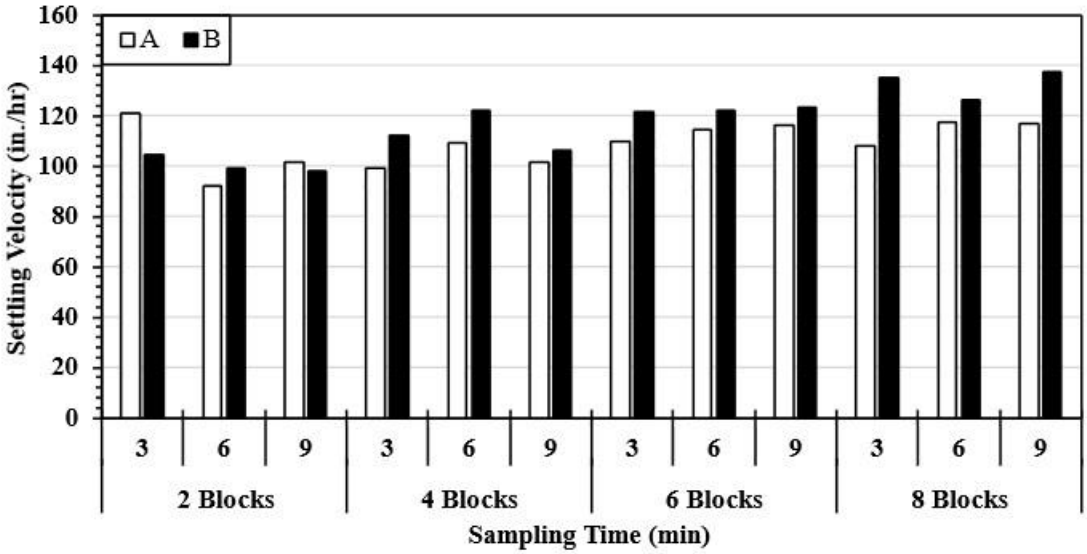

(a) settling velocity with respect to time

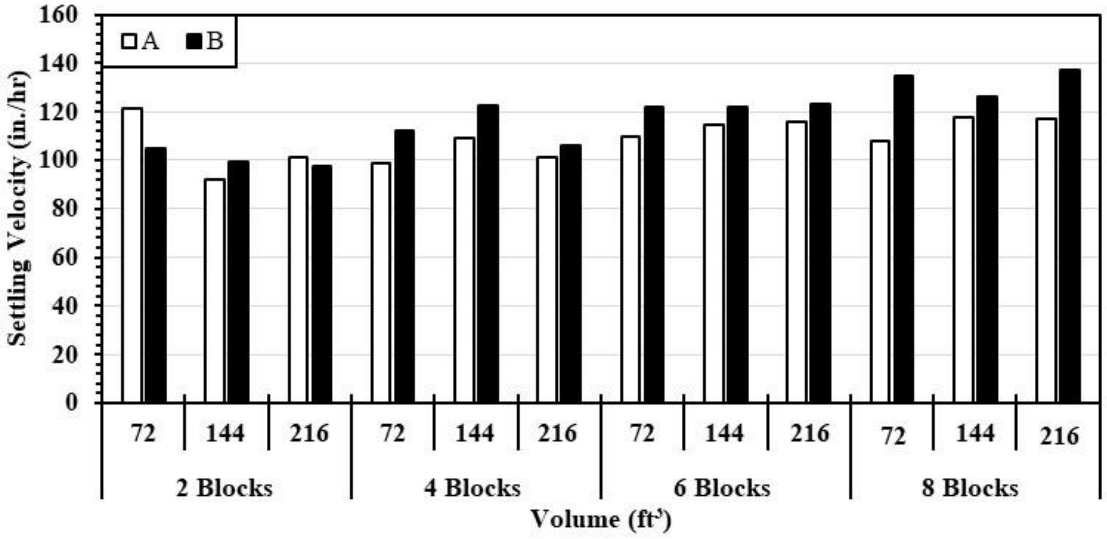

(b) settling velocity with respect to volume

Figure 3-43. B-PAM Large-Scale Test Settling Velocity Results

The sediment-laden pond water collected during large-scale testing that was used to confirm prediction values was also used for creating a prediction equation that was specific to the testing conditions. The measured amount of B-PAM and the soil settling velocity for each measured concentration is plotted in Figure 3-44(a). Samples with 0 mg/L were omitted as their oil settling velocities remained inconsistent across sample and test replications. The regression

equation in Figure 3-44(a) was used as the pond concentration prediction equation where y is the measured quantity of B-PAM concentration and x is the measured soil settling velocity for flocculant blocks. This equation was used to generate the data in Figure 3-44(b) which obtained concentration predictions between 0.0 and 8.6 mg/L. A general trend is more prominent in Figure 3-44(b) where the offset predicted flocculant concertation increases as the number of flocculant blocks are added in the channel. Overall, when predicting B-PAM concentrations, it is clear that it is difficult to accurately measure known concentrations with current methods and it is recommended to adapt testing methodologies that best account different flocculant forms.

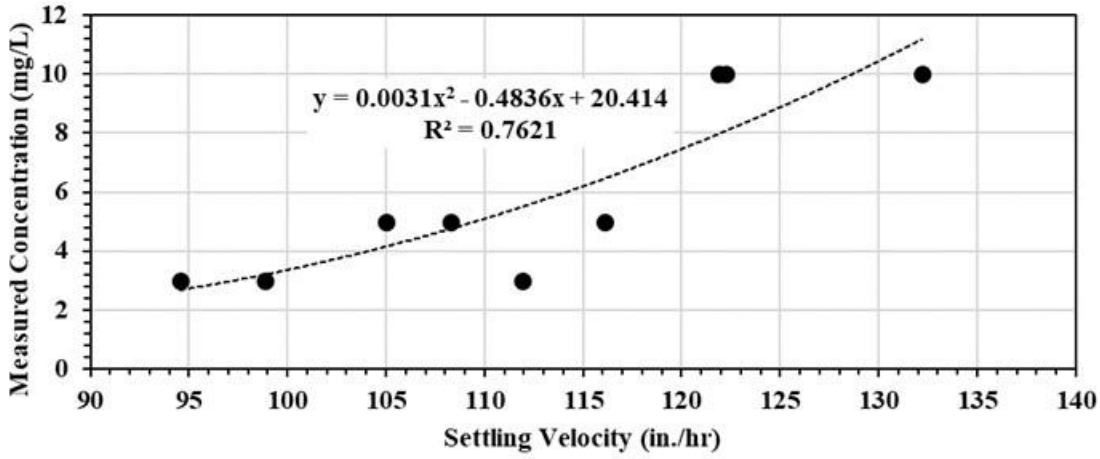

(a) B-PAM prediction trend and equation from pond water collected during testing

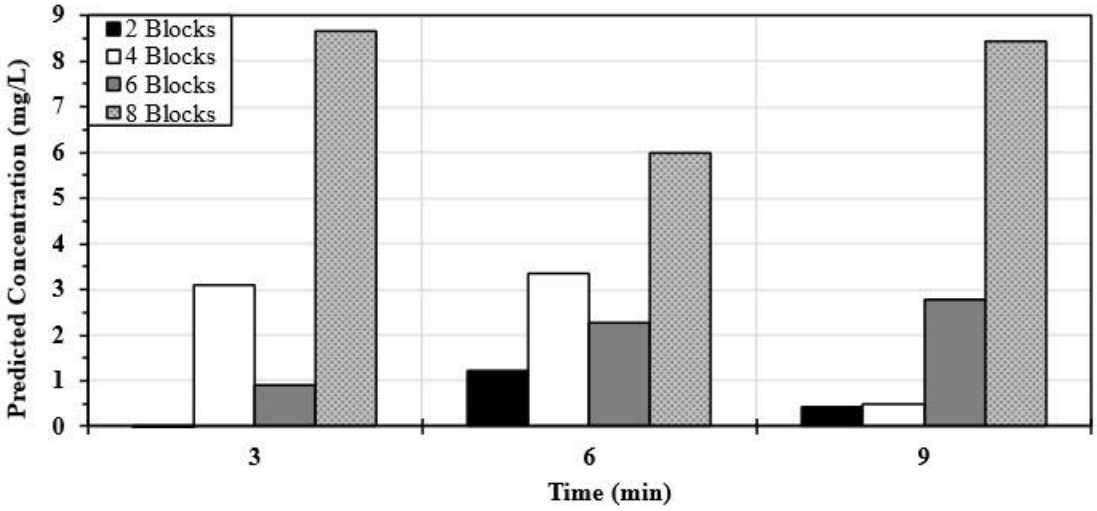

(b) B-PAM prediction results using pond concentration prediction equation

Figure 3-44. B-PAM Large-Scale Test from Pond Concentration Prediction

Since G-PAM and B-PAM consist of the same flocculating agent, the same SDS is used for both products. Once again, the oral rat toxicity LD_{50} > 5,000 mg/kg body weight with an 'unlikely aquatic toxicity' as B-PAM does not hydrolyze remains the same (Carolina Hydrologic, 2019), which matches information from Christofano et al. (1969) where an orally administrated LD_{50} for rats was not reached. Predicted B-PAM concentrations from Figure 3-44(b) indicate the maximum concentration reached was 8.6 mg/L with 8 blocks, which is well below the toxic ranges for all aquatic organisms mentioned in the literature review.

3.4.4.3 TURBIDITY REDUCTION

Turbidity reduction results were analyzed by calculating the percent change in turbidity between the initial turbidity against undisturbed turbidity and initial turbidity against disturbed turbidity. The percent change was then used to calculate the difference between the undisturbed percent change against disturbed percent change, referred to as Δ turbidity, making it easier to observe the difference between the two samples. The following sections discuss results for G-PAM and B-PAM large-scale tests.

3.4.4.3.1 GRANULAR PAM

Figure 3-45(a) and (b) contain the Δ turbidity results for G-PAM large-scale tests and are plotted in against the sampling location and sampling time, respectively. Negative Δ turbidity results indicate disturbed samples had a lower turbidity than the undisturbed, meaning flocculant was not sufficiently mixed in the channel at that location or time.

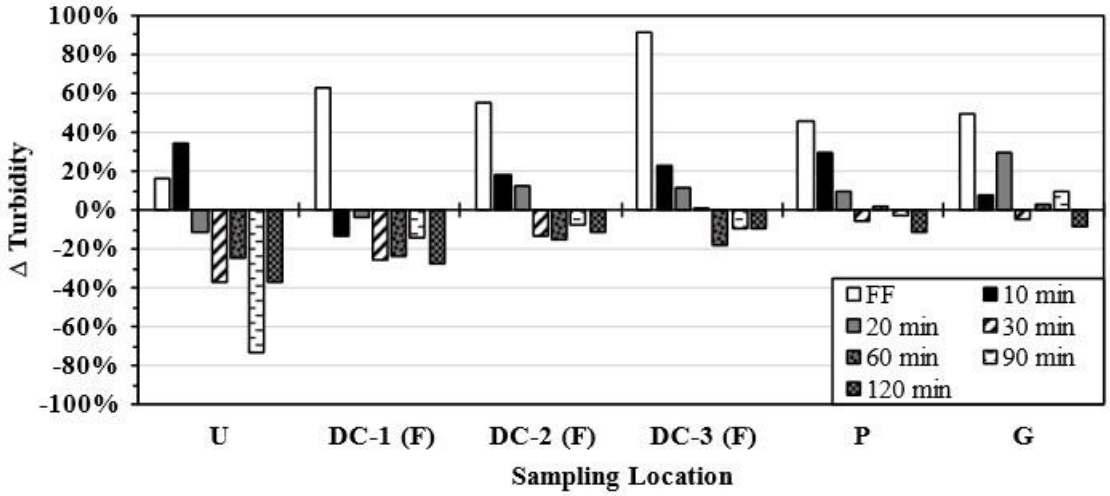

(a) sampling location

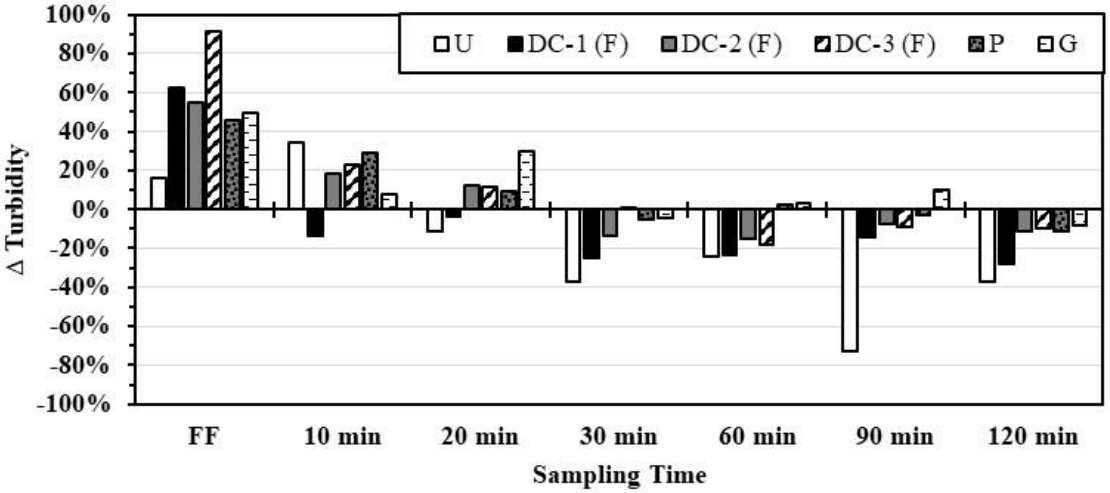

(b) sampling time

Figure 3-45. G-PAM Turbidity Reduction

High flocculant concentrations beginning from first flush (FF in figures) through the first 30 minutes of flow, that was discussed in the dosage and longevity results previously, is also displayed in the turbidity reduction plot in Figure 3-45(b), where the positive Δ turbidity indicates additional agitation is not needed to achieve similar turbidity reduction results. The trend in Figure 3-45(b) shows as time passes during testing and flocculant concentration decreases, the location where sufficient agitation (positive Δ turbidity values) occurs continues to move further

downstream in the channel. For example, at 20 minutes, U and DC-1(F) are not adequately mixed, whereas all other sampling locations are well mixed. Looking at samples from 90 minutes, U through P are all inadequately mixed as G is the last sampling location that indicates proper flocculant mixing. By the time the test reached 120 minutes, the flocculant concentration was predicted to be below 1 mg/L, where flocculation efficacy decreases compared to higher concentrations. Results indicate that one additional wattle without flocculant installed at the end of the channel would be beneficial to ensure sufficient mixing before discharging to a sediment basin.

Turbidity reduction results are also separated by sampling locations in Figure 3-45(b): upstream (U in figures), first ditch check (DC-1 in figures), second ditch check (DC-2 in figures), third ditch check (DC-3 in figures), after the underground pipe (P in figures), and at the end of the grass channel (G in figures). When upstream samples have a lower Δ turbidity value than any consecutive downstream samples, it indicates sediment is being captured in the channel with likely successful flocculation. When upstream samples have greater Δ turbidity values than downstream samples, it suggests minimal to no flocculation is occurring and additional sediment is being picked up throughout the channel.

3.4.4.3.2 BLOCK PAM

Since B-PAM large-scale test setup included only one silt fence ditch check with the purpose of determining the ideal number of flocculant blocks to target recommended dosing, the setup was not constructed for appropriate mixing. A negative Δ turbidity results indicates that the flocculant is not sufficiently mixed in the channel. Therefore, the results in Figure 3-46 confirm that nearly all samples collected were not subjected to sufficient mixing in the channel. This indicates that

flocculant blocks need to be installed where water would flow over at least one additional ditch check before discharging into a sediment basin to ensure sufficient mixing.

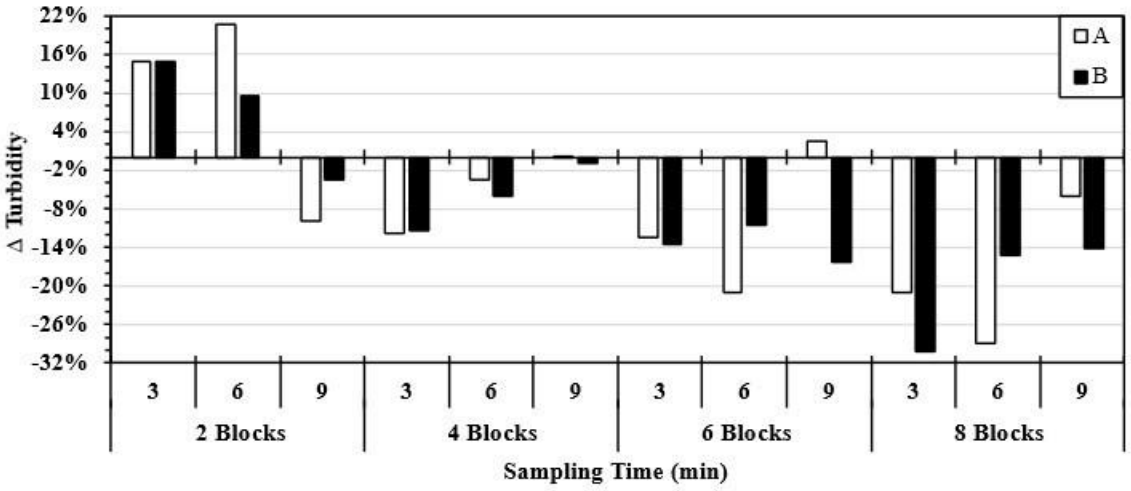

Figure 3-46. B-PAM Large-Scale Test Turbidity Reduction

Turbidity reduction results are also separated by upstream (A in figure), no flocculant, and downstream (B in figure), with flocculant, sampling locations in Figure 3-46. When upstream samples have a lower Δ turbidity value than downstream samples, it indicates sediment is being captured in the channel. Due to the channel design and downstream sampling location, sediment reduction between the two sampling locations is most likely due to flocculation. When upstream samples have greater Δ turbidity values than downstream samples, it suggests minimal to no flocculation is occurring and additional sediment is being picked up in the channel due to downstream scour. Figure 3-47 displays downstream scour that was observed after each test replication.

Figure 3-47. Observed Downstream Scour After Large-scale Block Test

3.4.4.4 VISUAL TESTS

Visual test sample recordings for both G-PAM and B-PAM were reviewed with a floc sizing template that was used during match testing (Figure 3-48). The following sections discuss results for G-PAM and B-PAM large-scale test results, respectively.

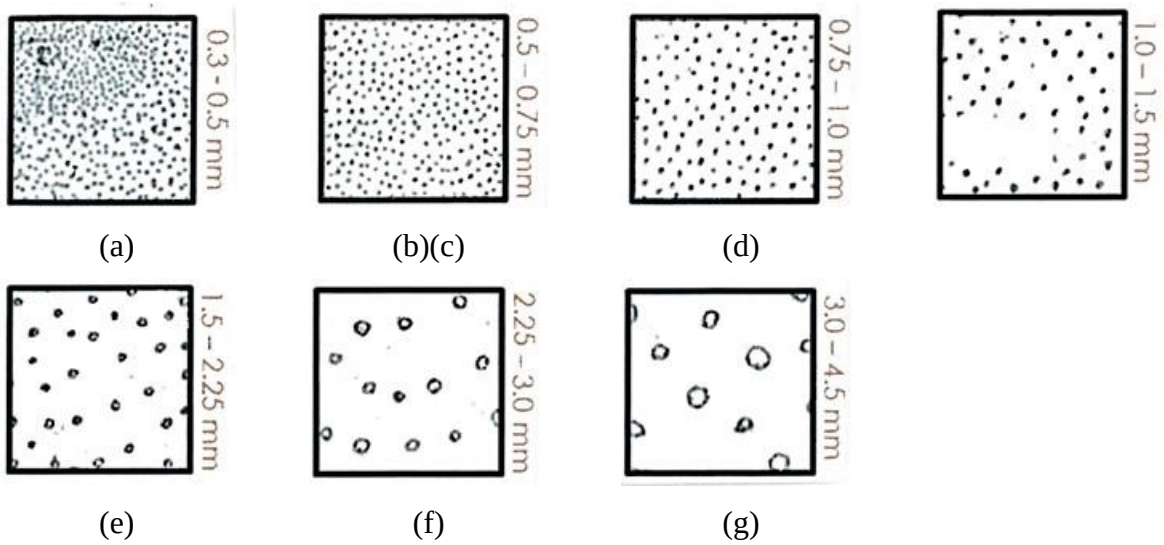

Figure 3-48. Visual Test Floc Sizing Observation Guide (Swift et al., 2015)

3.4.4.4.1 GRANULAR PAM

One test replication of visual test samples are shown in Figure 3-49, where after 5 seconds of settling, the observed floc size can be easily seen for the first two samples (D0 and D10 – first flush and 10 minute sample time for sampling location D, respectively), but becomes progressively more difficult to distinguish flocs as the sampling time continues.

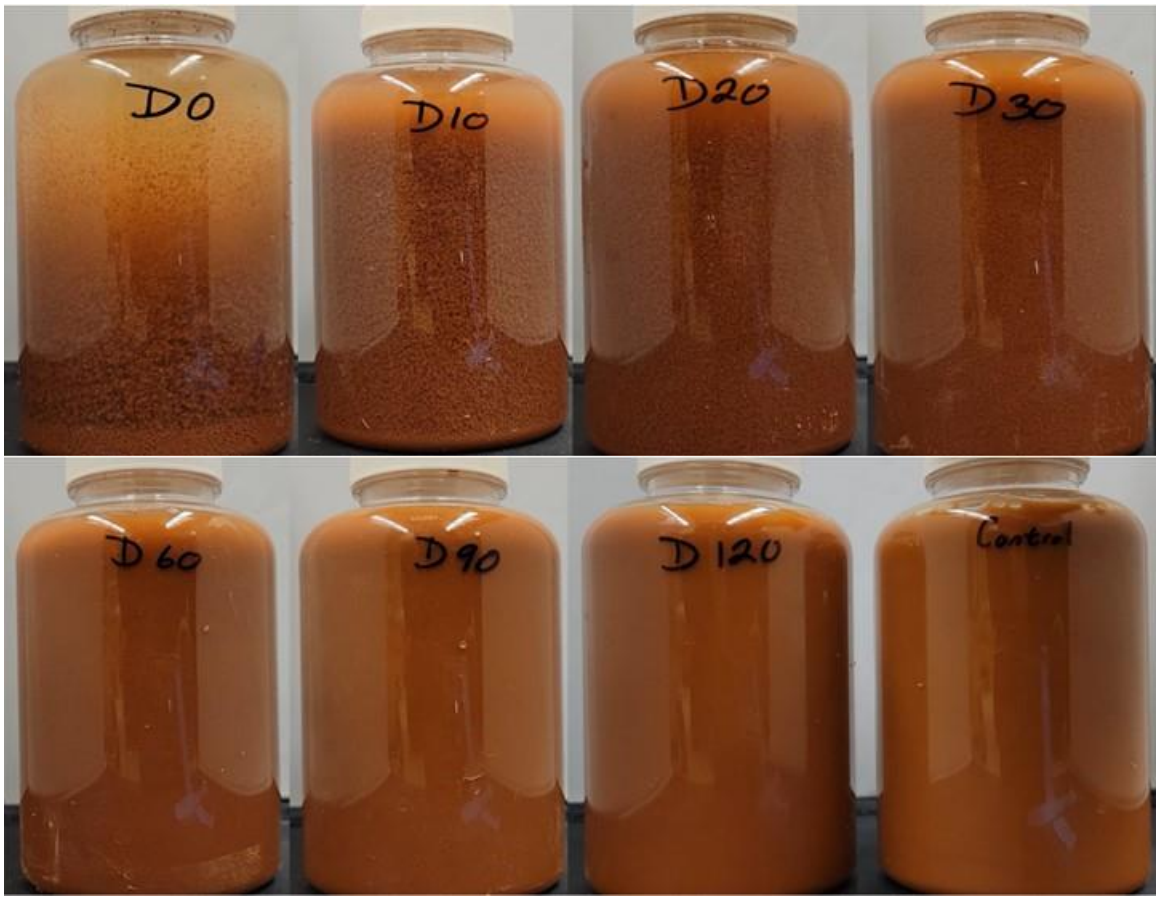

Figure 3-49. G-PAM Large-Scale Test Visual Jars after 5 Seconds of Settling Time

Once all the floc sizes were visually approximated using the template, the maximum range from the floc size template was used to quantify each sample. The results between all three test replications were averaged for each sampling time and results are shown in Figure 3-50. Here, trends are similar to the dosage and longevity results where after 60 min, flocs formed are very small, indicating that the dosing levels are below 1 mg/L but still marginally greater than 0 mg/L.

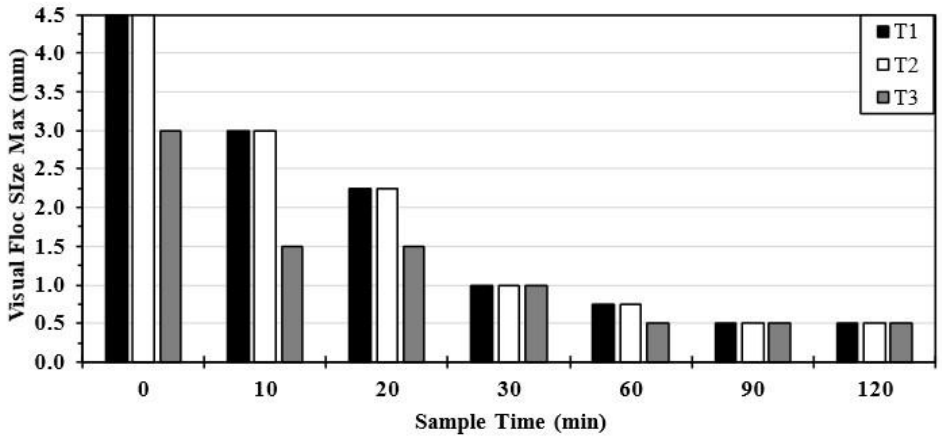

Figure 3-50. G-PAM Large-Scale Test Visual Results

3.4.4.4.2 BLOCK PAM

One test replication of visual test samples are shown in Figure 3-51, where after 1.5 minutes of settling, the observed flocs are difficult to see across all samples when compared to the control, however, a slight gradient difference can be observed in Figure 3-51 from all samples compared to the control.

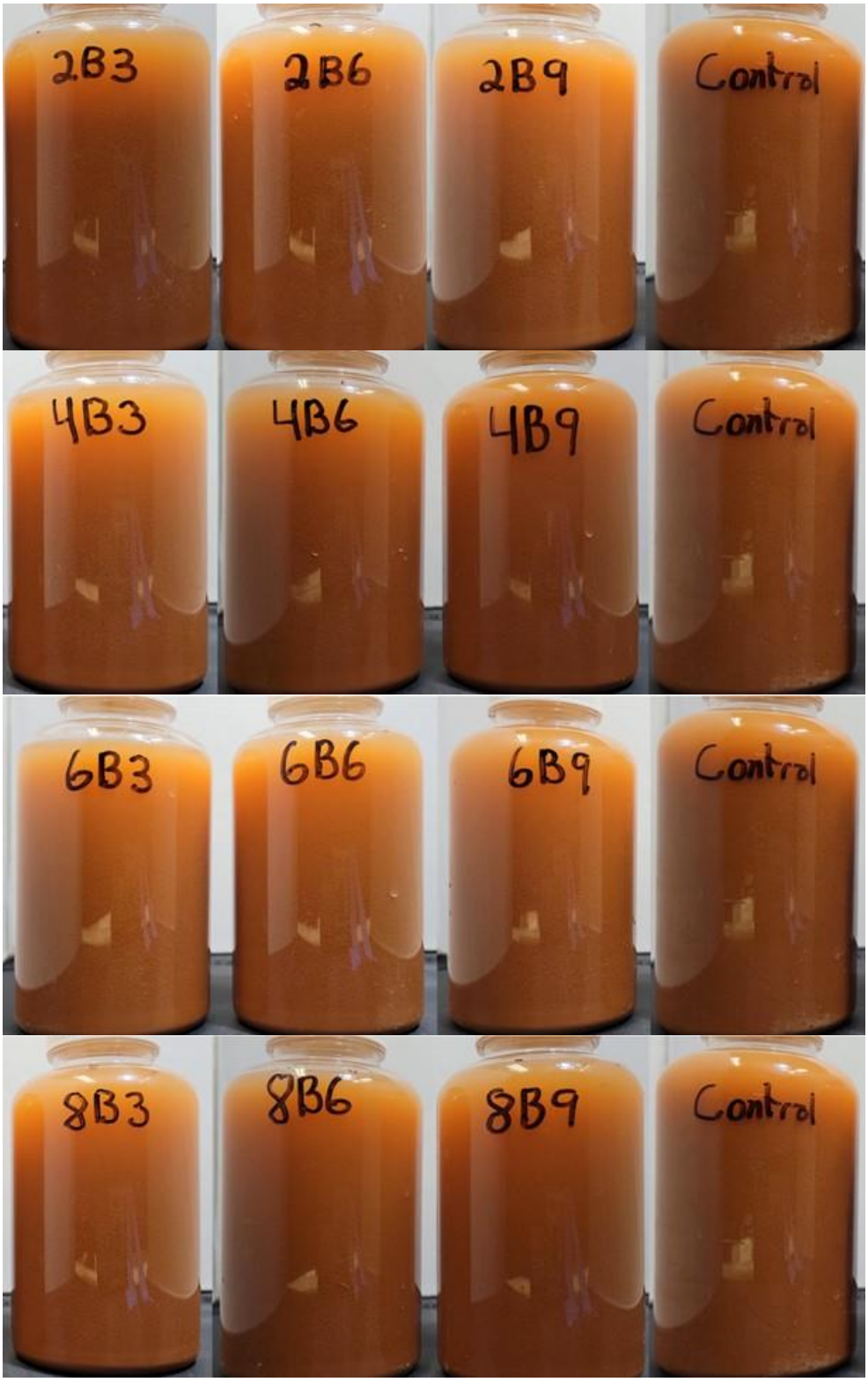

Figure 3-51. B-PAM Large-Scale Test Visual Jars after 1.5 Minutes of Settling Time

When quantifying and plotting the observed floc sizes in Figure 3-52, the trend shows that observed floc size increases over time with two flocculant blocks installed in the channel. Four, six, and eight flocculant blocks result in consistent observed floc sizes during testing. Six and eight flocculant blocks yielded the same observed floc size. Meaning six flocculant blocks are recommended to obtain maximum and consistent floc sizes under tested flow conditions.

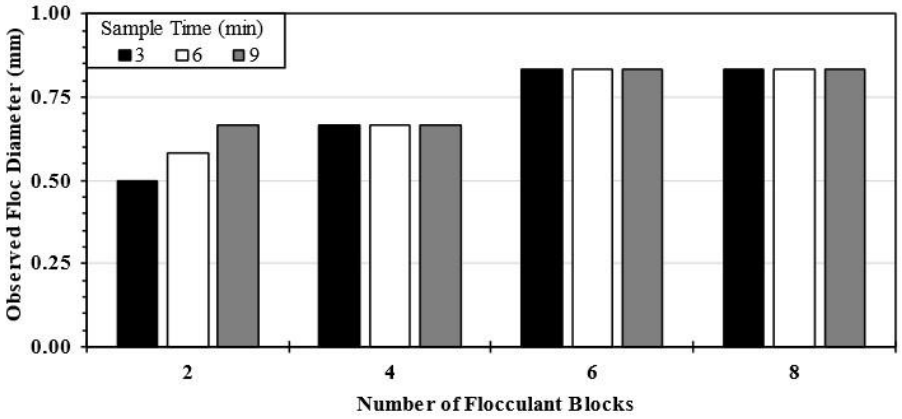

Figure 3-52. B-PAM Large-Scale Test Visual Results

3.5 SUMMARY

Research has investigated flocculant impacts in controlled or monitored settings ranging from uses in water, wastewater treatment, cosmetics, agriculture, mining industries, and more. However, the use of PAM in E&SC practices lacks guidance and consistency with application and maintenance that allows practitioners to maximize the use of the product without causing environmental harm. This work has identified requirements for proper dosage delivery mechanisms by validating bench- and intermediate-scale phase findings of this research through large-scale application sediment basin and channel-based evaluations. Performing large-scale test evaluations with granular and block form PAM using the expanded settling velocity residual detection method has enabled dosage rates over time to be quantified.

Initial large-scale testing showed promise of using residual settling plots initially developed for large-scale application of residual flocculant detection. However, it was clear that environmental conditions present in the field that influence flocculant efficacy needed to be accounted for. Residual settling plots were recreated by measuring the settling velocity for different flocculant concentrations at different pH values and temperatures to quantify flocculant efficacy across multiple factors that can vary by geographical region and season. Both G-PAM and B-PAM settling velocities were found to be significantly influenced by pH, temperature, and concentrations. G-PAM trends show that the soil settling velocity increases as the temperature and concentration increase and pH decreases. Whereas B-PAM soil settling velocity increases as temperature, concentration, and pH increases. However, further analysis should be conducted with B-PAM as it is unknown if the measured quantity of B-PAM fully dissolved in the sample before it was poured in graduated cylinders and the settling velocity was determined. Therefore, B-PAM settling velocity equation may not be an accurate representation of field conditions due to the ASTM jar testing methodology used.

Granular large-scale testing with G-PAM found that 180 g (6.36 oz.) spread across three wattles that were spaced over a total distance of 43 ft (13 m) initially dosed the channel with 19 mg/L and exponentially decreases to reach the recommended dosing concentration of 5.0 mg/L after 25.1 minutes and 1059.6 ft^3 (30.0 m^3) of flow. These results were developed by using the expanded residual settling velocity curves that include pH and temperature changes with various concentrations. Visual tests confirm predicted concentrations as visible flocs are progressively smaller as sampling time continues. After 60-minutes, very small flocs were observed, indicating dosing levels were under 1 mg/L but marginally greater than 0 mg/L. Results indicate that G-PAM should be reapplied after 3600 ft^3 (101.9 m^3) of flow or 1.0 in. (2.54 cm) of runoff per acre

(0.4 ha). This allows for underdosing above 1.0 mg/L to occur for an extended period of time to dilute initial increased dosing that is captured in a downstream sediment basin. Literature review found freshwater fleas to have the lowest LD_{50} of 14.1 mg/L which was exceeded during the first 20-minutes of flow. By reapplying flocculant after the recommended 3,600 ft^3 (101.9 m^3) of flow or 1.0 in. (2.5 cm) of runoff per 1.0 ac (0.4 ha), the reapplication rate can be justified by diluting residual concentrations to be below all aquatic organism toxicity limits before the effluent leaves the construction site. Turbidity results indicate G-PAM should be applied in a way where at least one ditch check at the end of the channel is left without flocculant application to mix flocculated water before discharging into a sediment basin.

Expanded residual settling velocity curves from Block form flocculant using B-PAM large-scale testing were inconclusive. However, using pond water collected during testing, a test-specific concentration prediction equation was established. B-PAM trends showed that settling velocities increased as the number of blocks in the channel grew, regardless of water volume or length of time. Large-scale testing showed that B-PAM quantification is problematic since current technologies cannot reliably detect known quantities. It is suggested that ASTM jar testing standards be modified to better account for the gelatinous flocculant form, or that improved methods for weighing out known concentrations while maintaining saturation consistency be determined. Turbidity data suggest applying B-PAM so that at least one ditch check at the end of a channel is flocculant-free to mix flocculated water before discharging into a sediment basin. Visual tests support residual predicted trends showing floc size rises with channel block count. Based on testing at AU-SRF using B-PAM that is developed by Manufacturer I with 1.80 ft^3/s (0.05 m^3/s) of flow and with sandy clay loam soil present at the AU-SRF, it was determined that six flocculant blocks were for channel flow applications. The number of blocks was determined

from visual tests as current residual detection methods using the ASTM jar testing method does not allow the product to fully dissolve and accurately reflect initial known concentrations. As products can vary greatly between manufacturers, the recommended number of flocculant blocks require testing based on product, flow, soils, and site-specific conditions. Based on testing at AU-SRF using B-PAM, block-form flocculants are not recommended for passive dosing systems as they were not as effective at flocculating the granular form flocculant (G-PAM) used. Passive dosing with flocculant blocks poses additional challenges to protect the product from drying out or sediment build-up, which can reduce its ability to treat stormwater. Further testing should be conducted to evaluate how long it takes for blocks to rehydrate to begin dosing during flow conditions or if the flocculation efficacy is impacted when the product is rehydrated after drying out. Additionally, flocculant block use in active treatment systems should be evaluated and compared to passive treatment methods using flocculant blocks to compare possible performance differences.

Large-scale evaluations on flocculants were essential to confirm results from intermediate-scale flume testing that contained controlled variables that would otherwise be uncontrolled in field applications. The findings of this research aim to guide practitioners in implementing adequate dosage delivery techniques on active job sites. This research demonstrated alternative ways of using residual concentration detection results to ensure proper dosage delivery in flocculant applications. Findings showed the importance of residual concentration detection not just for increased dosage monitoring, but also for identifying the agitation needs of the flocculant applications. It is important to note that these studies were conducted using PAM flocculants from Manufacturer I with AU-SRF sandy clay loam soil. Further analysis should be cautious when collecting large-scale test samples to ensure the use of single-use plastic bags when glass is not an

option. Proper cleaning is critical to minimize cross-contamination. Protecting samples from heating up and maintaining constant temperature and resting time between collection and processing is critical in maintaining consistency with residual flocculant predictions. This research provides insight on flocculant dosing during flow in field conditions to predict guidance on how and where to apply granular and block form flocculant to achieve effective flocculation without causing environmental harm and when reapplication should be performed. Therefore, these tests may not produce similar results for different flocculants or soil types. This research is meant to serve as a baseline for testing methodologies that can be used to evaluate other flocculant products to provide guidance on optimum flocculant implementation for construction sites. Future research should also focus on how to implement flocculants on different large-scale testing apparatuses different than sediment basins, determine better methods for quantifying residual flocculant block concentrations, and evaluate flocculant block uses in active treatment systems and compare the results to passive treatment systems. Moreover, the findings of this research would potentially pave the way for a future field monitoring study for flocculant applications on active construction sites.

CHAPTER FOUR: CONCLUSIONS AND RECOMMENDATIONS

4.1 INTRODUCTION

This research aimed to improve impoundment capabilities of wattles through simple and cost-effective solutions and improving the guidance available for the use of flocculants in construction stormwater applications. A comprehensive literature review for both wattles and flocculants detail the importance of each practice's role in E&SC. Wattle product evaluation procedures allow for emerging designs to be directly compared to existing products. Detailed evaluations on percent open area, encasement types, and fill densities all assess the components of wattles individually to assess areas of possible improvements. Various detection methods were assessed for quantifying residual flocculant concentrations for large-scale applications. Large-scale application testing was then conducted to develop guidance on large-scale application of flocculants. This section summarizes the conclusions of each of the investigated research areas in this project. General limitations of the research performed are also included, and explores avenues by which the knowledge base can be expanded by performing additional studies and investigations. The research identified universal applicability for improved wattle designs and identified common unknowns in flocculant application for construction stormwater treatment and developed methods to provide specialized guidance to ALDOT practitioners. Practical and implementable findings are provided in this chapter. The major findings of this research will ultimately promote improved wattle designs for impounding water and proper flocculant implementation on ALDOT construction sites to enhance the sediment capture function of temporary E&SC controls for protecting the waters of the U.S.

4.2 CONCLUSIONS AND RECOMMENDATIONS

This section summarizes the conclusions of each of the investigated research objectives in this thesis. The presented research identified how encasements and fill density can influence a wattle's impoundment abilities and identify how applied flocculant doses in a channel over time when environmental factors are accounted. The information provided contains specialized guidance for designers and practitioners to apply to constriction sites to improve E&SC practices. The major findings of this research will ultimately promote proper wattle product selection and flocculant implementation on construction sites to enhance sediment retention on temporary E&SC and protect downstream water bodies.

4.2.1 WATTLE PERFORMANCE

To achieve the first objective of this thesis, product, fabric, encasement, and density evaluations were conducted to assess how various wattle encasement material types with low percent open areas or fill densities impact a wattle's impoundment abilities. Wattle testing used a hydraulic flume located at Auburn University to conduct product evaluations and fabric impoundment evaluations that were independent of fill materials. Encasement evaluations that included fill material and fill density evaluations were evaluated through a collaboration with Iowa State University. The sections below include the individual tasks completed to achieve this specific research objective.

4.2.1.1 SMALL SCALE WATTLE PROTOTYPE EVALUATIONS

Small-scale product evaluations on wattles can help designers create novel products. A 15.00 ft (4.57 m) fiberglass hydraulic flume with a 1.00 ft (0.30 m) width and 1.50 ft (0.457 m) deep

rectangular open channel was sufficient to compare manufactured wattles and an impervious barrier to a new wattle product. For those wishing to improve their design before investing, a small-scale impoundment test can provide product insight quickly and cheaply. However, it is important to communicate with the product designer to agree on products to test and compare, evaluate manufactured products from different manufacturers to ensure fair product comparison, and explain the results and their meanings to the product designer for optimal outcomes.

4.2.1.2 Encasement Percent Open Area

The fabrics selected for wattle applications were chosen based on their capacity for impoundment. Phase II wattle application testing used the top-performing fabric encasement per fabric type from Phase I, adjusted for a tighter weave. Polypropylene, cotton, bamboo cotton blend, and polyester-polypropylene encasement materials were examined. Scanning each fabric and calculating its POA allows for direct comparison of hydraulic performance and wattle applications. To compare and expand results, Phase II's study technique was reproduced from Whitman et al. (2021a).

The encasement selection study indicated that decreasing the POA by 97.3% more than the control yielded a maximum impoundment length of 139 in. (354 cm) and depth of 8.42 in. (21.3 cm). Additionally, cotton fabrics with larger POA performed equally to polyester and polyester-polypropylene mix fabrics with smaller POA [e.g., C3, PP1, and P4 had POA values of 49.1, 39.9, and 29.1%, respectively, but yielded similar impoundment lengths of 24.7, 21.9 and 27.2 in. (62.7, 55.7, and 69.0 cm) and depths of 3.38, 3.30, and 3.45 in. (8.59, 8.38, and 8.76 cm), respectively].

Impoundment length and depth ratio graphs demonstrate that most wattles impound water within or near the PTW during high flow. Since water had less time to move through the wattles before overtopping, high impoundment capacities were likely related to channel volume. Low-flow wattles were more likely to impound water poorly. This difference in performance depends

greatly on the material type and density (Donald et al., 2015). This deficient performance during low flow conditions is the target area to seek improvement.

Low flow [0.250 ft^3/s (0.00708 m^3/s)] and high flow [0.750, 1.25, and 2.00 ft^3/s (0.0212, 0.0354, and 0.0566 m^3/s)] were used to evaluate the wattles hydraulic performance. C2M improved length and depth ratios most for low and high flow in the MLR. C2MT outperformed C2M but not enough to warrant the extra cost. In low and high flow, P2M increased impoundment length and depth less than C2M. C2M surpasses P2M and is more environmentally friendly.

Only PP1M consistently lowered hydraulic performance for length, depth, and low and high flow conditions, demonstrating that materials may impair impoundment. The MLR study found no correlation between encasement POA and impoundment length and depth ratios, supporting the idea that fabric type has a greater impact on a wattle's hydraulic performance. A material made of only polypropylene had an adverse effect on the hydraulic performance than when polyester is mixed with polypropylene.

4.2.1.3 Fill Density

Contrary to previous research, increasing fill density appeared to significantly decrease the overall hydraulic performance, regardless of flow conditions. The repacking of the two denser wattles was a variable that could not be accounted for when exchanging or adding additional fill material to create different wattles from the control. Therefore, this procedure may not have been representative of how the control wattle was packed, resulting in the formation of additional pores throughout the media. Future studies that account for this variable may produce differing outcomes.

4.2.1.4 LIMITATIONS AND RECOMMENDATIONS

It's worth noting that this investigation was carried out with clean water. Since encasement blinding and soil buildup may impair performance, future studies should incorporate soil introduction. POA was examined using dry encasement fabrics. Understanding the fabrics' hydraulic performance may require studying their saturated POA. Evaluation materials were difficult to acquire due to a global supply shortage. Therefore, exploring the hydraulic performance of additional biodegradable encasement choices, such as bamboo cotton blend (B1), which performed well in the encasement evaluation phase of this study but could not be woven to the requisite dimensions due to its age and fragility. As the industry strives to reduce plastic in E&SC, investigating the hydraulic performance of alternative biodegradable materials might be beneficial. To determine overall costs, a life cycle cost study of encasement materials should be done.

This investigation could also be expanded by conducting durability tests, large-scale applications, and quantifying flow-through rates of various fill materials. Further research should also expand on the hydraulic performance of wattles with lower densities while maintaining the wattle dimensions. All wattle evaluations that involve altering existing packing methods performed from a manufacturer should consider alternative ways to control for the possibility of altering the fill media. Packing wattles by hand may bring error to evaluations as additional pores through the media or uneven packing densities throughout the product.

Lastly, future wattle performance evaluations should consider assessing the shear stress reduction in the channel. The evaluation method used in this thesis quantifies wattle performance based on impoundment length and depth ratios. Light rain events that produce a small amount of surface runoff, result in minimal channel flow with low shear stresses. These low shear stresses

do not lead to erosion in the channel but would be disguised as poor-performing products using the impoundment ratio method. This is due to when the water depth reaches the wattle height and the throughflow rate, via wattle voids, is larger than the incoming runoff flowrate, the water will not overtop the wattle. Which would be considered as poor-performance as defined by the impoundment ratio method. However, the small impoundment created curing these low flow events may have already reduced the shear stress sufficiently to reduce/avoid channel erosion. Quantifying shear stress reductions in the channel would better account for assessing the wattle's performance across all flow conditions.

4.2.2 FLOCCULANTS

The flocculant portion of this research aimed to improve residual flocculant detection methods for large-scale application and perform large-scale experiments to evaluate flocculant form, placement, agitation, mixing, and reapplication requirements for granular and block form flocculant in a large-scale setting with less controlled variables. These two research objectives are broken down in the following sections.

4.2.2.1 FLOCCULANT DETECTION METHODS FOR LARGE-SCALE APPLICATION

The second objective of this thesis was to expand on large-scale application methods for residual flocculant concentration detection. This study evaluated two viscosity methods, one SCV method, and expanded on the existing settling velocity residual detection method developed by Kazaz et al. (2022).

There are several methods for quantifying flocculants, but the challenge was to find a detection method that is simple and easy to perform without extensive lab training, low cost, works with sediment-ladened samples, produces reliable results in a short time, and can quantify

concentrations above and below the PAM manufacturer's recommendation of 5.0 mg/L. A Cannon-Fenske Routine Viscometer and Brookfield Digital Viscometer were not sensitive enough to discern concentration changes below 20 mg/L. Cannon-Fenske tubes also required samples to be silt-free before evaluation since debris could block the tubes and affect results.

LCA was performed using two anionic forms of flocculant, G and B-PAM, and one cationic form, chitosan. G-PAM and chitosan were not viable options for determining increased dosing by measuring the sample's SCV in the presence of sediment, whereas B-PAM was able to quantify concentrations between 3 and 7 mg/L. When soil is present at 0.125 to 7.00 mg/L, 3.00 to 7.00 mg/L, and 20 to 200 mg/L, G-PAM, B-PAM, and chitosan flocculants dramatically lower pH values. Using sample pH change versus SCV may be able to approximate concentration ranges that would be difficult to distinguish from concentration versus SCV plots alone. Future evaluations should include additional flocculants and soil types because trends and connections may vary.

Initial residual settling plots created by Kazaz et al., (2022), had shown promise in preliminary large-scale testing for initial large-scale application of residual flocculant detection. Nonetheless, it was evident that environmental conditions present in the field that affect flocculant efficacy must be accounted for in this method. Residual settling plots were produced by monitoring the settling velocity for different flocculant concentrations at varied pH values and temperatures to assess flocculant efficacy across many parameters that can vary by geographical region and season. The settling velocities of G-PAM and B-PAM were found to be substantially affected by pH, temperature, and concentrations. According to G-PAM trends, temperature, concentration, and pH increase soil settling velocity, while B-PAM soil settling velocity trends increase as temperature, concentration, and pH increase. As it is uncertain whether the measured

amount of B-PAM was completely dissolved in the sample before it was poured into graduated cylinders and the settling velocity was measured, additional analysis should be conducted with B-PAM. Therefore, B-PAM settling velocity equation may not be an accurate representation of field conditions due to the ASTM jar testing methodology used.

4.2.2.2 LARGE-SCALE FLOCCULANT APPLICATION

The last objective of this thesis was to provide flocculant application placement and reapplication timing guidance on construction sites to achieve optimum dosing and mixing for granular and block-form flocculants. This study performed large-scale tests using granular and block form flocculant that focused on dosage, longevity, quantity, turbidity reduction, and visual tests to provide insight of how flocculant is dosed and mixed in a channel during a flow event. The following subsections review the two flocculant forms evaluated in large-scale evaluations.

4.2.2.2.1 GRANULAR FLOCCULANT

Channelized testing using straw wattles found that 6.4 oz. (180 g) spread across three wattles spaced 43 ft (13 m) initially dosed the channel with 19 mg/L and exponentially decreased to the target dosing concentration of 5.0 mg/L after 25.1 minutes and 1,060 ft^3 (30.02 m^3) of flow. Expanded residual settling velocity curves with pH and temperature variations at varied concentrations were used to obtain concentration results. Visual observations show decreasing floc formation over time, confirming projected concentrations. After 60 minutes, minimally discernible flocs showed dosage levels <1 mg/L but above 0 mg/L. Results suggest reapplying G-PAM granular flocculant after 3,600 ft^3 (101.9 m^3) of flow or 1.0 in. (2.54 cm) of runoff per acre (0.4 ha) into a channel. This allows prolonged underdosing above 1.0 mg/L to dilute downstream sediment basin increased dosing. Turbidity data suggest applying granular flocculant so that at

least one ditch check at the channel's terminus should be flocculant-free to ensure sufficient mixing is achieved for flocculated water before discharging into a sediment basin.

4.2.2.2.2 FLOCCULANT BLOCK

Unlike the granular form flocculant, block form flocculants evaluated using the expanded residual settling velocity curves were inconclusive for B-PAM used during large-scale tests. However, using pond water collected during testing, a test-specific concentration prediction equation was established. Block form flocculant trends showed that settling velocities increased as the number of blocks in the channel grew, regardless of water volume or length of time. Large-scale testing showed that flocculant blocks quantification is problematic since current technologies cannot reliably detect known quantities.

Visual tests support residual predicted trends showing floc size increases with block count. Testing was conducted in a 4 ft (1 m) wide trapezoidal channel with 3:1 side slopes at a 5% slope. A standard ALDOT silt fence ditch check was installed within the channel and flocculant blocks were placed immediately downstream of the ditch check. A sandy clay loam soil was introduced at a rate of 42.8 lb./min (19.4 kg/min) to create a turbidity of approximately 1500 ± 500 NTU. At the flow rate of 1.80 ft^3/s (0.05 m^3/s), it was determined that six flocculant blocks were effective providing proper dosage concentration. The number of blocks was determined from visual tests as residual detection methods using the ASTM Jar Testing Method did not allow the product to fully dissolve and accurately reflect initial known concentrations. Further testing is recommended by evaluating block requirements for different products and flow rates. In addition, passive dosing with flocculant blocks poses challenges to protect the product from drying out or from accumulating sediment build-up, which may impact its ability to treat stormwater. Evaluation of hydration requirements and longevity of flocculant blocks is needed.

Large-scale evaluations on flocculants were essential in this research to elevate the knowledge gained in the bench-scale and intermediate-scale phases by replicating construction conditions. The findings of this research aim to guide practitioners in implementing adequate dosage delivery techniques on active construction sites. This research demonstrated alternative ways of using residual concentration detection results to ensure proper dosage delivery in flocculant applications. Findings showed the importance of residual concentration detection not just for increased dosage monitoring, but also for identifying the agitation needs of the flocculant applications.

4.2.2.3 Lessons Learned, Limitations, and Future Research Recommendations

It is important to note that these studies were conducted using PAM flocculants from Manufacturer I with AU-SRF sandy clay loam soil and findings may be limited. Further analysis should be cautious when collecting field samples to ensure the use of single-use plastic bags when glass is not an option. Proper cleaning is critical to minimize cross-contamination. Protecting samples from heating up and maintaining constant temperature and resting time between collection and processing is critical in maintaining consistency with residual flocculant predictions. This research provides insight on flocculant dosing during flow in field conditions to predict guidance on how and where to apply granular and block form PAM using G-PAM and B-PAM, respectively, to achieve effective flocculation without causing environmental harm and when reapplication should be performed. Therefore, these tests may not produce similar results for different flocculants, soil types, or flow rates. This research is meant to serve as a baseline for testing methodologies that can be used to evaluate other flocculant products to provide guidance on optimum flocculant implementation for construction sites.

As flocculants are highly soil-dependent, future research efforts should emanate from this research by allowing opportunities to evaluate more soils with different types of flocculant products and expand knowledge on soil-dependent dosage requirements. These evaluations should strive to build a bank of standard residual concentration plots for different products and soil types. These standard residual concentration plots should include a range of temperatures, pH values, concentrations, soil types, and flocculant products from different manufacturers to build a bank of data that can be used to predict residual flocculant concentrations regardless of the season, geographical location, or product used. Additionally, using the SCV to predict residual flocculant concentrations should be further explored using additionally flocculant products and soil types to track trend changes. Even though this detection method may not be as feasible for large-scale applications due to time and cost restrictions, further evaluations with this product may aid in flocculant monitoring in more controlled environments.

The ASTM jar testing methodology (ASTM International D2035-19, 2008) is not ideal for block form flocculant due to its gelatinous consistency that is designed to slowly dissolve. Future studies should focus on identifying methods for reliably quantifying residual flocculant block concentrations to allow for additional time for the block to dissolve where it can create flocs and correlate those results to settling velocities collected in large-scale testing. Subsequent studies should focus on how to implement flocculants on different large-scale testing apparatuses that can treat stormwater prior to being captured in a sediment basin, determine better methods for quantifying residual flocculant block concentrations, and evaluate flocculant block uses in active treatment systems and compare the results to passive treatment systems. Future testing should be conducted to evaluate how long it takes for blocks to rehydrate to begin dosing during flow conditions or if the flocculation efficacy is impacted when the product is rehydrated after drying

out. Additionally, flocculant block use in active treatment systems should be evaluated and compared to passive treatment methods using flocculant blocks to compare possible performance differences.

REFERENCES

Aguilar, M. I., Sáez, J., Lloréns, M., Soler, A., Ortuño, J. F., Meseguer, V., & Fuentes, A. (2005). Improvement of coagulation-flocculation process using anionic polyacrylamide as coagulant aid. *Chemosphere*, *58*(1), 47–56. https://doi.org/10.1016/j.chemosphere.2004.09.008

Al Momani, F. A., & Örmeci, B. (2014). Measurement of polyacrylamide polymers in water and wastewater using an in-line UV-vis spectrophotometer. *Journal of Environmental Chemical Engineering*, *2*(2), 765–772. https://doi.org/10.1016/j.jece.2014.02.015

Alabama Department of Environmental Management. (2020). *303(d) Information and Map*. https://adem.alabama.gov/programs/water/303d.cnt

Alabama Department of Environmental Management. (2021a). Alabama Department of Environmental Management Construction General Permit. In *Alabama Department of Environmental Management*. https://adem.alabama.gov/programs/water/constructionstormwater.cnt

Alabama Department of Environmental Management. (2021b). National Pollutant Discharge Elimination System General Permit. In *ADEM* (Code of Alabama 1975, §§22-22A-1 to 22-22A-15). chrome-extension://efaidnbmnnnibpcajpcglclefindmkaj/https://adem.alabama.gov/newsEvents/notices/jul21/pdfs/ALR040000.pdf

Alabama Department of Transportation. (2020). Best Management Practice. In *Alabama Department of Transportation* (Vol. 100, Issue c). https://www.dot.state.al.us/publications/Construction/pdf/Specifications/2022/StandardDrawings.pdf

Al-Hashmi, A. R., & Luckham, P. F. (2010). Characterization of the adsorption of high molecular weight non-ionic and cationic polyacrylamide on glass from aqueous solutions using modified atomic force microscopy. In *Colloids and Surfaces A: Physicochemical and Engineering Aspects* (Vol. 358, Issues 1–3, pp. 142–148).

Anderson, F. A. (2005). Amended final report on the safety assessment of polyacrylamide and acrylamide residues in cosmetics. *International Journal of Toxicology*, *24*(SUPPL. 2), 21–50. https://doi.org/10.1080/10915810590953842

ASTM International D446-12. (2009). Standard Specifications and Operating Instructions for Glass Capillary Kinematic Viscometers. In *American Society for Testing and Materials International* (Vol. 12, Issue Reapproved). https://doi.org/10.1520/D0446-12R17.2

ASTM International D789-19. (2008). Standard Test Method for Determination of Relative Viscosity of Concentrated Polyamide (PA) Solutions. In *American Society for Testing and Materials International*. https://doi.org/10.1520/mnl10913m

ASTM International D2035-19. (2008). Standard Practice for Coagulation-Flocculation Jar Test of Water. In *American Society for Testing and Materials International*. https://doi.org/10.1520/D2035-19.2

ASTM International D4751-21a. (2021). Standard Test Methods for Determining Apparent Opening Size of a Geotextile. *American Society for Testing and Materials International*. https://doi.org/10.1520/D4751-21A

ASTM International D7208-14e1. (2018). *Standard Test Method for Determination of Temporary Ditch Check Performance in Protecting Earthen Channels from Stormwater-Induced Erosion*. https://doi.org/10.1520/D7208-14E01

Australian and New Zealand Environment and Conservation Council, & Agriculture and Resource Management Council of Australia and New Zealand. (2000). Australian and New Zealand Guidelines for Fresh and Marine Water Quality. *National Water Quality Management Strategy*, *1*, Chapters 1-7.

Aydilek, A. H., & Edil, T. B. (2004). Evaluation of Woven Geotextile Pore Structure Parameters Using Image Analysis. *Geotechnical Testing Journal*, *27*(1), 99–110. https://doi.org/10.1520/gtj11070

Bachand, P. A. M., Bachand, S. M., Lopus, S. E., Heyvaert, A., & Werner, I. (2010). Treatment with chemical coagulants at different dosing levels changes ecotoxicity of stormwater from the Tahoe basin, California, USA. In *Journal of Environmental Science and Health - Part A Toxic/Hazardous Substances and Environmental Engineering* (Vol. 45, Issue 2). https://doi.org/10.1080/10934520903425459

Beim, A. A., & Beim, A. M. (1994a). Comparative ecological - toxicological data on determination of maximum permissible concentrations (mpc) for several flocculants. *Environmental Technology (United Kingdom)*, *15*(2), 195–198. https://doi.org/10.1080/09593339409385420

Beim, A. A., & Beim, A. M. (1994b). Comparative ecological - toxicological data on determination of maximum permissible concentrations (mpc) for several flocculants. *Environmental Technology (United Kingdom)*, *15*(2), 195–198. https://doi.org/10.1080/09593339409385420

Besaratinia, A., & Pfeifer, G. P. (2007). A review of mechanisms of acrylamide carcinogenicity. *Carcinogenesis*, *28*(3), 519–528. https://doi.org/10.1093/carcin/bgm006

Bhatia, S. K., Khachan, M. M., Stallings, A. M., & Smith, J. L. (2014a). Alternatives for the detection of residual polyacrylamide in geotextile tube dewatering-streaming current detection and china clay settling rate methods. *Geotechnical Testing Journal*, *37*(4). https://doi.org/10.1520/GTJ20130162

Bhatia, S. K., Khachan, M. M., Stallings, A. M., & Smith, J. L. (2014b). Alternatives for the detection of residual polyacrylamide in geotextile tube dewatering-streaming current detection and china clay settling rate methods. *Geotechnical Testing Journal*, *37*(4). https://doi.org/10.1520/GTJ20130162

Bhattarai, R., Kalita, P., Garcia, C. B., & Schumacher, P. (2016). Evaluation of Ditch Checks for Sediment Retention. *Illinois Center for Transportation/Illinois Department of Transportation*, *FHWA-ICT-16-002*.

Biesinger, K. E., & Stokes, G. N. (1986). Effects of synthetic polyelectrolytes on selected aquatic organisms. *Journal of the Water Pollution Control Federation*, *58*(3), 207–213.

Bjorneberg, D. L. (2013). Temperature, Concentration, and Pumping Effects on PAM Viscosity. *American Society of Agricultural Engineers*, *41*(208), 1651–1655. WWW.PADYCHBOOKS.COM

Brookfield. (2014). Brookfield Dial Viscometer (Operating Instructions). *Brookfield Engineering Laboratories, Inc.* https://www.brookfieldengineering.com/-/media/ametekbrookfield/manuals/obsolete manuals/dial m85-150-p700.pdf?la=en

Brookfield Engineering Laboratoried, Inc. (1985). *Brookfield Dial reading Viscometer Brookfield Digital Viscometer Model DV-I (Operating Instructions)*. LabWrench. https://photos.labwrench.com/equipmentManuals/4807-1512.pdf

Brown, P. M., Stanley, D. A., & Scheiner, B. J. (1989). An explanation of flocculation using Lewis acid-base theory. *Mining, Metallurgy & Exploration*, *6*, 196–200. https://doi.org/https://doi.org/10.1007/BF03403463

Buczek, S. B., Cope, W. G., McLaughlin, R. A., & Kwak, T. J. (2017). Acute toxicity of polyacrylamide flocculants to early life stages of freshwater mussels. *Environmental Toxicology and Chemistry*, *36*(10), 2715–2721. https://doi.org/10.1002/etc.3821

Butler, T. O., Acurio, K., Mukherjee, J., Dangasuk, M. M., Corona, O., & Vaidyanathan, S. (2021). The transition away from chemical flocculants: Commercially viable harvesting of Phaeodactylum tricornutum. *Separation and Purification Technology*, *255*(April 2020), 117733. https://doi.org/10.1016/j.seppur.2020.117733

Calhoun, C. C. (1972). Development of Design Criteria and Acceptance Specifications for Plastic Filter Cloths. *U.S. Army Engineer WaterWays Experiment Station*, *Technical*.

Canadian Centre for Occupational Health and Safety. (2023). Chemicals and Materials What is a LD 50 and LC 50 ? *Canadian Centre for Occupational Health and Safety*.

Cannon Instrument Company. (2018). *Calculation of Viscometer Constants for Cannon-Fenske Routine and Cannon-Fenske Opaque Viscometers (Tech Brief 101)*. Cannon Instrument Company. https://cannoninstrument.com/pub/media/assets/product/documents/Whitepapers/GENERAL VISCOSITY/Calculation of Viscometer Constants for Cannon-Fenske Routine and Cannon-Fenske Opaque Viscometers (Tech Brief 101) .pdf

Cannon Instrument Company. (2023). CANNON-FENSKE ROUTINE VISCOMETER. In *Cannon Instrument Company*. https://cannoninstrument.com/manual-glass-viscometers/cannon-fenske-routine-viscometer.html

Carere, A. (2006). Genotoxicity and carcinogenicity of acrylamide: A critical review. *Annali Dell'Istituto Superiore Di Sanita*, *42*(2), 144–155.

Carolina Hydrologic, L. (2019). H30 PAM Safety Data Sheet. In *Carolina Hydrologic, LLC*. https://us.vwr.com/assetsvc/asset/en_US/id/16490607/contents

Caulfield, M. J., Hao, X., Qiao, G. G., & Solomon, D. H. (2003). Degradation on polyacrylamides. Part I. Linear polyacrylamide. *Polymer*, *44*(5), 1331–1337. https://doi.org/10.1016/S0032-3861(03)00003-X

Chang, Q., Hao, X., & Duan, L. (2008). Synthesis of crosslinked starch-graft-polyacrylamide-co-sodium xanthate and its performances in wastewater treatment. *Journal of Hazardous Materials*, *159*(2–3), 548–553. https://doi.org/10.1016/j.jhazmat.2008.02.053

Chapman, J. M., Proulx, C. L., Veilleux, M. A. N., Levert, C., Bliss, S., André, M. È., Lapointe, N. W. R., & Cooke, S. J. (2014). Clear as mud: A meta-analysis on the effects of sedimentation on freshwater fish and the effectiveness of sediment-control measures. *Water Research*, *56*, 190–202. https://doi.org/10.1016/j.watres.2014.02.047

Chmtrac Systems Inc. (2017). *Laboratory Charge Analyzer (Operations Manual - Models: LCA-1, LCA-2, LCA-2)*. Chmtrac Systems Inc. https://chemtrac.com/downloads-3/

Christofano, E. E., Frawley, J. P., Fancher, O. E., & Keplinger, M. L. (1969). The toxicology of modified polyacrylamide resin. *Toxicology and Applied Pharmacology*, *14*, 616.

Christopher, B. R., & Fischer, G. R. (1992). Geotextile filtration principles, practices and problems. *Geotextiles and Geomembranes*, *11*(4–6), 337–353. https://doi.org/10.1016/0266-1144(92)90018-6

Code of Federal Regulations. (2023). *Electronic Code of Federal Regulations*. Code of Federal Regulations. https://www.ecfr.gov/

Colen, C. Van, Rossi, F., Montserrat, F., Andersson, M. G. I., Gribsholt, B., Herman, P. M. J., Degraer, S., Vincx, M., Ysebaert, T., & Middelburg, J. J. (2012). Organism-Sediment Interactions Govern Post-Hypoxia Recovery of Ecosystem Functioning. *PLoS ONE*, *7*(11). https://doi.org/10.1371/journal.pone.0049795

Dao, V. H., Cameron, N. R., & Saito, K. (2016). Synthesis, properties and performance of organic polymers employed in flocculation applications. *Polymer Chemistry*, *7*(1), 11–25. https://doi.org/10.1039/c5py01572c

Dente, S. K., Gucciardi, B. M., Griskowitz, N., Chang, L. L., & Raudenbush, D. L. (2000). Chemistry . Function , and Fate of Acrylamide-Based. *Chemical Water and Wastewater Treatment VI*, 1–2.

Donald, W. N., Zech, W. C., & Fang, X. (2015). Comparative Evaluation of Wattle Ditch Checks Composed of Differing Materials and Properties. *Journal of Irrigation and Drainage Engineering*, *141*(2), 04014051. https://doi.org/10.1061/(asce)ir.1943-4774.0000794

Donald, W. N., Zech, W. C., Fang, X., & Lamondia, J. J. (2013). Evaluation of wheat straw wattles for velocity reduction in ditch check installations. *Transportation Research Record*, *2358*, 69–78. https://doi.org/10.3141/2358-08

Donald, W. N., Zech, W. C., Fang, X., & Perez, M. A. (2016). Hydraulic Method to Evaluate the Performance of Ditch Check Practices and Products. *Journal of Hydrologic Engineering*, *21*(11), 04016042. https://doi.org/10.1061/(asce)he.1943-5584.0001311

Druschel, S. J. (2014). Flocculation Treatment BMPs for Construction Water Discharges. *Minnesota Department of Transportation Research Services & Library*, *August*.

Duggan, K. L., Morris, M., Bhatia, S. K., Khachan, M. M., & Lewis, K. E. (2019). Effects of Cationic Polyacrylamide and Cationic Starch on Aquatic Life. *Journal of Hazardous, Toxic, and Radioactive Waste*, *23*(4), 1–12. https://doi.org/10.1061/(asce)hz.2153-5515.0000467

Erkekoglu, P., & Baydar, T. (2014). Acrylamide neurotoxicity. *Nutritional Neuroscience*, *17*(2), 49–57. https://doi.org/10.1179/1476830513Y.0000000065

Forbes, E. (2011). Shear, selective and temperature responsive flocculation: A comparison of fine particle flotation techniques. *International Journal of Mineral Processing*, *99*(1–4), 1–10. https://doi.org/10.1016/j.minpro.2011.02.001

Fort, D. J., & Stover, E. L. (1995). Impact of toxicities and potential interactions of flocculants and coagulant aids on whole effluent toxicity testing. *Water Environment Research*, *67*(6), 921–925. https://doi.org/10.2175/106143095x133149

Glover, S. M., Yan, Y. de, Jameson, G. J., & Biggs, S. (2004). Dewatering properties of dual-polymer-flocculated systems. *International Journal of Mineral Processing*, *73*(2–4), 145–160. https://doi.org/10.1016/S0301-7516(03)00070-X

Greenwood, J. (2022). *How are coagulants and flocculants used in water and wastewater treatment?* WCS Group Safe Efficient Compliance. https://www.wcs-group.co.uk/wcs-

blog/coagulants-flocculants-wastewater-treatment#:~:text=Coagulation and flocculation are two,easily separated from the liquid.
Guezennec, A. G., Michel, C., Bru, K., Touze, S., Desroche, N., Mnif, I., & Motelica-Heino, M. (2015). Transfer and degradation of polyacrylamide-based flocculants in hydrosystems: A review. *Environmental Science and Pollution Research*, *22*(9), 6390–6406. https://doi.org/10.1007/s11356-014-3556-6
Hancock, B. (2017). Flocculants: How Do They Work and Why? *Mainland Machinery Ltd*.
Hench, L. L., & Wilson, J. (1984). Surface-Active Biomaterials. *Science*, *226*(4675), 630–636. https://doi.org/10.1126/science.6093253
Howard, P. H., Bosch, S. J., & Lande, S. S. (1978). Degradation and Leaching of Acrylamide in Soil. *ACS Division of Environmental Chemistry, Preprints*, *18*(2). https://doi.org/10.2134/jeq1979.00472425000800010029x
Hunter, R. J. (1986). Foundations of Colloid Science. In *Oxford Science* (Vol. 1).
International Programme on Chemical Safety. (1985). *Environmental Health Criteria No. 49, Acrylamide*. International Programme on Chemical Safety. http://www.inchem.org/documents/ehc/ehc/ehc49.htm.
Jensen, W. B. (1978). The Lewis Acid-Base Definitions: A Status Report. *American Chemical Society*, *78*(1).
Jung, J., Jang, J., & Ahn, J. (2016). Characterization of a polyacrylamide solution used for remediation of petroleum contaminated soils. *Materials*, *9*(1), 1–13. https://doi.org/10.3390/ma9010016
Kajihara, M. (1971). Settling velocity and porosity of large suspended particle. *Journal of the Oceanographical Society of Japan*, *27*(4), 158–162. https://doi.org/10.1007/BF02109135
Kang, J., Sowers, T. D., Duckworth, O. W., Amoozegar, A., Heitman, J. L., & McLaughlin, R. A. (2013). Turbidimetric Determination of Anionic Polyacrylamide in Low Carbon Soil Extracts. *Journal of Environmental Quality*, *42*(6), 1902–1907. https://doi.org/10.2134/jeq2013.07.0279
Kaufman, M. M. (2000). Erosion control at construction sites: The science-policy gap. *Environmental Management*, *26*(1), 89–97. https://doi.org/10.1007/s002670010073
Kay-Shoemake, J. L., Watwood, M. E., Lentz, R. D., & Sojka, R. E. (1998). Polyacrylamide as an organic nitrogen source for soil microorganisms with potential effects on inorganic soil nitrogen in agricultural soil. *Soil Biology and Biochemistry*, *30*(8–9), 1045–1052. https://doi.org/10.1016/S0038-0717(97)00250-2
Kazaz, B. (2022). Improvements in Construction Stormwater Treatment using Flocculants. In *Auburn University Electronic Thesis and Dissertations*.
Kazaz, B., Perez, M. A., & Donald, W. N. (2021). State-of-the-Practice Review on the Use of Flocculants for Construction Stormwater management in the United States. *Transportation Research Record*, *2675*(7), 248–258. https://doi.org/10.1177/0361198121995192
Kazaz, B., Perez, M. A., Donald, W. N., Fang, X., & Shaw, J. N. (2022). Detection of Residual Flocculant Concentrations in Construction Stormwater Runoff. *Transportation Research Record: Journal of the Transportation Research Board*, *2676*(7), 036119812210779. https://doi.org/10.1177/03611981221077985
Khoo, S. C., Phang, X. Y., Ng, C. M., Lim, K. L., Lam, S. S., & Ma, N. L. (2019). Recent technologies for treatment and recycling of used disposable baby diapers. *Process*

Safety and Environmental Protection, *123*, 116–129. https://doi.org/10.1016/j.psep.2018.12.016

King, D. J., & Noss, R. R. (1989). Toxicity of polyacrylamide and acrylamide monomer. *Reviews on Environmental Health*, *8*(1–4), 3–16. https://doi.org/10.1515/reveh-1989-1-403

K.Labahn, S., C. Fisher, J., A. Robleto, E., H. Young, M., & P. Moser, D. (2010). Microbially Mediated Aerobic and Anaerobic Degradation of Acrylamide in a Western United States Irrigation Canal. *Journal of Environmental Quality*, *39*(5), 1563–1569. https://doi.org/10.2134/jeq2009.0318

Kurenkov, V. F., Hartan, H.-G., & Lobanov, F. I. (2002). Application of Polyacrylamide Flocculants for Water Treatment. *Ул. К. Маркса Казань. Татарстан. Россия*, *3*(31), 31–40.

Labeeuw, L., Commault, A. S., Kuzhiumparambil, U., Emmerton, B., Nguyen, L. N., Nghiem, L. D., & Ralph, P. J. (2021). A comprehensive analysis of an effective flocculation method for high quality microalgal biomass harvesting. *Science of the Total Environment*, *752*, 141708. https://doi.org/10.1016/j.scitotenv.2020.141708

Lentz, R. D., & Sojka, R. E. (1994). Field results using polyacrylamide to manage furrow erosion and infiltration. *Soil Science*, *158*(4), 274–282. https://doi.org/10.1097/00010694-199410000-00007

Li, X., Xu, Z., Yin, H., Feng, Y., & Quan, H. (2017). Comparative Studies on Enhanced Oil Recovery: Thermoviscosifying Polymer Versus Polyacrylamide. *Energy and Fuels*, *31*(3), 2479–2487. https://doi.org/10.1021/acs.energyfuels.6b02653

Liao, K., & Bhatia, S. K. (2005). Geotextile Tube: Filtration Performance of Woven Geotextiles Under Pressure. *Syracuse University, Civil and Environmental Engineering Department, Syracuse, NY, USA*, 1–15.

Liebert, M. A. (1991). Final Report on the Safety Assessment of Polyacrylamide. *Journal of the American College of Toxicology*, *10*(1), 193–203.

Long, Y., You, X., Chen, Y., Hong, H., Liao, B. Q., & Lin, H. (2020). Filtration behaviors and fouling mechanisms of ultrafiltration process with polyacrylamide flocculation for water treatment. *Science of the Total Environment*, *703*, 135540. https://doi.org/10.1016/j.scitotenv.2019.135540

Ma, J., Wang, R., Wang, X., Zhang, H., Zhu, B., Lian, L., & Lou, D. (2019). Drinking water treatment by stepwise flocculation using polysilicate aluminum magnesium and cationic polyacrylamide. *Journal of Environmental Chemical Engineering*, *7*(3), 103049. https://doi.org/10.1016/j.jece.2019.103049

Mainland Machinery. (2023). *Dry Flocculant Mixing and Feeding Design Considerations*. In Equipment, Informative, Manufacturing, Mining. https://mainlandmachinery.com/dry-flocculant-mixing-feeding/

Maurya, N. K., & Mandal, A. (2016). Studies on behavior of suspension of silica nanoparticle in aqueous polyacrylamide solution for application in enhanced oil recovery. *Petroleum Science and Technology*, *34*(5), 429–436. https://doi.org/10.1080/10916466.2016.1145693

McCollister, D. D., Hake, C. L., Sadek, S. E., & Rowe, V. K. (1965). Toxicologic investigations of polyacrylamides. *Toxicology and Applied Pharmacology*, *7*(5), 639–651. https://doi.org/10.1016/0041-008X(65)90119-5

Mclaughlin, R. A., & Zimmerman, A. (2008). Best Management Practices for Chemical Treatment Systems for Construction Stormwater and Dewatering. *Federal Highway Administration U.S. Department of Transportation*, *October*, 12.

Menter, P. (2012). Electrophoretic mobility shift assay (EMSA) technical bulletin. Acrylamide Polymerization - A Practical Approach (tech note 1156). *Bio-Rad Laboratories*. https://www.bio-rad.com/webroot/web/pdf/lsr/literature/Bulletin_1156.pdf

Mikulec, J., Polakovičová, G., & Cvengroš, J. (2015). Flocculation Using Polyacrylamide Polymers for Fresh Microalgae. *Chemical Engineering and Technology*, *38*(4), 595–601. https://doi.org/10.1002/ceat.201400639

Muzi Sibiya, S. (2014). Evaluation of the streaming current detector (SCD) for coagulation control. *Procedia Engineering*, *70*, 1211–1220. https://doi.org/10.1016/j.proeng.2014.02.134

Narejo, D. B. (2003). Opening size recommendations for separation geotextiles used in pavements. *Geotextiles and Geomembranes*, *21*(4), 257–264. https://doi.org/10.1016/S0266-1144(03)00028-1

Narkis, N., & Rebhun, M. (1966). Ageing effects in measurements of polyacrylamide solution viscosities. *Polymer*, *7*(10), 507–512. https://doi.org/10.1016/0032-3861(66)90032-2

National Oceanic and Atmospheric Administration. (2022). River Habitat. In *National Oceanic and Atmospheric Administration*. https://www.fisheries.noaa.gov/national/habitat-conservation/river-habitat#:~:text=Roughly%203.5%20million%20miles%20of,%2C%20ecological%2C%20and%20cultural%20value.

North Carolina Department of Transportation. (2015). *Erosion and Sediment Control Design and Construction Manual*. North Carolina Department of Transportation. https://connect.ncdot.gov/resources/roadside/SoilWaterDocuments/Erosion and Sediment Control Design and Construction Manual_Rev20220519.pdf

Occupational Safety and Health Administration 1910.1200. (2012). Occupational Safety and Health Standards - Toxic and Hazardous Substances - Safety Data Sheets (Mandatory). In *Occupational Safety and Health Administration*.

O'Shea, J. P., Qiao, G. G., & Franks, G. V. (2010). Solid-liquid separations with a temperature-responsive polymeric flocculant: Effect of temperature and molecular weight on polymer adsorption and deposition. *Journal of Colloid and Interface Science*, *348*(1), 9–23. https://doi.org/10.1016/j.jcis.2010.04.063

Parsapour, G. A., Hossininasab, M., Yahyaei, M., & Banisi, S. (2014). Effect of settling test procedure on sizing thickeners. *Separation and Purification Technology*, *122*, 87–95. https://doi.org/10.1016/j.seppur.2013.11.001

Pérez, L., Salgueiro, J. L., Maceiras, R., Cancela, Á., & Sánchez, Á. (2016). Study of influence of pH and salinity on combined flocculation of Chaetoceros gracilis microalgae. *Chemical Engineering Journal*, *286*, 106–113. https://doi.org/10.1016/j.cej.2015.10.059

Perez, M. A., Zech, W. C., Donald, W. N., & Fang, X. (2015). Installation Enhancements to Common Inlet Protection Practices Using Large-Scale Testing Techniques. *Transportation Research Record: Journal of the Transportation Research Board*, *2521*(1), 151–161. https://doi.org/10.3141/2521-16

Pillai, J. (1997). Flocculants and Coagulants: The Keys to Water and Waste Management in Aggregate Production. *Nalco, Stone Review*, 1,3. http://www.aniq.org.mx/pqta/pdf/Flocculants and Coagulants NALCO (LIT).pdf

Rasband, W. S. (n.d.). *ImageJ*. U. S. National Institutes of Health. https://imagej.nih.gov/ij/

Rawat, A., Mahavar, H. K., Chauhan, S., Tanwar, A., & Singh, P. J. (2012). Optical band gap of polyvinylpyrrolidone/polyacrylamide blend thin films. In *Indian Journal of Pure & Applied Physics* (Vol. 50).

Roselet, F., Vandamme, D., Roselet, M., Muylaert, K., & Abreu, P. C. (2015). Screening of commercial natural and synthetic cationic polymers for flocculation of freshwater and marine microalgae and effects of molecular weight and charge density. *Algal Research*, *10*(1), 183–188. https://doi.org/10.1016/j.algal.2015.05.008

Roselet, F., Vandamme, D., Roselet, M., Muylaert, K., & Abreu, P. C. (2017). Effects of pH, Salinity, Biomass Concentration, and Algal Organic Matter on Flocculant Efficiency of Synthetic Versus Natural Polymers for Harvesting Microalgae Biomass. *Bioenergy Research*, *10*(2), 427–437. https://doi.org/10.1007/s12155-016-9806-3

Schussler, J. C., Kazaz, B., Perez, M. A., Whitman, J. B., & Cetin, B. (2021). Field evaluation of wattle and silt fence ditch checks. *Transportation Research Record*, *2675*(6), 281–293. https://doi.org/10.1177/0361198121992073

Seybold, C. D. (1994). Polyacrylamide review: Soil conditioning and environmental fate. *Communications in Soil Science and Plant Analysis*, *25*(11–12), 2171–2185. https://doi.org/10.1080/00103629409369180

Shanker, R., Ramakrishna, C., & Seth, P. K. (1990). Microbial degradation of acrylamide monomer. *Archives of Microbiology*, *154*(2), 192–198. https://doi.org/10.1007/BF00423332

Shin, S., & Cho, Y. I. (1993). Temperature effect on the non-Newtonian viscosity of an aqueous polyacrylamide solution. *International Communications in Heat and Mass Transfer*, *20*(6), 831–844.

Shukor, M. Y., Gusmanizar, N., Azmi, N. A., Hamid, M., Ramli, J., Shamaan, N. A., & Syed, M. A. (2009). Isolation and characterization of an acrylamide-degrading Bacillus cereus. *Journal of Environmental Biology*, *30*(1), 57–64.

Singh, R., & Adhikari, R. (2018). Generalized Stokes laws for active colloids and their applications. *Journal of Physics Communications*, *2*(2). https://doi.org/10.1088/2399-6528/aaab0d

Smith, E. A., Prues, S. L., & Oehme, F. W. (1997). Environmental degradation of polyacrylamides. II. Effects of environmental (outdoor) exposure. *Ecotoxicology and Environmental Safety*, *37*(1), 76–91. https://doi.org/10.1006/eesa.1997.1527

SNF Floeger, & de Milieux, Z. (2003). Coagulation - Flocculation. *SNF Floerger*, *33*(0), 10. http://www.snf-group.com/wp-content/uploads/2017/02/Water-Treatment-Coagulation-Flocculation-E.pdf

Sojka, R. E., & Lentz, R. D. (1996). PAM in Furrow Irrigation, an Erosion Control Breakthrough. *First European Conference & Trade Exposition on Erosion Control*, *1*, 183–189.

Stechemesser, H., & Dobiáš, B. (2005). Coagulation and Flocculation. In *Coagulation and Flocculation, Second Edition* (pp. 1–862). https://doi.org/10.1680/bwtse.63341.061

Stephan, C. E. (2009). Methods for Calculating an LC. *Aquatic Toxicology and Hazard Evaluation*. https://doi.org/10.1520/stp32389s

Swift, T., Swanson, L., Bretherick, A., & Rimmer, S. (2015). Measuring poly(acrylamide) flocculants in fresh water using inter-polymer complex formation. *Environmental Science: Water Research and Technology*, *1*(3), 332–340. https://doi.org/10.1039/c4ew00092g

Syed, S., Karadaghy, A., & Zustiak, S. (2015). Simple Polyacrylamide-based Multiwell Stiffness Assay for the Study of Stiffness-dependent Cell Responses. *Journal of Visualized Experiments*, *2015*(97). https://doi.org/10.3791/52643

Tang, X. W., Tang, L., She, W., & Gao, B. S. (2013). Prediction of pore size characteristics of woven slit-film geotextiles subjected to tensile strains. *Geotextiles and Geomembranes*, *38*, 43–50. https://doi.org/10.1016/j.geotexmem.2013.05.001

Tolikonda, R., & Quaranta, J. D. (2012). Environmental factors affecting geotextile filter design in coal refuse impoundments. *International Journal of Mining, Reclamation and Environment*, *26*(2), 163–181. https://doi.org/10.1080/17480930.2011.603511

Touzé, S., Guerin, V., Guezennec, A. G., Binet, S., & Togola, A. (2015). Dissemination of acrylamide monomer from polyacrylamide-based flocculant use—sand and gravel quarry case study. *Environmental Science and Pollution Research*, *22*(9), 6423–6430. https://doi.org/10.1007/s11356-014-3177-0

United States Environmental Protection Agency. (1992). *Sediment and Erosion Control*. https://www3.epa.gov/npdes/pubs/chap03_conguide.pdf

United States Environmental Protection Agency. (2007a). Construction Site Soil Erosion and Sediment Control [Fact Sheet]. In *Natural Resources Conservation Service*. https://www.nrcs.usda.gov/wps/portal/nrcs/detail/il/home/?cid=nrcs141p2_031319

United States Environmental Protection Agency. (2007b). Developing Your Stormwater Pollution Prevention Plan: A Guide for Construction Sites. In *United States Environmental Protection Agency*. chrome-extension://efaidnbmnnnibpcajpcglclefindmkaj/https://dep.wv.gov/WWE/Programs/stormwater/MS4/guidance/Documents/Developing your SWPPP A Guide for Construction Sites.pdf

United States Environmental Protection Agency. (2022a). *Basic Information about Nonpoint Source (NPS) Pollution*. https://www.epa.gov/nps/basic-information-about-nonpoint-source-nps-pollution

United States Environmental Protection Agency. (2022b). National Pollutant Discharge Elimination System (NPDES) Construction General Permit (CGP) for Stormwater Discharges from Construction Activities. In *United States Environmental Protection Agency* (Issue January).

United States Environmental Protection Agency. (2022c). Stormwater Discharges from Construction Activities. In *United States Environmental Protection Agency*. https://www.epa.gov/npdes/stormwater-discharges-construction-activities

United States Environmental Protection Agency. (2023). National Primary Drinking Water Regulations. In *United States Environmental Protection Agency*. https://www.epa.gov/ground-water-and-drinking-water/national-primary-drinking-water-regulations#Organic

Uthra, C., Shrivastava, S., Jaswal, A., Sinha, N., Reshi, M. S., & Shukla, S. (2017). Therapeutic potential of quercetin against acrylamide induced toxicity in rats. *Biomedicine and Pharmacotherapy*, *86*, 705–714. https://doi.org/10.1016/j.biopha.2016.12.065

Vajihinejad, V., Gumfekar, S. P., Bazoubandi, B., Rostami Najafabadi, Z., & Soares, J. B. P. (2019). Water Soluble Polymer Flocculants: Synthesis, Characterization, and Performance Assessment. *Macromolecular Materials and Engineering*, *304*(2), 1–43. https://doi.org/10.1002/mame.201800526

WATERTECH of America Inc. (2023). *Polymer Flocculants in Detail*. WATERTECH of America Inc. https://www.watertechusa.com/Polymer-Flocculants-in-Detail

Whitman, J. B., Schussler, J. C., Perez, M. A., & Liu, L. (2021a). Hydraulic Performance Evaluation of Wattles Used for Erosion and Sediment Control. *Journal of Irrigation and Drainage Engineering*, *147*(7), 1–11. https://doi.org/10.1061/(asce)ir.1943-4774.0001586

Whitman, J. B., Schussler, J. C., Perez, M. A., & Liu, L. (2021b). Hydraulic Performance Evaluation of Wattles Used for Erosion and Sediment Control. *Journal of Irrigation and Drainage Engineering*, *147*(7), 1–11. https://doi.org/10.1061/(asce)ir.1943-4774.0001586

Whitman, J. B., Zech, W. C., & Donald, W. N. (2019). Full-Scale Performance Evaluations of Innovative and Manufactured Sediment Barrier Practices. *Transportation Research Record*, *2673*(8), 284–297. https://doi.org/10.1177/0361198119827905

Wong, S. S., Teng, T. T., Ahmad, A. L., Zuhairi, A., & Najafpour, G. (2006). Treatment of pulp and paper mill wastewater by polyacrylamide (PAM) in polymer induced flocculation. *Journal of Hazardous Materials*, *135*(1–3), 378–388. https://doi.org/10.1016/j.jhazmat.2005.11.076

Xepapadeas, A. (2011). The Economics of Non-Point-Source Pollution. *Annual Review of Resource Economics*, *3*, 355–373. https://doi.org/10.1146/annurev-resource-083110-115945

Xiong, B., Loss, R. D., Shields, D., Pawlik, T., Hochreiter, R., Zydney, A. L., & Kumar, M. (2018). Polyacrylamide degradation and its implications in environmental systems. *Npj Clean Water*, *1*(1). https://doi.org/10.1038/s41545-018-0016-8

Xylem. (2023). *What is the pH of water and how is pH measured? What does pH measure?* YSI. https://www.ysi.com/parameters/ph

Young, M. H., Tappen, J. J., Miller, G. C., Carroll, S., & Susfalk, R. B. (2007). Using Linear Anionic Polyacrylamide (LA-PAM) as an Alternative to Reduce Seepage Losses in Water Delivery Canals. *U.S. Bureau of Reclamation*.

Yu, H., Wang, C., Meng, F., Xiao, J., Liang, J., Kim, H., Bae, S., Zou, D., Kim, E. S., Kim, N. Y., Zhao, M., & Li, B. (2021). Microwave humidity sensor based on carbon dots-decorated MOF-derived porous Co3O4 for breath monitoring and finger moisture detection. *Carbon*, *183*, 578–589. https://doi.org/10.1016/j.carbon.2021.07.031

Zolfaghari, R., Katbab, A. A., Nabavizadeh, J., Tabasi, R. Y., & Nejad, M. H. (2006). Preparation and characterization of nanocomposite hydrogels based on polyacrylamide for enhanced oil recovery applications. *Journal of Applied Polymer Science*, *100*(3), 2096–2103. https://doi.org/10.1002/app.23193

APPENDICES

Appendix A: Manufacturer

Appendix B: Settling Velocity Calibration Testing Procedure

Appendix C: Residual Concentration Testing Procedure

APPENDIX A: MANUFACTURER IDENTIFICATION

Table 5-1. Manufacturer Identification

ID	Manufacturer Name
Manufacturer A	Carolina Hydrologic
Manufacturer B	Dober

APPENDIX B: SETTLING VELOCITY CALIBRATION TESTING PROCEDURE

Settling Velocity Calibration Testing Procedure

Equipment

1) Jar Test Multiple Stirrer
2) 1500 mL Glass Beakers
3) Stopwatch
4) 1000 mL Glass Graduated Cylinder
5) GoPro Camera
6) Digital Clock (with seconds!)
7) pH meter
8) Glass thermometer
9) Scale
10) Precision Scale
11) Acid and Base pH Buffering Solutions
12) Large Plastic Tub (27 gal. plastic tub recommended)
13) Cheese Grater
14) White Poster Board

Pre-Test

1) Fill a large plastic tub with tap water that is close to the desired testing temperature. Low temperatures (50°F [10°C] and below) will require water to be chilled overnight prior to testing.
2) Depending on the desired pH range, add acid or base buffering solution to tap water to raise or lower the pH, respectively. Use a paint mixer to sufficiently mix solution before taking a pH reading. Note: adjusting the pH can take some time so temperature adjustments will be necessary later. Set pH range to a value between 5.35 to 5.45, 6.35 to 6.45, 7.35 to 7.45, or 8.35 to 8.45 to ensure consistency between samples.
3) Once the pH is within the desired range, set the temperature by using heat lamps to raise the temperature. To cool samples, proceed to the next step.
4) Fill glass beakers with 1000 mL of pH set water. If samples need cooled a couple degrees, place in a refrigerator for 15-30 minutes. For lower temperatures, place beakers in a salted ice bath, being careful to not contaminate the pH water with any salt. Samples will need stirred periodically to ensure samples reach low temperature sets. While waiting for the temperature to reach the desired value, proceed to the next step.

5) Clean Jar Test Multiple Stirrer machine by rinsing the stirring rods, paddles, and paddle rest with deionized water, spraying with Alconox® Liquinox cleaning solution, and wipe clean with a paper towel.
6) Equip graduated cylinder with ruler tape on the side with zero starting at the cylinder base.
7) Insert microSD card in GoPro and ensure the video frame includes the top and bottom of the graduated cylinder, ruler tape on cylinder is visible on the side without obstructing the view of the sample in the cylinder, and digital clock visible and legible in frame. Place white poster board behind cylinder for a solid background to make it easier to see gradient when sample is poured.

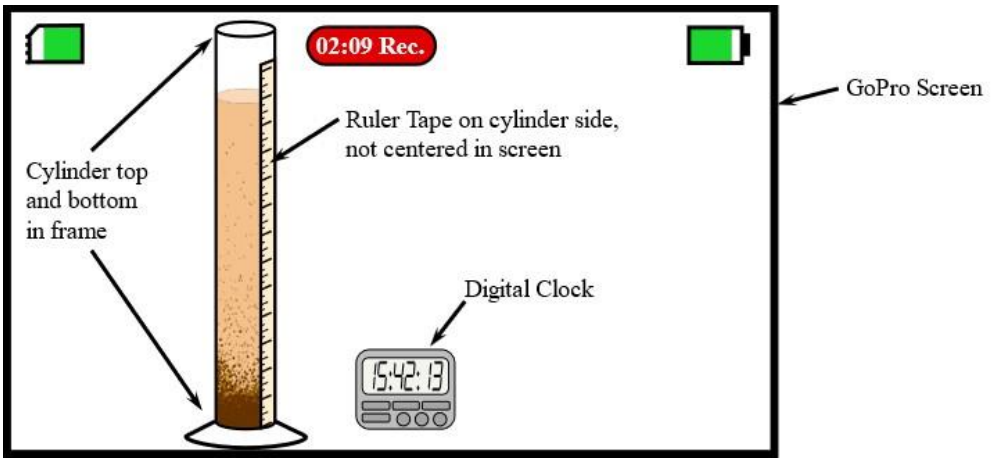

8) Weigh 20g of testing soil that was sieved through a #200 sieve and set aside.
9) Calibrate precision scale and use to weigh out desired flocculant in mg with ±0.1 mg acceptable error. If weighing out block form PAM, use the cheese grater to break up the block into smaller pieces. Fresh material will need grated daily and stored in an airtight jar as it will dry out and impact weights otherwise. Weighed block form PAM will need used within 1 hour of weighing to ensure flocculant does not dry out and harden, which could impact results.
10) Once the pH water reaches the desired temperature, proceed to the testing section.

Testing

1) Start GoPro video recording of the graduated cylinder.
2) Add 20g of sieved testing soil to the sample and place on jar test multiple stirrer machine and flash mix (120 rpm) for 1 min.

3) Remove sample and add the desired flocculant in center of cylinder. Do not add flocculant while stirrers are still in sample as the flocculant may stick to the beaker walls or stirrer rod and not make it into the sample.
4) Place samples back on jar test multiple stirrer machine and flash mix (120 rpm) again for 1 min.
5) Quickly pour the sediment-supernatant sample into the graduated cylinder, being sure to pour fast enough so that all sediment in sample remains suspended while pouring.
6) Record the start hour and minute sample was poured and the sample total height.
7) Wait until sample is fully settled before stopping GoPro video. If sample gradient is not easily visible, allow for sample to settling for 1 hour before stopping video.

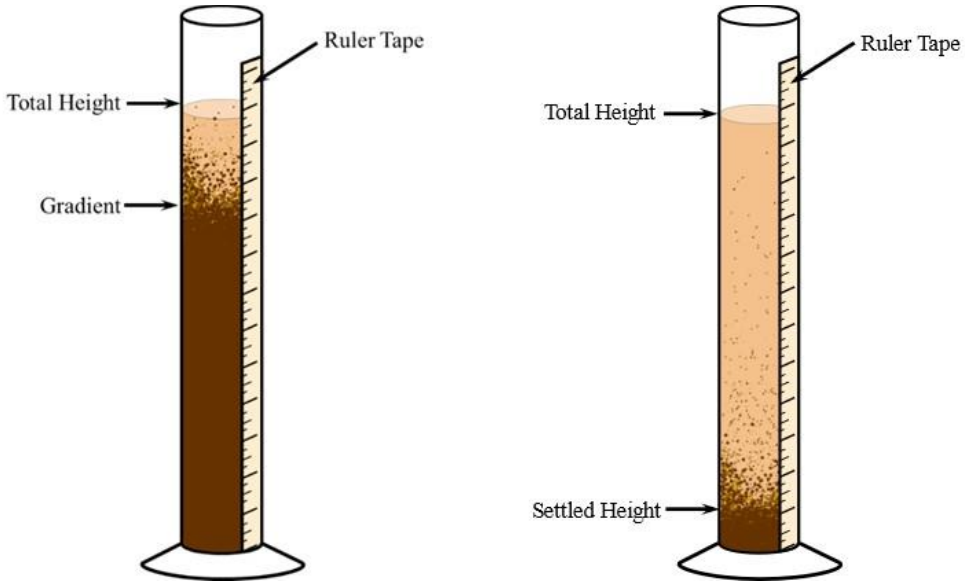

Post-Test

1) Wash glass beakers and cylinders with hot water and scrub clean with Alconox® Liquinox cleaning solution.
2) Clean Jar Test Multiple Stirrer machine by rinsing the stirring rods, paddles, and paddle rest with deionized water, spraying with Alconox® Liquinox cleaning solution, and wipe clean with a paper towel. If sample flocculated under 30 sec, it is recommended to repeat the cleaning process two or three time to ensure all flocculant is removed.
3) Review residual video to capture the seconds that the sample was poured and the settle time and height. Note that depending on the floc size, settle height will vary. Sample

is considered as settled when the lowest gradient point touches the fully settled sediment. Samples that are difficult to distinguish a gradient and take longer to settle, multiple videos may need stitched together in a video editing software to be able to see gradient since GoPro videos record in 10-minute sections.

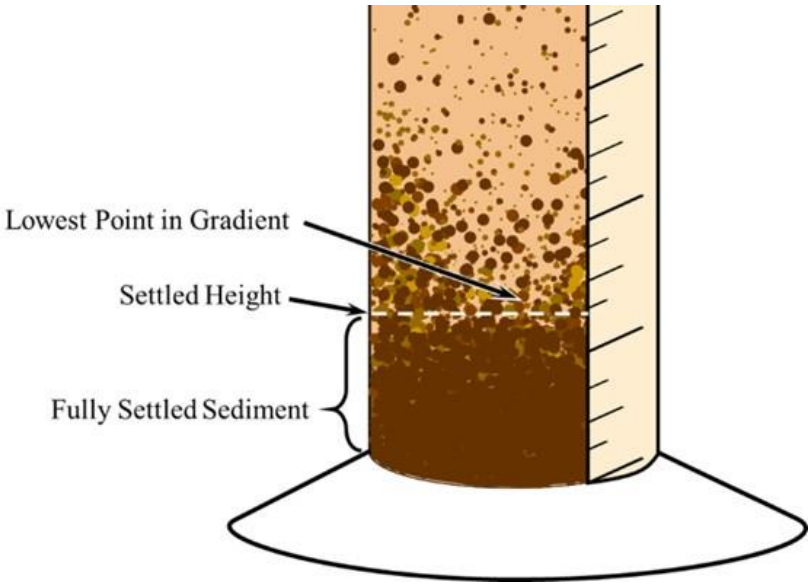

APPENDIX C: RESIDUAL CONCENTRATION TESTING PROCEDURE

Residual Testing Procedure

Equipment

1) Jar Test Multiple Stirrer
2) 1500 mL Glass Beakers
3) Stopwatch
4) 1000 mL Glass Graduated Cylinder
5) GoPro Camera
6) Digital Clock (with seconds!)
7) pH meter
8) Glass thermometer
9) Scale

Pre-Test

1) Shake samples for 1 min, then pour >1,000 mL of sample into three clean 1,500 mL glass beakers and label.
2) Wait 15 min for sediment in sample to fully settle.
3) Clean Jar Test Multiple Stirrer machine by rinsing the stirring rods and paddles with deionized water, spraying with Alconox® Liquinox cleaning solution, and wipe clean with a paper towel.
4) Equip graduated cylinder with ruler tape on the side with zero starting at the cylinder base.
5) Insert microSD card in GoPro and ensure the video frame includes the top and bottom of the graduated cylinder, ruler tape on cylinder is visible on the side without obstructing the view of the sample in the cylinder, and digital clock visible and legible in frame.

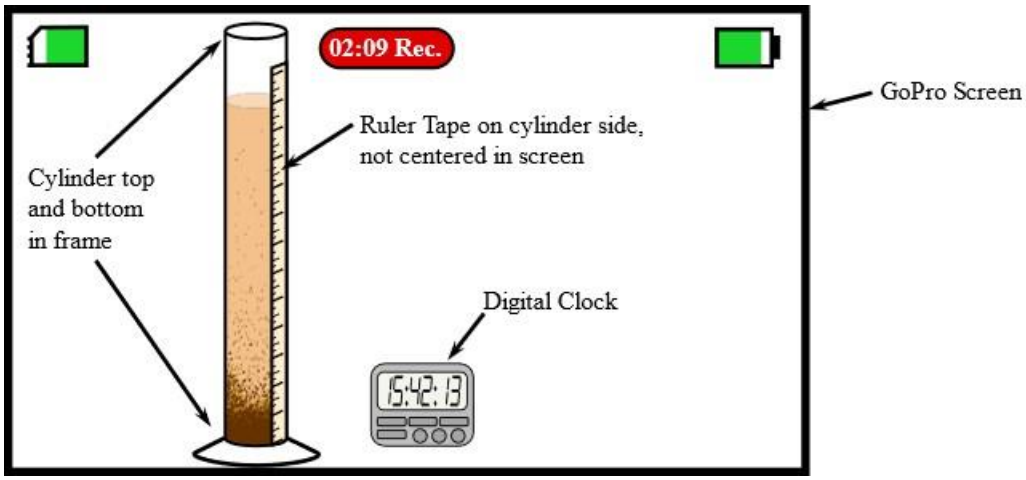

6) Weigh 20g of testing soil that was sieved through a #200 sieve and set aside.
7) Transfer 1,000 mL of supernatant into a new clean 1,500 mL glass beaker and label beaker.
8) Take pH reading and temperature of sample

Testing

1) Start GoPro video recording of the graduated cylinder.
2) Add 20g of sieved testing soil to the supernatant sample and place on jar test multiple stirrer machine and flash mix (120 rpm) for 1 min.
3) Quickly pour the sediment-supernatant sample into the graduated cylinder, being sure to pour fast enough so that all sediment in sample remains suspended while pouring.
4) Record the start hour and minute sample was poured and the sample total height.
5) Wait until sample is fully settled before stopping GoPro video. If sample gradient is not easily visible, allow for sample to settling for 1 hour before stopping video.

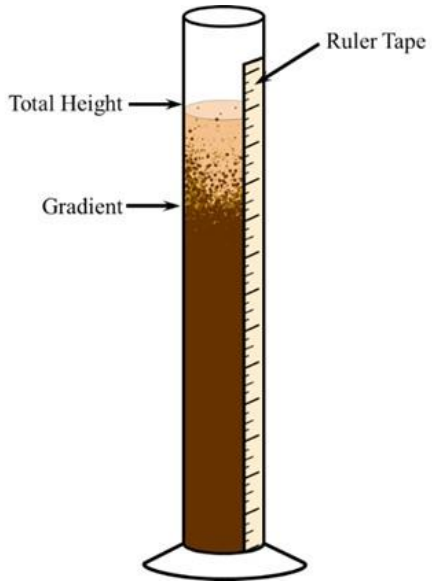

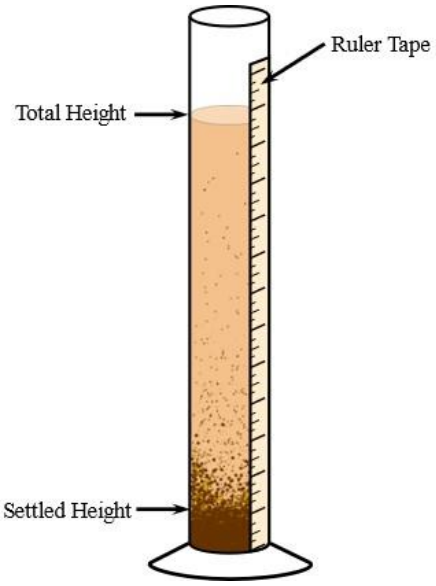

Post-Test

1) Wash glass beakers and cylinders with hot water and scrub clean with Alconox® Liquinox cleaning solution.
2) Clean Jar Test Multiple Stirrer machine by rinsing the stirring rods, paddles, and paddle rest with deionized water, spraying with Alconox® Liquinox cleaning solution, and wipe clean with a paper towel. If sample flocculated under 30 sec, it is recommended to repeat the cleaning process two or three time to ensure all flocculant is removed.
3) Review residual video to capture the seconds that the sample was poured and the settle time and height. Note that depending on the floc size, settle height will vary. Sample is considered as settled when the lowest gradient point touches the fully settled sediment. Samples that are difficult to distinguish a gradient and take longer to settle, multiple videos may need stitched together in a video editing software to be able to see gradient since GoPro videos record in 10-minute sections.

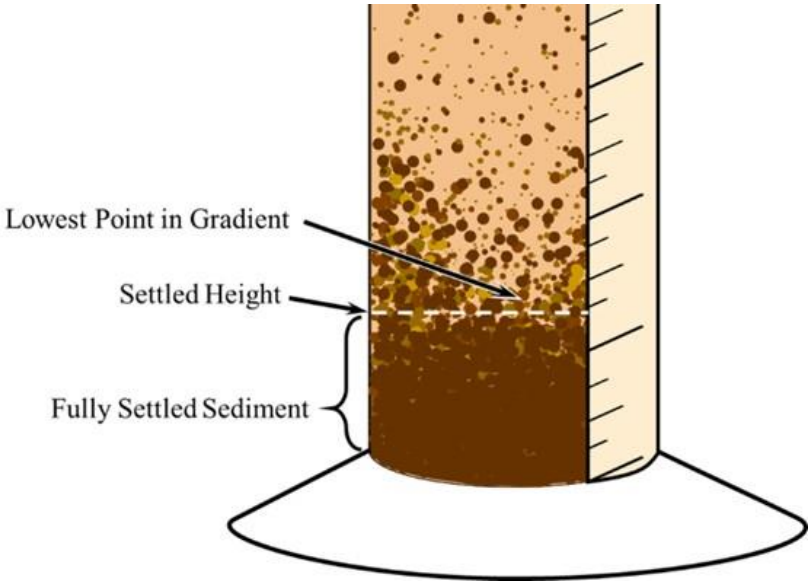
Lowest Point in Gradient
Settled Height
Fully Settled Sediment